

Conclusion

6.1 Summary of the present research work

- Three crude oils—LCO (Light, 33.4 API, Middle East), MCO (Medium, 21.4 API, Canada), and EHCO (Extra Heavy, 9.5 API, South America)—were analyzed.
- Complete analysis, followed by detailed investigations regarding the chemical composition were performed for the above-mentioned crude oils.
- ASTM D2892 & ASTM D5236 were thoroughly utilized to understand the nature of the distillates obtained from the crude oil.
- Aromatic, Resin, and Asphaltene (ARA) fractions were investigated for the presence of CCR, density, carbon, nitrogen, and metals.
- Heat treatment of Aromatic, Resin, and Asphaltene (ARA) fractions was conducted in three stages: green carbon (Stage I), calcined carbon (Stage II), and graphitized carbon (Stage III).
- Possibility of dehydrogenative polymerization and dehydrative polycondensation reactions were studied by elemental analysis, which figured % hydrogen, nitrogen, sulfur, and oxygen.
- Three types of materials such as green, calcined and graphitized carbon were derived from VRO.
- Another set of materials based on graphene oxide, were synthesized by thermal as well as microwave method.
- Optimization of rGO-M synthesis using Box-Behnken Design (BBD) was done.
- Thermogravimetric Analysis (TGA) was performed to analyse the thermal stability of the three types of materials synthesized from VRO.
- XRD analysis, Raman spectroscopy, Elemental analysis, Electron microscopy studies, nitrogen adsorption studies and FTIR were used to assure the formation of carbon materials.
- Effectiveness of Reduced Graphene Oxide in wastewater treatment and oil spill remediation was also studied to emphasize the utility of the synthesized material in environmental protection.

6.2 Conclusions of the present research work

This thesis comprehensively explored the transformation of petroleum-derived heavy fractions into high-value carbon materials, with a particular focus on reduced graphene oxide synthesized via microwave-assisted techniques (rGO-M). The research spanned the characterization of crude oil fractions, synthesis and structural transformation of carbon materials, and evaluation of their practical environmental applications. The work demonstrates a significant advancement in both crude oil analysis methodologies and the development of functional carbon-based materials for environmental remediation.

In the early stages of the research, the development and validation of a refined TLC-FID analytical method for SARA fraction quantification offered a fast, reliable, and accurate tool to assess crude oil compatibility and stability. The ability to predict incompatibility using defined thresholds ($CII < 1.0$; $P > 1.45$) has significant implications for the refining industry, reducing operational risks and improving decision-making in crude blending.

The study also provided deep insights into the molecular and structural features of Aromatic, Resin, and Asphaltene (ARA) fractions using FTIR, GPC, and NMR techniques. Heavier fractions were found to exhibit greater heterogeneity, increased aromaticity, and higher concentrations of heteroatoms and metals. These characteristics have direct consequences on refining behaviour, asphaltene precipitation, and potential for value-added product synthesis.

A major outcome of the work lies in the successful synthesis of graphitized carbon materials from VRO-derived ARA fractions through a three-stage heat treatment process. The transition from amorphous to graphitic structure was clearly established using XRD, Raman spectroscopy, and TGA. The findings confirmed the feasibility of producing high-purity carbon materials (carbon content $\sim 99.99\%$) with excellent thermal stability and structural order, independent of the originating fraction type.

The centrepiece of the study was the synthesis and optimization of microwave-assisted reduced graphene oxide (rGO-M). Compared to thermally reduced rGO, rGO-M exhibited

superior structural restoration, porosity, and thermal stability. Microwave reduction was shown to be a highly efficient method for producing high-quality graphene derivatives with minimal defects, as confirmed by advanced characterization tools such as XRD, Raman, FTIR, TGA, and electron microscopy.

In environmental applications, rGO-M demonstrated exceptional performance in both wastewater treatment and oil spill remediation. Its high surface area, hierarchical pore structure, and active surface functionalities contributed to rapid and efficient adsorption of pollutants. The material achieved impressive removal efficiencies—up to 85% for total hardness and 60–61% for TOC in wastewater, and 190 mg/g oil uptake capacity with 95% efficiency in oil spill simulations. These results clearly illustrate the superior functional performance of rGO-M over conventional rGO and standard adsorbents.

In conclusion, this research bridges fundamental studies in petroleum chemistry with applied materials science, offering scalable pathways to convert crude oil by-products into valuable nano-materials. It lays a strong foundation for future advancements in carbon material synthesis and their deployment in environmental and industrial applications. The strategic integration of analytical, synthetic, and application-oriented approaches underlines the novelty and practical relevance of this work.

6.3 Future Work

- The findings of this research open multiple avenues for continued exploration and application:
- While the synthesis of high-purity graphitized carbon materials and rGO-M has been demonstrated at the lab scale, future efforts should focus on process scale-up, energy efficiency optimization, and economic viability. Microwave-assisted reduction, in particular, holds promise for industrial-scale graphene production due to its rapid processing time and minimal energy loss.
- The surface chemistry of rGO-M can be further tailored through chemical or biological functionalization to enhance selectivity and efficiency in specific

environmental applications such as heavy metal capture, gas adsorption, or catalysis.

- Incorporating rGO-M into composite materials, membranes, or filtration systems could significantly enhance the performance of existing water and air purification technologies. Pilot-scale studies in real-world environmental conditions would be a logical next step to validate practical feasibility.
- Given the high surface area, porosity, and conductivity of the synthesized carbon materials, future research could explore their application in energy storage systems such as supercapacitors or lithium-ion batteries, expanding the scope beyond environmental remediation.
- The refined SARA analysis technique developed in this study can be further applied to a broader range of crude oil types, aiding in better compatibility prediction, refining strategy design, and selection of optimal feedstocks for carbon material synthesis.
- A thorough life-cycle analysis (LCA) of the carbon material synthesis process from petroleum fractions would provide insights into the environmental benefits and trade-offs, guiding sustainable material development strategies.
- While this study focused on petroleum-derived fractions, future work could investigate the conversion of other carbon-rich waste streams (e.g., bio-oil, plastic waste, or used lubricants) into graphene-based materials using similar methodologies, promoting circular economy principles.



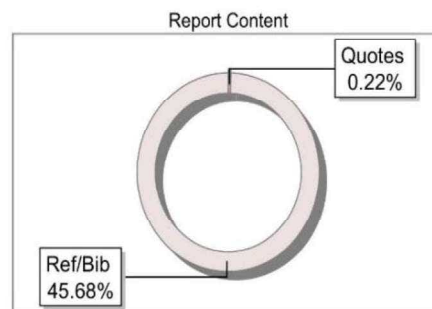
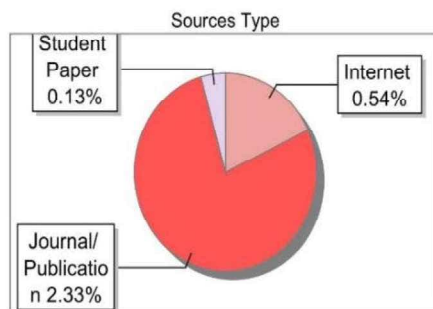
The Report is Generated by DrillBit Plagiarism Detection Software

Submission Information

Author Name	Ravi Dalsaniya
Title	SYNTHESIS OF NANOMATERIAL FROM HEAVY FRACTION OF CRUDE OIL
Paper/Submission ID	4285309
Submitted by	director.rit@atmiyauni.ac.in
Submission Date	2025-08-28 09:13:25
Total Pages, Total Words	253, 60188
Document type	Thesis

Result Information

Similarity **3 %**



Exclude Information

Quotes	Excluded
References/Bibliography	Excluded
Source: Excluded < 1 Words	Excluded
Excluded Source	0 %
Excluded Phrases	Excluded

Database Selection

Language	English
Student Papers	Yes
Journals & publishers	Yes
Internet or Web	Yes
Institution Repository	Yes

A Unique QR Code use to View/Download/Share Pdf File





DrillBit Similarity Report

3

SIMILARITY %

89

MATCHED SOURCES

A

GRADE

A-Satisfactory (0-10%)
B-Upgrade (11-40%)
C-Poor (41-60%)
D-Unacceptable (61-100%)

LOCATION	MATCHED DOMAIN	%	SOURCE TYPE
1	Thesis Submitted to Shodhganga Repository	1	Publication
4	Thesis Submitted to Shodhganga Repository	<1	Publication
6	REPOSITORY - Submitted to VTU Examination 2 on 2024-03-26 11-48	<1	Student Paper
7	Quality and Authenticity Control of Fruit Juices-A Review, by Dasenaki, Marilena- 2019	<1	Publication
8	Thesis Submitted to Shodhganga Repository	<1	Publication
9	degruyter.com	<1	Internet Data
12	www.dx.doi.org	<1	Publication
13	Chemical Composition of Athabasca Bitumen The Distillable Aromatic Fraction by Strausz-2011	<1	Publication
14	Dry Ashing Preparation of (Quasi)solid Samples for the Determination of Inorgani by Shen-2015	<1	Publication
16	Thesis submitted to shodhganga - shodhganga.inflibnet.ac.in	<1	Publication
17	www.nap.edu	<1	Internet Data
26	redcol.minciencias.gov.co	<1	Publication
27	Thesis Submitted to Shodhganga Repository	<1	Publication

Conferences

- [1] Ravi Dalsania, Mahesh Savant. (2024), The major concern of the crude oil compatibility for process, operation and environment. 2nd International Conference On Emerging Trends & Contemporary Practices - ICETPC-2024. Atmiya university, Rajkot, India.



- [2] Ravi Dalsania, Vipul Audichya, Mahesh Savant. (2024), A review of Green Hydrogen Potential And Viable Renewable Source In India. Recent Trends In Chemical Science. Shri U. P. Arts, Smt. M. G. Panchal Science & Shri V. L. Shah Commerce College, Pilvai, Gujarat, India




- [3] Ravi Dalsania, Mahesh Savant. (2024), A review of on sustainable source as bio CNG from bio-waste. Green Energy And Sustainable Development, R R Lalan College, Bhuj, Gujarat, India




Publications

International Journals

- [1] Ravi Dalsania, Hasmukh Gajera, Mahesh Savant, Microwave-Assisted Reduced Graphene Oxide from vacuum gas oil derived graphitic carbon: An Innovative Solution for Wastewater Treatment and Oil Spill Control. Desalination and Water Treatment Volume 323, July 2025.




Author Search Sources ?  RD

Source details

Feedback > Compare sources >

Desalination and Water Treatment

Open Access 

Years currently covered by Scopus: from 2009 to 2025

Publisher: Elsevier


ISSN: 1944-3994 E-ISSN: 1944-3986


Subject area: Engineering: Ocean Engineering Environmental Science: Water Science and Technology Environmental Science: Pollution


Source type: Journal


View all documents >

Set document alert

 Save to source list

CiteScore 2024
2.3 

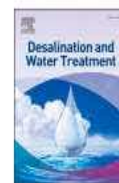
SJR 2024
0.247 

SNIP 2024
0.255 



Contents lists available at ScienceDirect

Desalination and Water Treatment

journal homepage: www.sciencedirect.com/journal/desalination-and-water-treatment/

Microwave-assisted reduced graphene oxide from vacuum gas oil derived graphitic carbon: An innovative solution for wastewater treatment and oil spill control

Ravi Dalsania^{a,b,*}, Hasmukh Gajera^a, Mahesh Savant^b^a Reliance Industries Limited, Village Motikhavdi, Jamnagar, Gujarat 361140, India^b Department of Chemistry, Atmiya University, Rajkot, Gujarat 360005, India

HIGHLIGHTS

- rGO-M synthesized using VGO-derived graphite via microwave-assisted reduction.
- rGO-M exhibited 136 mg/g for hardness and 13.65 mg/g for TOC, over heat-treated rGO.
- rGO-M reduced total hardness by 80 % and TOC by 60 % at 1.0 g/L.
- rGO-M achieved 190 mg/g oil adsorption in 30 min with 95 % efficiency.
- rGO-M provides a sustainable solution for wastewater treatment and oil spills.

ARTICLE INFO


Keywords:


Vacuum gas oil
Reduced graphene oxide
Microwave-assisted reduction
Wastewater treatment
Oil spill remediation, adsorption capacity

ABSTRACT

Graphitic carbon derived from vacuum gas oil (VGO) was chemically oxidized to produce graphene oxide (GO), which was then reduced through sudden thermal treatment and microwave-assisted reduction to obtain reduced graphene oxide (rGO) and rGO-M, respectively. Leveraging VGO's rich carbon content, this eco-friendly synthesis produced graphene-based materials with enhanced adsorption capacity, thermal stability, and structural integrity. The rGO-M synthesis was optimized using Box-Behnken Design (BBD), adjusting microwave power (200 W), reduction time (30 s), and H₂O₂ concentration (5 mL), achieving up to 95 % removal efficiency. Structural, surface, and adsorption characteristics were evaluated for both rGO and rGO-M, particularly in wastewater treatment and oil spill cleanup. rGO-M showed superior adsorption capacity, removing 80 % of total hardness (initial: 170 mg/L) and 60 % of total organic carbon (TOC; initial: 22.74 mg/L) at 1.0 g/L dosage. At 1.5 g/L, it achieved 85 % and 61 % reductions in total hardness and TOC, respectively. For oil removal, rGO-M adsorbed 190 mg/g in 30 min, improving from 40 % efficiency at one minute to 95 % at thirty. While rGO had slightly higher efficiency, rGO-M stands out for its energy-efficient, simple preparation process and excellent performance.

- [2] Ravi Dalsania, Hasmukh Gajera, Mahesh Savant. (2025), Advanced Analytical Techniques for Comprehensive Characterization of Vacuum Residue Oil (VRO): A State-of-the-Art Review JCHR (2025) 15(2), 1398-142.



Author Search Sources ?  RD

Source details [Feedback](#) [Compare sources](#)

Journal of Chemical Health Risks

Years currently covered by Scopus: from 2019 to 2025

Publisher: Islamic Azad University

ISSN: 2251-6719 E-ISSN: 2251-6727

Subject area: [Medicine: Public Health, Environmental and Occupational Health](#) [Chemical Engineering: Chemical Health and Safety](#)
[Environmental Science: Health, Toxicology and Mutagenesis](#) [Environmental Science: Environmental Chemistry](#)

Source type: Journal

[View all documents](#) [Set document alert](#) [Save to source list](#)

CiteScore 2023
1.3

SJR 2023
0.217

SNIP 2023
0.328



Advanced Analytical Techniques for Comprehensive Characterization of Vacuum Residue Oil (VRO): A State-of-the-Art Review

^{1,2*} Ravi Dalsania, ¹ Hasmukh Gajera, ² Mahesh Savant

¹ Reliance Industries Limited, Village Motikhavdi, Jamnagar 361140, Gujarat, India.

² Department of Chemistry, Atmiya University, Rajkot-360005, Gujarat, India.

(Received: 26 February 2025 Revised: 30 March 2025 Accepted: 22 April 2025)


KEYWORDS


Analytical
Techniques,
Comprehensive
Characterization,
Vacuum Residue Oil

ABSTRACT:

The characterization of vacuum residue oil (VRO) presents substantial challenges due to its complex and diverse composition, including a wide range of heavy hydrocarbons and high molecular weight compounds. Existing literature has extensively documented various advanced analytical techniques for assessing VRO, yet the complexity of this material continues to pose difficulties in fully understanding its properties and optimizing its industrial applications. This review builds on prior research by providing a comprehensive overview of the latest characterization methods, categorizing them into three primary areas: physical and chemical bulk property analysis, saturates, aromatics, resins, and asphaltenes (SARA) fractionation, and molecular modeling approaches. The report highlights global standards and variations in VRO properties, with particular focus on the intricate correlations between physical properties such as refractive index and density, and the molecular weight of specific fractions. By compiling and synthesizing these advancements, this review not only underscores the significant diversity within VROs but also clarifies the crucial role of advanced techniques, such as FTIR, NMR spectroscopy, and chromatographic methods, in enhancing our understanding and optimizing the processing of VROs in industrial applications. The insights provided here aim to bridge the gap between existing characterization methods and their practical application in optimizing conversion processes in commercial residual oil units.

- [3] Ravi Dalsania, Hasmukh Gajera, Mahesh Savant. (2025), Exploration of graphitic carbon from crude oil vacuum residue. Carbon Trends Volume 17, December 2024.

 Scopus Preview

Author Search Sources ?  RD

Source details

Feedback > Compare sources >

Carbon Trends

Open Access ?

Years currently covered by Scopus: from 2020 to 2025

Publisher: Elsevier

E-ISSN: 2667-0569

Subject area: Materials Science: Materials Science (miscellaneous) Chemistry: Chemistry (miscellaneous)

Materials Science: Materials Chemistry

Source type: Journal

[View all documents >](#) [Set document alert](#) [Save to source list](#)

CiteScore 2023

4.6 ?

SJR 2023

0.542 ?

SNIP 2023

0.781 ?



Contents lists available at ScienceDirect

Carbon Trends

journal homepage: www.elsevier.com/locate/cartre

Exploration of graphitic carbon from crude oil vacuum residue

Ravi Dalsania^{a,b,*}, Hasmukh Gajera^a, Mahesh Savant^b^a Reliance Industries Limited, Village Motikhavdi, Jamnagar 361140, Gujarat, India^b Department of Chemistry, Atmiya University, Rajkot, Gujarat 360005, India

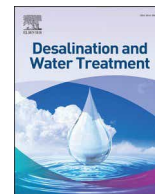
ARTICLE INFO

Keywords:

ARA analysis
Characterization
¹H and ¹³C NMR
Vacuum residue
Graphitic carbon

ABSTRACT

Preparation of graphitic carbon from low value refinery waste has captivated immense interest in past years owing to its low cost and abundant nature. Successful utilization of petroleum vacuum residue is a major challenge in the petroleum industry. In this study pyrolysis of vacuum residue fractions has been carried out for the preparation of graphitic carbon like material. The vacuum residue fractions were obtained from three different crude oils originated from Middle East, Canada and South America. The purity of the Aromatic, Resin and Asphaltene (ARA) fractions were confirmed using TLC-FID which denoted complete separation. The chemical composition were determined using elemental analysis and it revealed ARA fractions to be carbon rich regardless of its origin. Further, sulphur content was found to be high in ARA fractions from Heavy Crude oil (HCO). The degree of polymerization and molecular weight measured using GPC specify that asphaltene has high accumulation with high molecular weight compared with aromatic and resins. ARA derived carbon and heat-treated materials were analysed by TGA, XRD and Raman spectroscopy to study microstructural changes in formation of graphite like material. Thermogravimetric analysis of all ARA samples revealed the different decomposition stages for pyrolyzed, calcined and graphitized samples. The results of XRD demonstrated that the distance between the planes (d-spacing) is above 3.35 Å for all high temperature treated ARA derived carbon materials irrespective of its origin, indicating formation of graphite like structure. In Raman analysis, the nature and intensity of G and D bands evolution during each step of pyrolysis is supporting XRD results for formation of highly ordered graphitic carbon material. Furthermore, understanding feed quality has direct influence on high efficiency, low costs and sustainability, the major issues for oil refinery business.



Microwave-assisted reduced graphene oxide from vacuum gas oil derived graphitic carbon: An innovative solution for wastewater treatment and oil spill control

Ravi Dalsania^{a,b,*}, Hasmukh Gajera^a, Mahesh Savant^b

^a Reliance Industries Limited, Village Motikhavdi, Jamnagar, Gujarat 361140, India

^b Department of Chemistry, Atmiya University, Rajkot, Gujarat 360005, India

HIGHLIGHTS

- rGO-M synthesized using VGO-derived graphite via microwave-assisted reduction.
- rGO-M exhibited 136 mg/g for hardness and 13.65 mg/g for TOC, over heat-treated rGO.
- rGO-M reduced total hardness by 80 % and TOC by 60 % at 1.0 g/L.
- rGO-M achieved 190 mg/g oil adsorption in 30 min with 95 % efficiency.
- rGO-M provides a sustainable solution for wastewater treatment and oil spills.

ARTICLE INFO

Keywords:

Vacuum gas oil
Reduced graphene oxide
Microwave-assisted reduction
Wastewater treatment
Oil spill remediation, adsorption capacity

ABSTRACT

Graphitic carbon derived from vacuum gas oil (VGO) was chemically oxidized to produce graphene oxide (GO), which was then reduced through sudden thermal treatment and microwave-assisted reduction to obtain reduced graphene oxide (rGO) and rGO-M, respectively. Leveraging VGO's rich carbon content, this eco-friendly synthesis produced graphene-based materials with enhanced adsorption capacity, thermal stability, and structural integrity. The rGO-M synthesis was optimized using Box-Behnken Design (BBD), adjusting microwave power (200 W), reduction time (30 s), and H₂O₂ concentration (5 mL), achieving up to 95 % removal efficiency. Structural, surface, and adsorption characteristics were evaluated for both rGO and rGO-M, particularly in wastewater treatment and oil spill cleanup. rGO-M showed superior adsorption capacity, removing 80 % of total hardness (initial: 170 mg/L) and 60 % of total organic carbon (TOC; initial: 22.74 mg/L) at 1.0 g/L dosage. At 1.5 g/L, it achieved 85 % and 61 % reductions in total hardness and TOC, respectively. For oil removal, rGO-M adsorbed 190 mg/g in 30 min, improving from 40 % efficiency at one minute to 95 % at thirty. While rGO had slightly higher efficiency, rGO-M stands out for its energy-efficient, simple preparation process and excellent performance.

1. Introduction

The world's growing environmental degradation has made widespread oil spills and water body contamination serious problems that endanger human health as well as aquatic ecosystems [1]. Hazardous pollutants, such as heavy metals and organic contaminants, have been introduced into natural water sources by industrial effluents, agricultural runoff, and inappropriate waste disposal. Among these contaminants, high levels of total organic carbon (TOC) present serious concerns

because they can create toxic disinfection byproducts during the water treatment process, which can cause respiratory and gastrointestinal problems in people [2,3]. Also, high concentrations of calcium and magnesium in water cause excessive hardness, which not only reduces the effectiveness of industrial and household cleaning products but also disturbs aquatic ecosystems by changing the chemistry of the water, which in turn affects aquatic organisms' metabolism and ability to reproduce. Oil spills from drilling operations and maritime mishaps simultaneously destroy marine life, contaminate food chains, and harm

* Corresponding author at: Reliance Industries Limited, Village Motikhavdi, Jamnagar, Gujarat 361140, India.

E-mail addresses: Ravi.Dalsania@ril.com (R. Dalsania), Hasmukh.Gajera@ril.com (H. Gajera), maheshsavant84@gmail.com (M. Savant).

<https://doi.org/10.1016/j.dwt.2025.101307>

Received 5 May 2025; Received in revised form 19 June 2025; Accepted 2 July 2025

Available online 3 July 2025

1944-3986/© 2025 Published by Elsevier Inc. This is an open access article under the CC BY-NC-ND license (<http://creativecommons.org/licenses/by-nc-nd/4.0/>).

the environment permanently [4]. Even though they are frequently employed, traditional remediation techniques like chemical dispersants, mechanical skimming, and bioremediation can worsen the environment. They are also expensive and inefficient [5].

Due to these challenges, researchers are looking into novel materials like reduced graphene oxide (rGO) in an attempt to reduce the risks of water pollution and oil spills in a way that is more durable and environmentally friendly [6]. Both water pollution and oil spills require efficient, sustainable remediation strategies that can address complex contaminants simultaneously. Because of its remarkable qualities, graphene oxide (GO) and its reduced form, rGO, have garnered a lot of interest. A key characteristic of graphene oxide (GO) for environmental applications is its high density of oxygen-containing functional groups, which offer sites for chemical interaction and enhance its water solubility [7]. In a more reduced form, rGO preserves some of the functional groups that help graphene interact with contaminants while restoring a large portion of its electrical conductivity. Because of its surface area, chemical reactivity, and conductivity, rGO is an excellent choice for applications such as oil spill containment and pollutant adsorption. Recent research has examined GO for cleaning up oil spills and removing contaminants, pointing to both its advantages and disadvantages. Zhang et al. [8] observed that GO has a propensity to agglomerate, which lowers efficiency, but they also reported high Pb^{2+} and Cd^{2+} adsorption. Although rGO was found to be successful at 150 mg/g for cleaning up oil spills, Wang et al. stressed the necessity of surface changes to increase hydrophobicity and recyclability. These studies show how our unique GO method improves stability, adsorption efficiency, and reusability. These findings, supported by earlier studies highlighting the adsorption potential and limitations of GO and rGO, reinforce the relevance of our approach in enhancing material stability, adsorption efficiency, and reusability through tailored synthesis methods.

A byproduct of the refining of petroleum, vacuum gas oil (VGO) is commonly used as a feedstock to make fuels like diesel [9]. But VGO provides more than just energy in the context of sustainability. Waste valorization and the need for circular economy solutions are addressed by its potential conversion into value-added materials like graphitic carbon [10]. A sustainable method of turning what would otherwise be a refinery byproduct into a high-performance material is to use VGO to create advanced carbon materials [11]. The authors of two recent studies by Zohal et al. (2021 and 2023) used vacuum gas oil (VGO) as a feedstock for their hydrotreating reactions and other catalytic processes that formed reduced graphene oxide (rGO) and integrated it into nanocomposites [12,13]. We adopted a new strategy, taking inspiration from their work, and synthesized microwave-treated reduced graphene oxide (rGO) by pyrolyzing VGO. This approach, which is different from the traditional heat treatment procedures previously employed, provides a fresh viewpoint on the productive pyrolysis of rGO by employing VGO as the carbon source.

As a result, we developed a novel and sustainable process for synthesizing reduced graphene oxide (rGO) from vacuum gas oil (VGO)-derived graphitic carbon. This work aims to utilize rGO's potential for addressing wastewater treatment and oil spill control, two significant environmental challenges, by utilizing a microwave-assisted reduction technique. Enhance the yield of GO and rGO using graphitic carbon derived from vacuum gas oil as the precursor material. To accomplish this goal and obtain the best material properties possible, parameters like oxidation and reduction conditions must be adjusted. Utilizing cutting-edge analytical methods, characterize the resultant GO and rGO to comprehend their surface characteristics, morphology, and structure. These analyses will validate that VGO has been successfully converted into high-grade materials based on graphene. Also, Assess the effectiveness of rGO in environmental applications, paying particular attention to how well it adsorbs contaminants from wastewater and how well it can absorb and hold onto oil spill residue. The results of this performance evaluation will shed light on how well rGO works in actual situations. Evaluate the process of microwave-assisted synthesis for

sustainability and scalability. To make sure the procedure complies with the principles of green chemistry, a thorough assessment of the energy usage, economic viability, and possibility for large-scale production will be conducted. By utilizing an industrial byproduct, the method reduces waste and advances the creation of materials with additional value. To determine its commercialization potential, further research should examine the process's scalability and economic viability, taking into account energy usage and cost analysis. By investigating the transformative potential of VGO-derived rGO, this research seeks to offer a high-performance, affordable, and environmentally friendly solution for important environmental challenges.

2. Materials and methods

2.1. Synthesis of GO from VGO

The starting material for the production of graphitic carbon is vacuum gas oil (VGO), a by-product of the distillation of crude oil. As per ASTM D4530, VGO is first pyrolyzed to produce green coke. This green coke is subjected to additional heat treatment at temperatures high around 2800 °C, which rearranges the carbon atoms into a stable graphitic structure, turning the material into more ordered graphitic carbon material [14]. To produce graphene oxide (GO) and reduced graphene oxide (rGO), the resulting graphitic carbon is purified to eliminate contaminants and modify its particle size. This increases its reactivity for the oxidation process that follows.

VGO-derived graphitic carbon is used as a basis in a modified Hummers' method to create graphene oxide (GO). In this procedure, a 1:25:3 ratio of potassium permanganate (KMnO_4) to 98 % pure sulfuric acid (H_2SO_4) and graphitic carbon is employed for oxidation [15]. For four hours, the reaction is kept at 5 °C to regulate the oxidation process. Next, 5 mL of hydrogen peroxide (H_2O_2) is added and stir for 15 min. Next, add 10 mL of 30 % concentrated hydrochloric acid (HCl). Before adding cold water to the mixture, the mixture is given 15 min to settle. Sulfuric acid helps the graphite layers intercalate, and KMnO_4 is added gradually in an ice-cold environment to stop uncontrollably occurring exothermic reactions. Following the gradual addition, the reaction mixture is heated to about 40 °C and agitated for a few hours in order to incorporate functional groups that contain oxygen and facilitate the oxidation of graphite into graphene oxide [16]. After the completion of oxidation, the reaction is quenched with water and any remaining permanganate is neutralized with hydrogen peroxide, which turns the byproducts of manganese dioxide into soluble manganese ions. The resultant GO is purified by repeatedly washing it in distilled water to get rid of extra metal ions and acids. Next, it is dried under vacuum to keep its structure rich in oxygen.

2.2. Synthesis of reduced graphene oxide (rGO) and microwave-assisted reduced graphene oxide (rGO-M)

GO becomes a more chemically active material as a result of the oxidation process, which adds functional groups containing oxygen to the graphene layers. The as-prepared GO was subjected to a sudden thermal shock, causing the rapid removal of most oxygen-containing functional groups in less than a minute. The thermal process was done at 550°C for less than a min time and 200 W of microwave power. By sudden thermal shock majority oxygen functional groups will be decomposed and generate high pressure between GO layers, which resulted in to exfoliation of GO and convert to reduced graphene oxide (rGO). Another way to reduction of graphene oxide by using microwave treatment, process was done for 30-second under microwave irradiation to reduced graphene oxide. By quickly producing targeted heating, this microwave treatment speeds up the reduction process, increases the surface area and electrical conductivity of the rGO, and further eliminates any remaining oxygen groups [17]. Fig. 1 illustrates this process schematically.

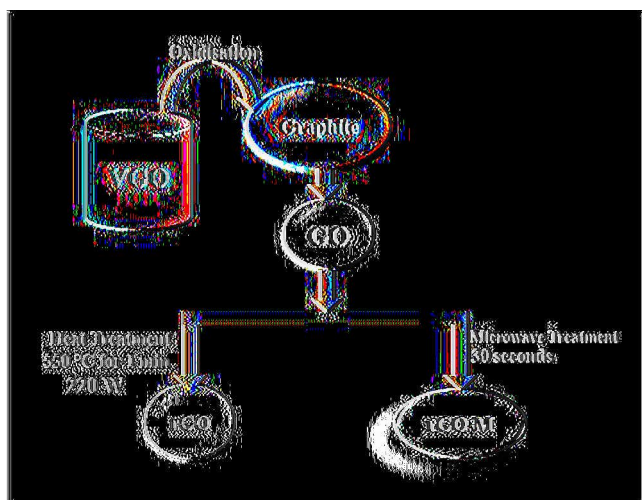


Fig. 1. Schematic diagram showing the synthesis of rGO & rGO-M from VGO via microwave assisted method.

2.3. Characterization of synthesized materials

A variety of cutting-edge methods are employed in the characterization of graphene oxide (GO) and reduced graphene oxide (rGO) and microwave assisted reduce graphene oxide (rGO-M) to evaluate their surface, thermal, and structural characteristics. Thermogravimetric analysis (TGA; PerkinElmer STA 6000) assesses the thermal stability of these materials by monitoring weight loss as temperature increases, revealing the breakdown of GO's oxygen-containing functional groups. The surface morphology of both materials is visualized using field emission scanning electron microscopy (FESEM; Carl Zeiss Sigma 300), producing higher-resolution images of rGO's crumpled sheets that emphasize surface defects and a reduction in oxygen groups. Atomic-level images of the crystallinity and layer stacking in GO and rGO are obtained by high-resolution transmission electron microscopy (HRTEM; JEOL JEM-2100), which also confirms exfoliation and the restoration of graphitic domains in rGO-M, along with any defects that affect adsorption and conductivity. Functional groups are identified using Fourier-transform infrared spectroscopy (FTIR; PerkinElmer Spectrum Two). A CHNSO analyzer (PerkinElmer 2400 Series II) was used to perform an elemental analysis of the samples in order to ascertain the weight percentages of carbon (C), hydrogen (H), nitrogen (N), sulfur (S), and oxygen (O). X-ray diffraction (XRD; Malvern Panalytical X'Pert Pro) analysis reveals crystallinity, with rGO-M shifting to a peak near 26° , indicating a return to the graphitic structure, while GO shows a peak around $10\text{--}12^\circ$ due to increased interlayer spacing from oxygen. Additionally, Raman spectroscopy (LabRAM HR Evolution, HORIBA Scientific) is employed to analyze the structural properties of these materials [18].

2.4. Wastewater treatment using rGO & rGO-M

This process evaluates how well rGO and rGO-M treat wastewater that contains a range of contaminants. The pH, conductivity, turbidity, total hardness, calcium hardness, magnesium hardness, chloride, iron, and total organic carbon are the first important parameters used to characterize the wastewater sample. At specified dosages, rGO and rGO-M are added to the wastewater. Experiments on batch adsorption are conducted in controlled environments with systematic variations in parameters such as temperature and contact time. By comparing initial and final values using adsorption studies, the reduction in pollutant concentrations, such as total hardness, calcium hardness, and organic carbon, is calculated. For every parameter, the efficiency of rGO and rGO-M in enhancing water quality is contrasted with industry standards

for potable water [19].

2.5. Oil spill remediation using rGO & rGO-M

The purpose of the oil spill remediation experiments is to assess rGO and rGO-M's oil absorption capacities. In these experiments, toluene is mixed with crude oil to simulate an oil spill. The capacities of rGO and rGO-M (0.5 g/L, 1.0 g/L, and 1.5 g/L) to absorb oil are added to toluene and their absorption rate is tracked over time. To mimic various environmental scenarios, the salinity and temperature of the experiment are changed. Weighing the adsorbents both before and after absorption allows us to determine the oil content gravimetrically. After exposure, the rGO and rGO-M with absorbed oil are extracted from the toluene. The performance of rGO and rGO-M is compared, and the oil absorption capacity is computed [20,21].

2.6. Adsorption studies for wastewater treatment of rGO & rGO-M

To ascertain its potential for pollutant removal, the adsorption effectiveness of microwave-treated reduced graphene oxide (rGO-M) in wastewater treatment was thoroughly assessed [22]. Using the following Eq. 1, the adsorption capacity (q_e) was determined:

$$q_e = \frac{(C_i - C_e) * V}{m} \quad (1)$$

where V is the wastewater volume, C_e is the equilibrium concentration following treatment, C_i is the contaminant's initial concentration, and m is the adsorbent's mass. In the experiments, different doses of rGO & rGO-M (0.5 g/L, 1.0 g/L, and 1.5 g/L) were used. Total hardness and total organic carbon (TOC) concentrations in wastewater samples were measured at the outset. To measure the concentrations of pollutants, controlled adsorption experiments were carried out with samples taken on a regular basis.

2.7. Adsorption studies of rGO-M in oil spill remediation

To determine rGO & rGO-M's adsorption capacity for oil spill remediation, an oil-toluene mixture is first made in a specified volume, typically 100 mL, at a known concentration. The oil's maximum absorbance wavelength is determined by measuring the initial oil concentration (C_o) using spectrophotometric techniques [23]. A known mass of rGO & rGO-M is added, and the mixture is then allowed to stand for predetermined amounts of time. At every interval, a sample is taken, and the ultimate oil concentration (C_t) is calculated. To find out how much oil rGO has adsorbed, use Eq. 2a as follows:

$$\frac{(C_o - C_t) * V}{m} \quad (2a)$$

where V is the volume of the mixture and m is the mass of rGO & rGO-M. Eq. 2b is used to calculate the removal efficiency (R). To guarantee accurate results, this procedure is repeated several times. The data is then analyzed to assess the adsorption kinetics and isotherms.

$$\frac{(C_o - C_t)}{C_o} \times 100 \quad (2b)$$

2.8. Optimization of rGO-M using Box-Behnken Design (BBD)

Three crucial factors are being optimized for rGO-M synthesis using BBD: exposure duration, lowering agent concentration, and microwave power. Maximizing reduction efficiency while minimizing defects is the aim. The variables include the following: 30 s of exposure time, and 200 W of microwave power. Response surface methodology (RSM) is used to optimize rGO-M's conductivity, surface area, and reduction [24]. To evaluate factor significance and interactions, statistical analysis, such as ANOVA, is conducted using Design Expert software (trial

version 15). Response surfaces increase the surface area and adsorption efficiency of rGO-M by identifying ideal conditions. The effectiveness of cleaning up oil spills is the response in this instance. The reliability and accuracy of the model are validated.

3. Results and discussion

3.1. Characterization studies

A thorough comparison of the functional group changes between graphite, graphene oxide (GO), reduced graphene oxide (rGO) and reduced graphene oxide with microwave assistance (rGO-M) is given by the FTIR spectra in Fig. 2. Graphite has very few peaks, suggesting that it is in its pure state with very few functional groups that incorporate oxygen. The oxidation process results in the appearance of significant O-H ($\sim 3400\text{ cm}^{-1}$), C-H ($\sim 2900\text{ cm}^{-1}$), C=O ($\sim 1720\text{ cm}^{-1}$), and C-O-C ($\sim 1100\text{ cm}^{-1}$) peaks, which indicate the addition of epoxy, hydroxyl, and carbonyl groups. These oxygen functionalities, particularly the carbonyl and hydroxyl groups, are significantly reduced in rGO-M, which is created by microwave reduction, indicating a successful partial restoration of the graphitic structure [25–27]. The FTIR analysis indicates that both rGO and rGO-M undergo partial restoration of the sp² carbon framework during the reduction process. Notably, rGO exhibits a relative decrease in hydroxyl functionalities compared to GO, although some are still present. In contrast, rGO-M shows a more significant reduction in carbonyl groups. These observations suggest subtle differences in the mechanisms of the two materials, with rGO being more effective at reducing hydroxyl groups and rGO-M showing enhanced removal of carbonyl functionalities.

There are notable variations in the carbon, hydrogen, nitrogen, sulfur, and oxygen content of the samples, including graphite, GO, rGO, and rGO-M, according to the elemental composition analysis (Table 1). Graphite is confirmed to be crystalline by its almost pure carbon content (99.99 %), minimal nitrogen concentration (0.01 %), and lack of hydrogen, sulfur, or oxygen. On the other hand, GO exhibits a significant drop in carbon content to 47.04 %, along with a high oxygen content (46.3 %) and a C/O ratio of 1.03, which suggests the presence of a variety of functional groups that contain oxygen. The oxidation process is further supported by the increases in sulfur (2.57 %), nitrogen (0.25 %), and hydrogen (3.84 %). After reduction, the carbon content of rGO shows a notable rebound to 91.81 %, while the oxygen content decreases to 5.60 %, increasing the C/O ratio to 16.39. Sulfur (0.84 %) and

nitrogen (0.94 %) indicate that these elements were included throughout the reduction process. The compound rGO-M has the lowest oxygen concentration (0.31 %) and the highest carbon content (96.18 %). Its C/O ratio of 310.26 indicates advanced reduction and modification. The higher sulfur (0.75 %) and hydrogen (2.76 %) in rGO-M suggest more functionalization. The transition from highly oxidized GO to more reduced forms is reflected in the changes in the C/O ratio between the samples. rGO-M exhibits the most advanced reduction, making it a potential material for applications requiring high conductivity and low oxygen content. Elemental analysis confirms that the synthesized graphite contains 99.99 % carbon with no detectable sulfur, indicating effective removal of VGO-derived impurities during high-temperature treatment.

The FESEM suggest how the morphological changes brought about by oxidation and reduction processes progressed from graphite to GO, rGO and rGO-M. The smooth, densely packed, and well-organized layers seen in graphite's pristine lamellar structure are depicted in Fig. 3(a). This order is upset by the addition of functional groups containing oxygen during the oxidation process, giving rise to the collapsed sheet-like morphology of GO in Fig. 3(b). The functionality of the carbon lattice, which presents strain and defects in the structure, is responsible for the increase in surface roughness and wrinkle appearance [28]. As shown in Fig. 3(c), the reduction of GO to rGO preserves some degree of exfoliation while only partially restoring the layered structure. This can be attributed to the elimination of oxygenated species, which preserves surface area for adsorption purposes while enabling the sheets to regain some structural cohesiveness more in rGO-M (Fig. 3d) than rGO [29]. Because of its improved adsorption capabilities, the resulting morphology plays a critical role in improving the material's use in environmental applications.

The XRD patterns in Fig. 4(a-d) illustrate the diffraction peaks corresponding to graphitic materials with varying levels of crystallinity and structural order. Fig. 4(a) represents graphite, where the prominent peak around 26° (20), indicative of the characteristic layered structure. The interlayer spacing and the hexagonal structure of graphite are further supported by distinct peaks at 44° and 77° showing moderate crystallinity. The sharp (002) diffraction peak observed around 26° (20) in graphite and rGO-M indicates a well-ordered layered structure. This peak was used to calculate the interlayer spacing. Fig. 4(b), representing GO, shows broader and less intense peaks, suggesting disruption of the graphitic layers due to oxidation, leading to an increased interlayer spacing and structural defects. Fig. 4(c) shows rGO, where the peaks are slightly sharper than those of GO, indicating partial restoration of the graphitic structure. However, the peaks are still broad, reflecting residual defects and disorder [30,31]. Lastly, Fig. 4(d) for rGO-M exhibits even sharper and more intense peaks, indicating a higher degree of crystallinity and better stacking order compared to rGO, demonstrating that microwave-assisted reduction more effectively restores the graphitic structure. These patterns illustrate a progressive recovery of graphitization, with graphite being the most crystalline (Fig. 4a) and GO the most disordered (Fig. 4b), while rGO (Fig. 4c) and rGO-M (Fig. 4d) show varying degrees of structural restoration. On the other hand, Table 2 displays the d-spacing values for GO, rGO, Graphite, and rGO-M. The organized structure of graphite is typified by its d-spacing of 3.3858 Å. Because of oxidation, GO has a substantially bigger d-spacing (7.6974 Å). Following reduction, rGO (3.6091 Å) and rGO-M (3.3960 Å) show decreasing d-spacing, with rGO-M being closer to pristine graphite, suggesting that microwave-assisted reduction improved structural restoration.

TGA curves in Fig. 5 illustrate the thermal stability of rGO-M in comparison to graphite, GO and rGO, providing significant information about the material. Similar to rGO-M, rGO has enhanced thermal stability in comparison to GO; however, it displays a unique pattern of thermal deterioration. Compared to rGO-M, rGO shows a more noticeable weight loss, especially between 200°C and 800°C , indicating that it keeps more oxygen-containing functional groups following reduction.

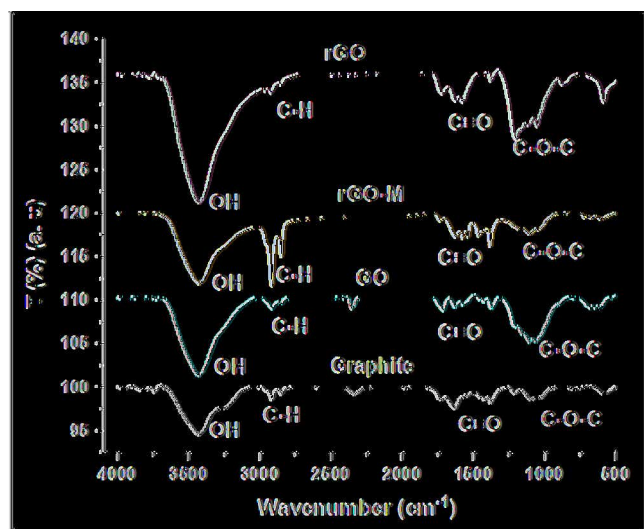


Fig. 2. FTIR spectra of graphite, GO, rGO, and rGO-M showing functional group transformations. GO displays oxygenated groups due to oxidation, while reduced peak intensity in rGO and rGO-M confirms successful reduction.

Table 1
Elemental composition of Graphite, GO, rGO, and rGO-M.

Sample	Carbon %	Hydrogen %	Nitrogen %	Sulphur %	Oxygen %	C/O Ratio
Graphite	99.99	0.00	0.01	0.00	0.00	-
GO	47.04	3.84	0.25	2.57	46.30	1.02
rGO	91.81	0.81	0.94	0.84	5.60	16.39
rGO-M	96.18	2.76	0.00	0.75	0.31	310.26

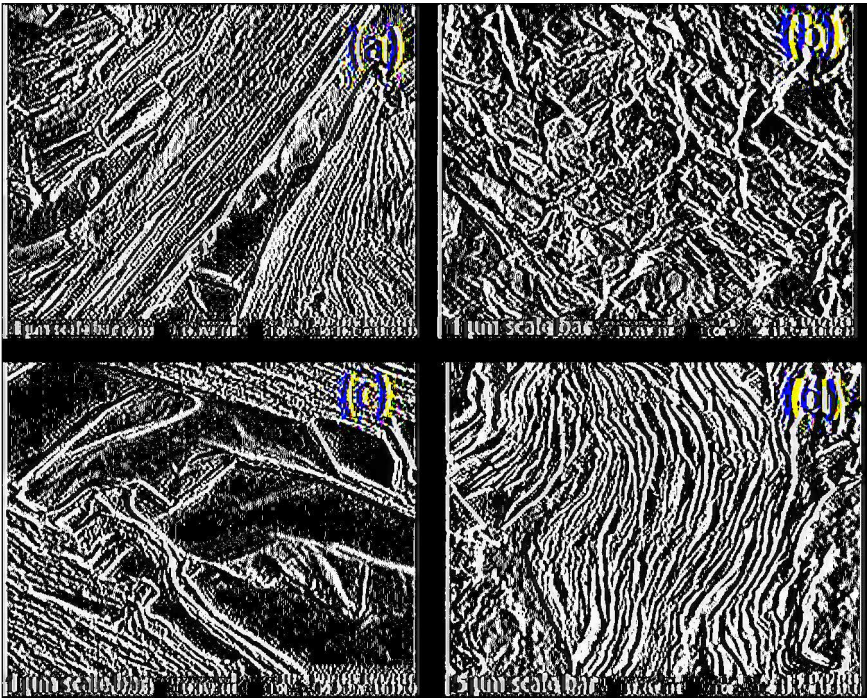


Fig. 3. FESEM images showing the morphological evolution: (a) graphite; (b) GO; (c) rGO and (d) rGO-M.

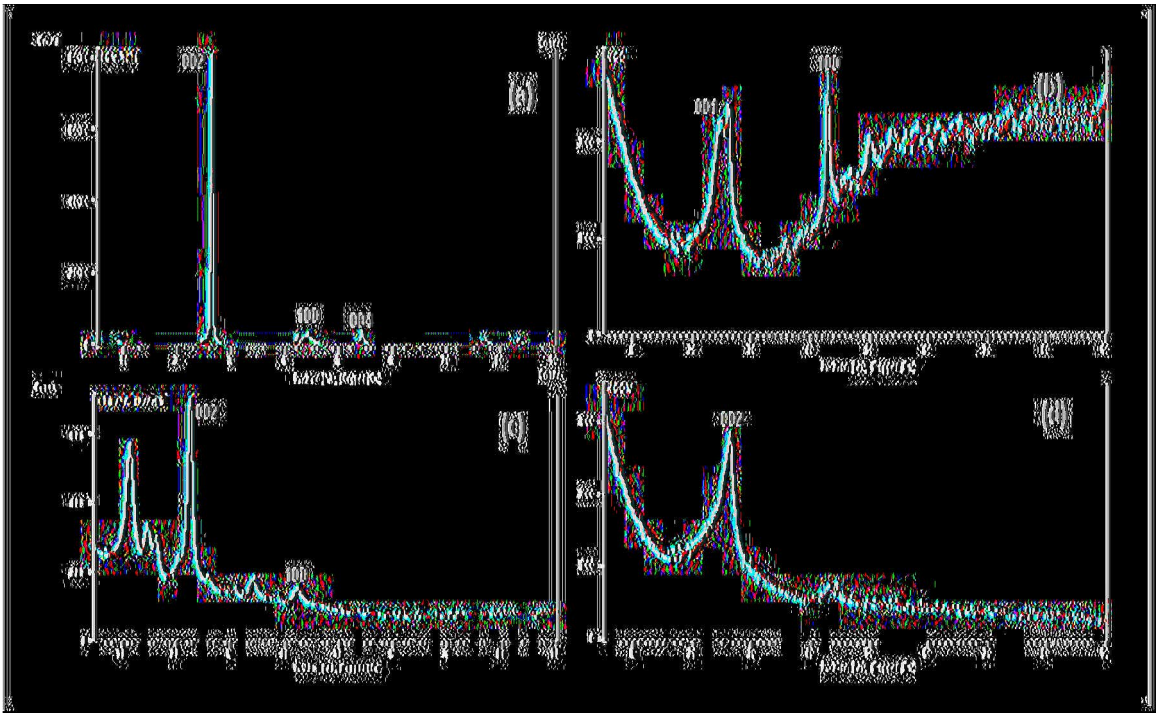


Fig. 4. X-ray diffraction (XRD) patterns of samples (a) Graphite, (b) GO, (c) rGO and (d) rGO-M.

Table 2

d-spacing values for Graphite, GO, RGO, and RGO-M, highlighting changes due to oxidation and reduction processes.

Samples	d-spacing [Å]
Graphite	3.3858
GO	7.6974
rGO	3.6091
rGO-M	3.3960

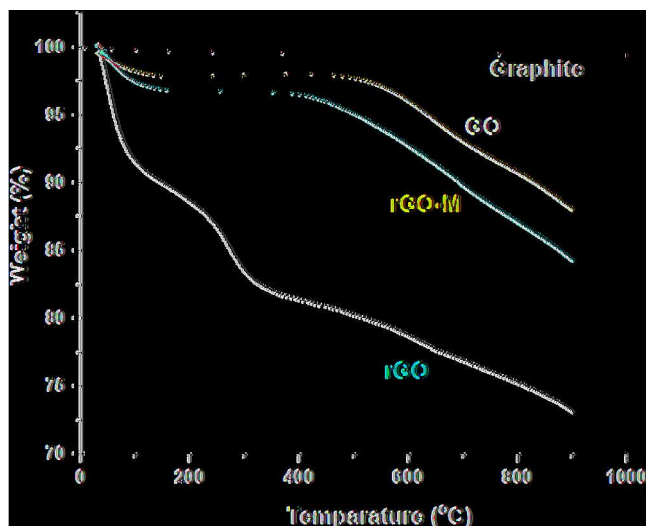


Fig. 5. TGA curves of graphite, GO, rGO, and rGO-M.

This suggests that, in comparison to rGO-M, the reduction process for rGO may not have been as successful in eliminating these groups. As a result of its more effective restoration of the sp^2 carbon network, rGO-M exhibits greater thermal stability when compared to other materials. In the same temperature range, rGO-M loses weight far less than rGO, indicating that the latter may still have more structural flaws and oxygen

functions that could jeopardize thermal stability [32,33]. As a result, although both rGO samples have better thermal characteristics than GO, rGO-M shows greater thermal resilience because functional groups are removed and reduced more successfully, giving it a better option for applications needing greater thermal stability.

The structural changes of graphitic carbon during the stages of GO, rGO, and rGO-M were examined by HRTEM (High-Resolution Transmission Electron Microscopy) analysis, as shown in Fig. 6. The crystalline and highly organized structure of pristine graphitic carbon (Fig. 6 (a)) with well-aligned carbon layers and few imperfections indicates robust graphitization. On the other hand, Fig. 6(b) illustrates GO, where the graphitic layers are severely disrupted and exfoliated by the oxidation process [34,35]. This results in disorderly and loosely packed structures because oxygen-containing functional groups like carboxyl, hydroxyl, and epoxide are introduced, amplifying interlayer spacing and improving chemical reactivity. The morphology of rGO, which is characterized by folds and wrinkles that may have an impact on its electrical conductivity, (Fig. 6(c)) shows a partial restructuring of the graphitic layers but retains a large amount of disorder and oxygen functions. On the other hand, rGO-M following microwave-assisted reduction is shown in Fig. 6(d), where the structure shows a significant restoration of the sp^2 -hybridized carbon network as well as more effective reorganization. While part of the defects and structural distortions common to materials created by microwaves is still present in rGO-M, the reduction effectively eliminates a large number of oxygen functional groups, increasing the material's electrical conductivity [36]. These structural modifications emphasize the benefits of using microwave-assisted reduction to produce functional graphene materials and place rGO-M in a favourable position for a range of environmental applications needing high conductivity and surface area.

The structural history of graphite, GO, rGO, and rGO-M may be clearly compared using the Raman spectra in Fig. 7. The D and G bands in graphite are distinct and crisp, signifying the material's high crystallinity and low defect content. On the other hand, GO exhibits wide, noticeable D ($\sim 1350\text{ cm}^{-1}$) and G ($\sim 1580\text{ cm}^{-1}$) bands, which indicate significant structural instability brought about by the addition of functional groups containing oxygen [37]. Both rGO and rGO-M exhibit sharper D and G bands after reduction, indicating a partial restoration of the graphitic structure; however, rGO-M has a more pronounced peak

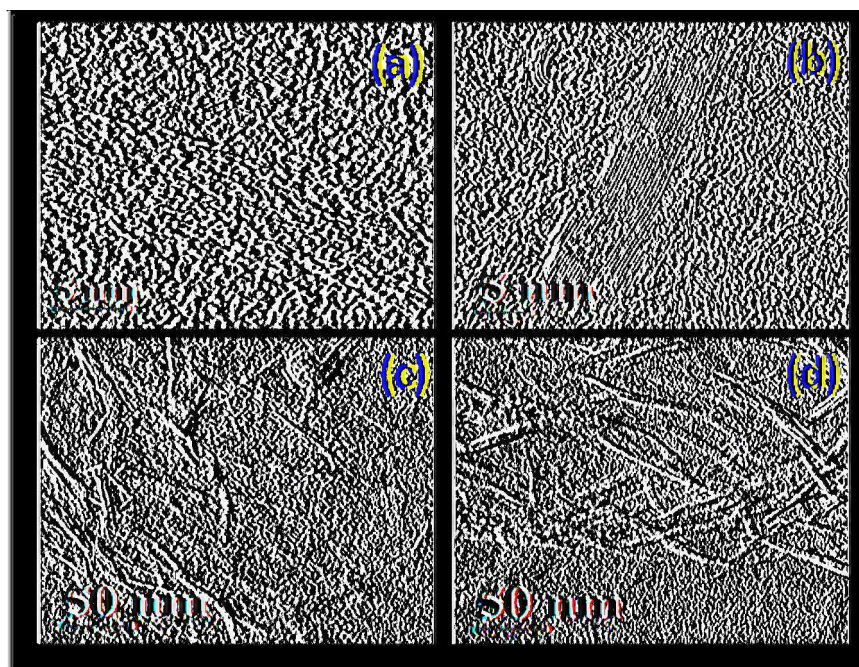


Fig. 6. HRTEM of (a) graphitic carbon, (b) GO, (c) rGO and (d) rGO-M.

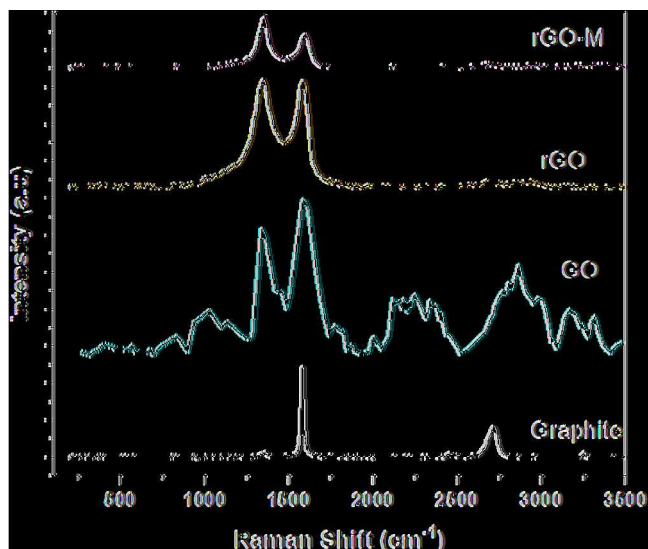


Fig. 7. Raman spectra of graphite, GO, rGO, and rGO-M. Sharper peaks in rGO-M indicate more effective reduction and restoration of the sp^2 carbon network compared to rGO and GO.

profile, indicating that microwave-assisted reduction, as opposed to heat treatment, more successfully restores the sp^2 carbon network while reducing defects. Table 3 also shows the placements of the D- and G-bands, their corresponding intensities, and the intensity ratio (ID/IG), which shows how disordered the carbon structure is. The lowest ID/IG ratio (0.05) in graphite indicates a well-ordered structure. The greater ID/IG ratio (0.82) of GO suggests more oxidation-related problems. The graphitic structure has partially recovered in rGO, as evidenced by its ID/IG ratio of 1.01. In contrast, rGO-M exhibits a higher ID/IG ratio of 1.52, suggesting that microwave-assisted reduction introduces more defects and edge sites due to rapid energy input. These structural alterations, consistent with the morphology observed in FESEM images, can enhance surface reactivity, making rGO-M more effective for adsorption-based applications.

The pore size distribution and porous structure of rGO and rGO-M were characterized by N_2 adsorption-desorption isotherms. Fig. 8 displays the corresponding BET plots of the two materials. The isotherms (Fig. 8a and Fig. 8c) show a typical type IV profile with a clear hysteresis loop at high relative pressures, indicating the existence of mesopores and macropores. The surface area of rGO-M was found to be $30 \text{ m}^2 \text{ g}^{-1}$ with a micropore volume of $0.04 \text{ cm}^3 \text{ g}^{-1}$, whereas rGO had a considerably higher surface area of $100 \text{ m}^2 \text{ g}^{-1}$ and a micropore volume of $0.14 \text{ cm}^3 \text{ g}^{-1}$. The higher micropore volume in rGO indicates a greater micropore density, while rGO-M showed a higher proportion of mesopores (2–50 nm) and macropores (>50 nm), as illustrated in the pore size distribution profiles (Fig. 8b and d). Such pore architecture is more favourable for adsorbing larger organic molecules than micropores, as supported by prior studies [38]. This structural development in rGO-M increases its application potential for wastewater treatment and oil spill cleanup, as meso/macropores allow for ion diffusion and fast adsorption, whereas micropores are mainly responsible for surface area

Table 3

Raman spectroscopy data of Graphite, GO, rGO, and rGO-M, showing D-band and G-band positions, intensities, and the ID/IG ratio.

Sample Details	D- Band Position	D- Band Intensity	G- Band Position	G- Band Intensity	ID/IG
Graphite	1358.6	6.1	1580.8	121.4	0.05
GO	1337.9	177.9	1582.4	216.3	0.82
rGO	1345.9	145.0	1583.9	143.1	1.01
rGO-M	1350.6	65.9	1594.7	43.5	1.52

without enhancing accessibility much for adsorption processes.

3.2. Adsorption efficiency of rGO & rGO-M in wastewater treatment

Adsorption experiments aimed at different contaminants were conducted to assess the effectiveness of rGO-M in wastewater treatment. Important parameters found in the initial characterization of the wastewater included pH (13.8), conductivity ($12,950 \mu\text{S}/\text{cm}$), turbidity (187 NTU), total hardness (170 ppm), calcium (66 ppm), magnesium (104 ppm), iron (0.3 ppm), chloride (250 ppm), and total organic carbon (TOC, 22.74 ppm). To evaluate their adsorption capacities, heat-treated rGO and rGO-M were added to the wastewater at doses of 0.5 g/L, 1.0 g/L, and 1.5 g/L. In order to maximize the removal of pollutants, batch adsorption experiments were carried out under carefully monitored circumstances, adjusting variables like temperature and contact time. Samples were taken periodically to track drops in the concentrations of pollutants.

The outcomes showed that rGO-M performed better than rGO at every tested dosage, exhibiting greater removal efficiencies for TOC, calcium hardness, magnesium hardness, and total hardness. At 1.0 g/L, for instance, rGO-M reduced total hardness and calcium hardness by 80 % and 85 %, respectively, at a dosage higher than rGO's 70 % and 75 %. Furthermore, rGO-M recorded a 60 % reduction in TOC, compared to rGO's 55 % reduction. Additionally highlighting rGO-M's exceptional performance was the calculation of its adsorption capacity at 1.0 g/L dosage, which came out to be 136 mg/g for total hardness and 13.65 mg/g for TOC. At the highest dosage of 1.5 g/L, rGO-M accomplished outstanding reductions of 85 % in total hardness as well as 61 % in TOC. These results demonstrate the enhanced adsorption efficacy of rGO-M, which is an intriguing material for wastewater treatment and environmental remediation applications due to its greater surface area and functional groups developed during microwave treatment.

3.3. Oil spill remediation performance

The Fig. 9 compares the stages of oil spill remediation using rGO-M in the presence of toluene, highlighting both qualitative and quantitative aspects of the process. In Fig. 10 (a), the initial oil is dispersed across the toluene's surface, simulating a spill with visible patches of floating oil. After the introduction of rGO-M in Fig. 10(b), dark areas form as the rGO begins to selectively adsorb the oil, significantly reducing the visible oil on the surface. The oil adsorption capacity of rGO was calculated to be 190 mg of oil/g of rGO-M, demonstrating 85 % removal efficiency within 30 min. By Fig. 10(c), most of the oil has been absorbed by the rGO-M, with the surface appearing clearer and a scraping tool indicating the collection of the rGO-M-oil aggregate. Finally, in Fig. 10 (d), the water is almost clear, with the oil-toluene mixture largely removed by the rGO, which has formed a dark clump. This progression illustrates the effectiveness of rGO-M in adsorbing and removing oil from the toluene mixture, demonstrating its potential for oil spill remediation in organic solvent environments.

3.4. Adsorption studies of rGO in oil spill remediation

The quantity of oil adsorbed (mg/g rGO-M) as a function of contact time (minutes) is shown in Fig. 11(a). The data demonstrate a notable increase in oil adsorption over time, with a peak of about 190 mg/g at 30 min, following a rapid rise from 0 mg/g at 0 min to 80 mg/g at 1 min. The pattern shows that rGO-M has quick adsorption, especially in the first few minutes, and then the rate of increase starts to slow down, indicating that saturation is approaching. The oil removal efficiency (%) over the same contact times is shown in Fig. 11(b). At 0 min, the removal efficiency is 0 %; after 1 min, it rises to 40 %; by 5 min, it reaches 85 %; and at 30 min, it reaches 95 %. The adsorption data and the steady increase in removal efficiency support the effectiveness of rGO-M in rapidly eliminating oil impurities from the solution. Taken as a whole,

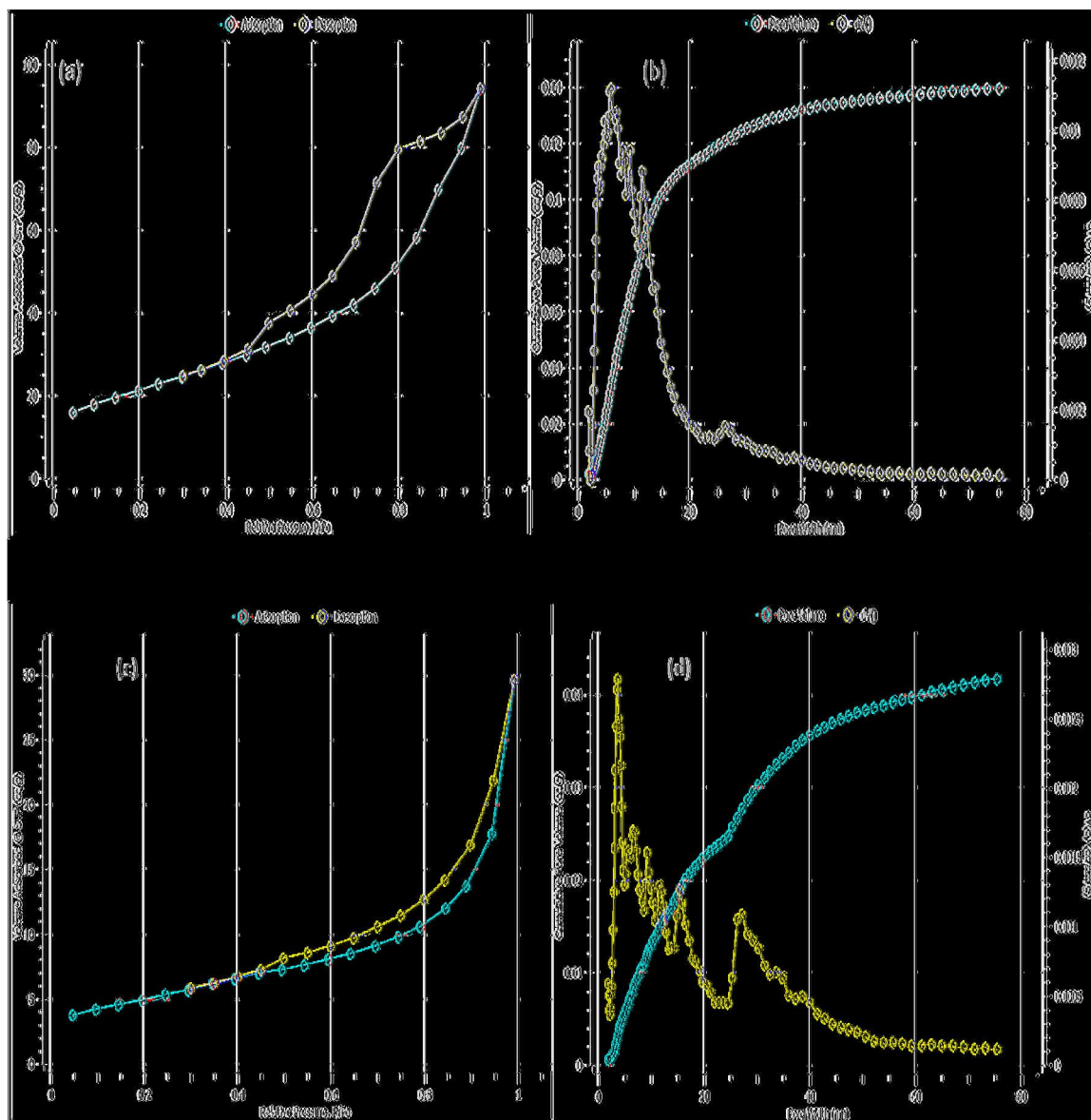


Fig. 8. N_2 adsorption-desorption isotherms and pore size distribution of rGO and rGO-M.

these graphs demonstrate the effectiveness of rGO-M as a potential adsorbent for cleaning up oil spills, showcasing its quick adsorption kinetics and high removal efficiency.

3.5. Optimization of rGO-M synthesis using Box-Behnken Design (BBD)

Using Design Expert software, the synthesis of rGO-M was optimized by analyzing the removal efficiency of pollutants in a wastewater treatment process using a quadratic model. With a Model F-value of 30.18 and a p-value of less than 0.0001, the quadratic model assessing the removal efficiency's ANOVA results show that the model is significant. This implies that the factors and interactions under investigation can account for the variances in removal efficiency that have been observed. Microwave power (A), exposure time (B), and reducing agent concentration (C), along with their interactions (AB, AC, BC) and quadratic terms (A^2 , B^2 , C^2), are the factors that are tested. The p-values less than 0.0500 indicate that the following factors are significant: microwave power (A), exposure time (B), reducing agent concentration (C), the interaction between reducing agent concentration and exposure time (BC), and the quadratic term for microwave power (A^2). According

to the significant interaction term BC, maximizing removal efficiency requires a combination of lowering agent concentration and exposure time. However, with p-values higher than 0.1000, it was discovered that interactions AB and AC as well as B^2 and C^2 were not significant.

Strong correlation between observed and predicted values is shown by the model fit statistics, which show an adjusted R^2 of 0.9426 and a R^2 value of 0.9749. The adjusted R^2 and the predicted R^2 of 0.7835 agree well, indicating that the model can produce accurate predictions within the design space. The model's precision is further highlighted by its low standard deviation (1.5409) and high coefficient of variation (C.V.) of 1.726 %. A strong signal-to-noise ratio is indicated by the Precision value of 20.691, which is significantly higher than the 4 thresholds, indicating that the model is robust for navigating the design space 3D response surface plots in Fig. 12(a–c) demonstrate how the response varies with these variables, demonstrating the effects of microwave power, exposure time, and reducing agent concentration on removal efficiency [39]. These plots show that a moderate concentration of the reducing agent combined with an increase in microwave power and exposure time improves removal efficiency. A two-dimensional depiction of the same data is given by the contour plots in Fig. 12(d–f), which

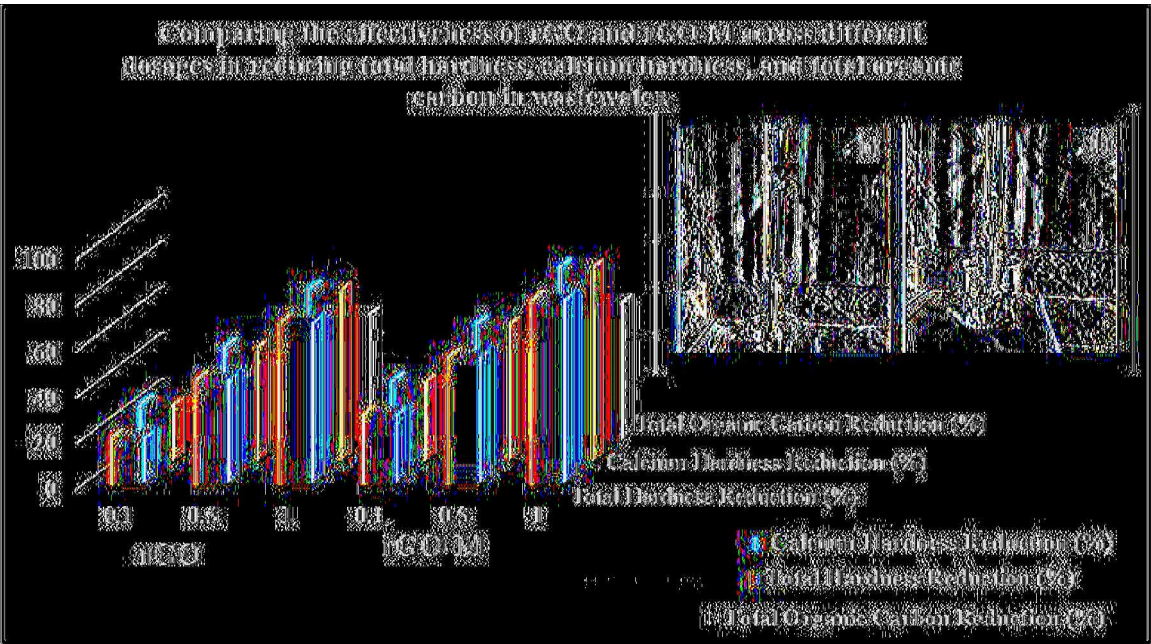


Fig. 9. Comparing the effectiveness of rGO and rGO-M across different dosages in reducing total hardness, calcium hardness, and total organic carbon in wastewater. Insight showing Adsorption capacity of (a) rGO treated wastewater and (b) rGO-M treated wastewater Treated with rGO-M Showing Improved Water Quality.

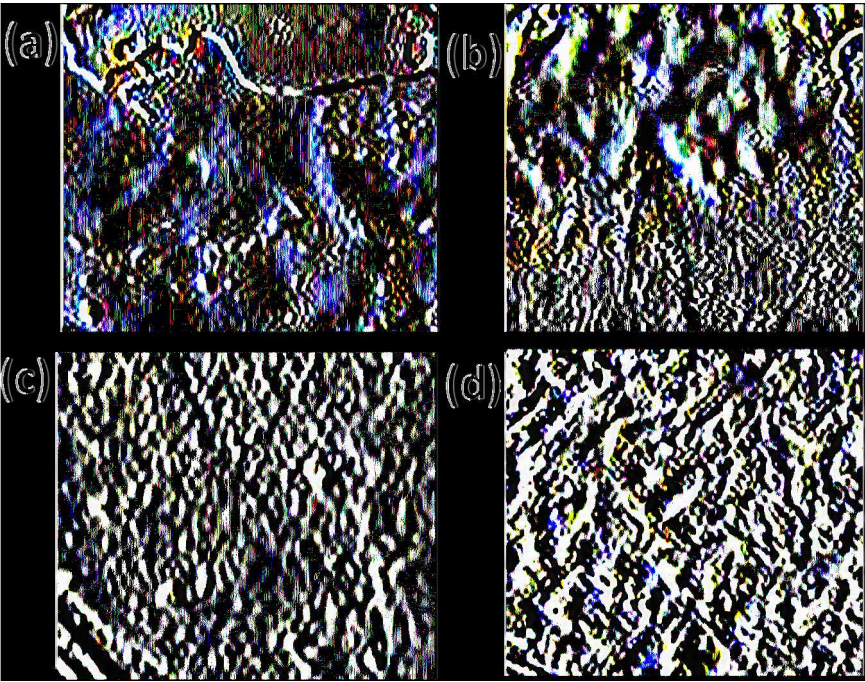


Fig. 10. Stages of oil spill remediation using rGO-M in toluene. (a) Initial oil patches on the surface. (b) rGO-M adsorbs oil, reducing visible oil. (c) Surface clears as rGO-M absorbs more oil. (d) Toluene is nearly clear, with rGO-M forming a dark clump. Adsorption capacity: 190 mg oil/g, 85 % removal in 30 min.

highlight the interactions between the variables and pinpoint the ideal circumstances for maximum efficiency. With a significance level of less than 0.001, the model demonstrated strong confidence in the effects that were observed.

3.6. Mechanism of GO to rGO-M

A number of crucial processes that take advantage of GO's special dielectric qualities are involved in the mechanism by which GO produces rGO-M. The polarity of graphene oxide (GO) allows for energy

absorption under 2.45 GHz microwave radiation, which selectively excites the functional groups that contain oxygen that are affixed to the graphene sheets. The removal of these functional groups and the restoration of graphene's conjugated carbon network characteristic are made possible by the selective heating that accelerates the cleavage of carbon-oxygen bonds [40]. Zhao *et al.* (2021) reported that the GO sample exhibits consistent reduction throughout due to the uniform energy distribution achieved through microwave-assisted heating, which ultimately produces high-quality rGO-M with enhanced electrical conductivity [41]. Furthermore, side reactions that might introduce

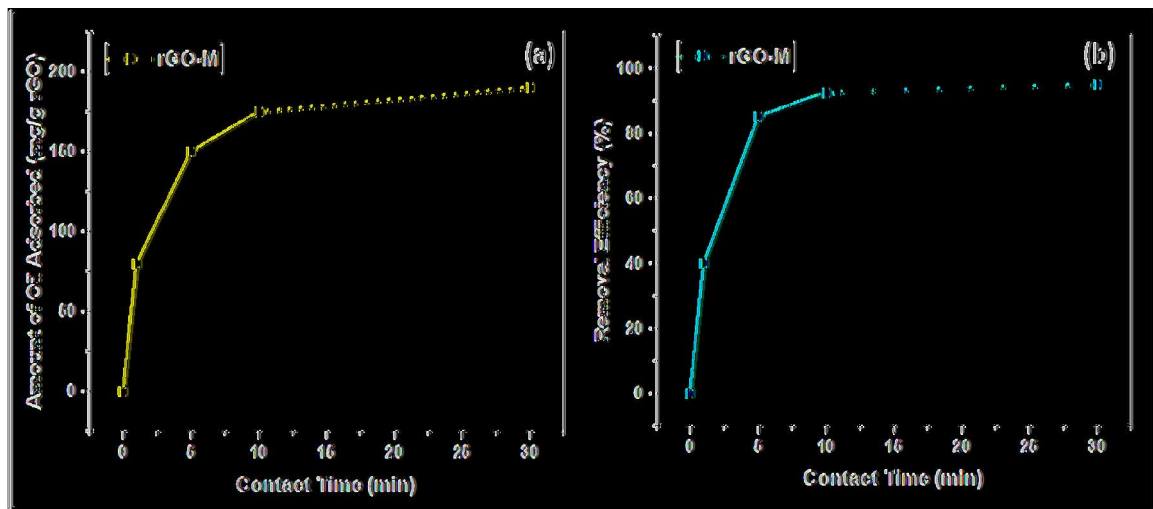


Fig. 11. Adsorption performance of rGO-M for oil spill remediation (a) oil Adsorbed vs time and (b) Removal efficiency vs time.

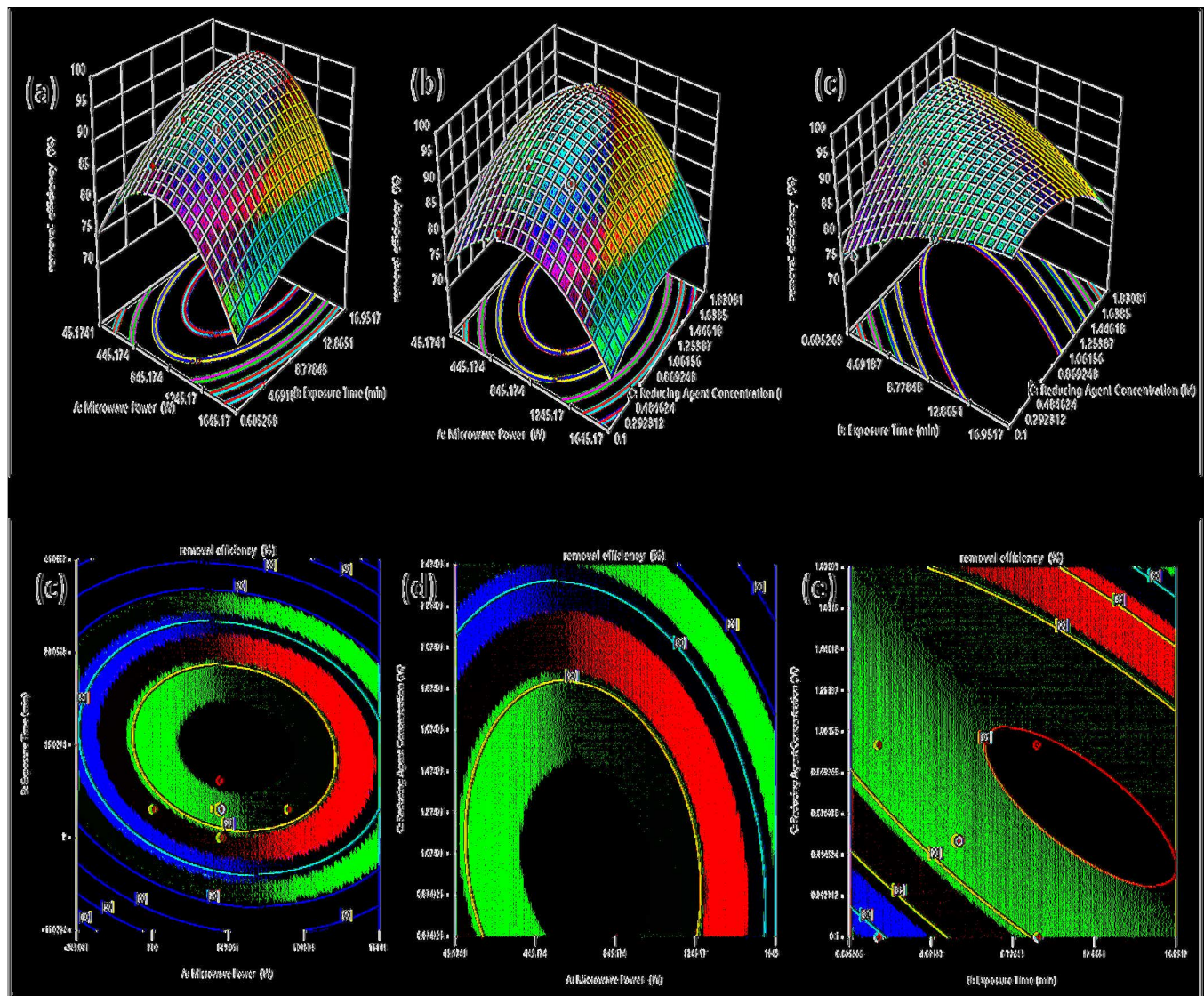


Fig. 12. (a-c) 3D response surface plots showing the effects of microwave power, exposure time, and reducing agent concentration on removal efficiency. Increasing microwave power and exposure time, with moderate reducing agent concentration, enhances efficiency. (d-f) Contour plots highlighting the interaction effects between the variables, identifying optimal conditions for achieving maximum removal efficiency.

defects or impurities are reduced in the controlled microwave environment, resulting in an improved rGO-M product with enhanced surface area and better adsorption capabilities. This makes it appropriate for a variety of applications, especially environmental remediation processes.

4. Conclusion

This work offers a practical way to use the plentiful carbon resources in VGO to create high-performance microwave based reduced graphene oxide (rGO-M) with enhanced adsorption capabilities. The BBD optimization method greatly increased the efficiency of pollutant removal, with rGO-M exhibiting exceptional efficacy in eliminating TOC and total hardness from wastewater. Its potential for resolving global issues like oil spills is further highlighted by its capacity to absorb oil quickly and effectively. rGO-M is more active than rGO due to its unique reduction mechanism and energy-efficient process. This study uniquely demonstrates the sustainable synthesis of rGO-M from VGO with optimized microwave parameters, achieving up to 95 % oil removal efficiency and 85 % total hardness reduction, highlighting its adsorption performance. These characteristics make rGO-M a superior option compared to traditional reduction methods. Moreover, the microwave treatment used in its production is a scalable process for GO reduction, offering a promising solution to environmental challenges such as oil spills and water pollution. This finding paves the way for further investigation of graphene-based materials in a range of environmental applications by developing sustainable pollution management solutions.

CRedit authorship contribution statement

Hasmukh Gajera: Writing – review & editing, Supervision, Resources, Project administration, Methodology, Conceptualization. **Ravi Dalsania:** Writing – original draft, Visualization, Validation, Software, Methodology, Investigation, Formal analysis, Data curation, Conceptualization. **Mahesh Savant:** Writing – review & editing, Visualization, Supervision, Project administration, Data curation, Conceptualization.

Funding

This research did not receive any specific grant from funding agencies in the public, commercial, or not-for-profit sectors.

Declaration of Competing Interest

The authors declare the following financial interests/personal relationships which may be considered as potential competing interests: Ravi Dalsania reports administrative support and writing assistance were provided by Atmiya University. Ravi Dalsania reports a relationship with Reliance Industries Limited that includes: employment. If there are other authors, they declare that they have no known competing financial interests or personal relationships that could have appeared to influence the work reported in this paper.

Data Availability

Data will be made available on request. The datasets generated and analysed during the current study are available from the corresponding author on reasonable request.

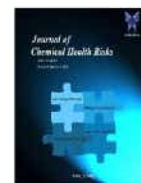
References

- [1] Hader DP, Banaszak AT, Villafañe VE, Narvarte MA, González RA, Helbling EW. Anthropogenic pollution of aquatic ecosystems: emerging problems with global implications. *Sci Total Environ* 2020;713:136586. <https://doi.org/10.1016/j.scitotenv.2020.136586>.
- [2] Huang G, Ng TW, Chen H, Chow AT, Liu S, Wong PK. Formation of assimilable organic carbon (AOC) during drinking water disinfection: a microbiological

prospect of disinfection byproducts. *Environ Int* 2020;135:105389. <https://doi.org/10.1016/j.envint.2019.105389>.

- [3] Yang H, Ye S, Wang J, Wang H, Wang Z, Chen Q, et al. The approaches and prospects for natural organic matter-derived disinfection byproducts control by carbon-based materials in water disinfection progresses. *J Clean Prod* 2021;311:127799. <https://doi.org/10.1016/j.jclepro.2021.127799>.
- [4] Mook WT, Chakrabarti MH, Aroua MK, Khan GMA, Ali BS, Islam MS, et al. Removal of total ammonia nitrogen (TAN), nitrate and total organic carbon (TOC) from aquaculture wastewater using electrochemical technology: a review. *Desalination* 2012;285:1–13. <https://doi.org/10.1016/j.desal.2011.09.029>.
- [5] Singh H, Bhardwaj N, Arya SK, Khatri M. Environmental impacts of oil spills and their remediation by magnetic nanomaterials. *Environ Nanotechnol Monit Manag* 2020;14:100305. <https://doi.org/10.1016/j.enmm.2020.100305>.
- [6] Ivshina IB, Kuyukina MS, Krivoruchko AV, Elkin AA, Makarov SO, Cunningham CJ, et al. Oil spill problems and sustainable response strategies through new technologies. *Environ Sci Process Impacts* 2015;17(7):1201–19. <https://doi.org/10.1039/c5em00070j>.
- [7] Onwurah I.N.E., Ogugua V.N., Onyike N.B., Ochonogor A.E., Otiotoju O.F. Crude oil spills in the environment, effects and some innovative clean-up biotechnologies. (<https://www.scirp.org/journal/jgis>).
- [8] Zhang B, Matchinski EJ, Chen B, Ye X, Jing L, Lee K. Marine oil spills—oil pollution, sources and effects. In: *World seas: an environmental evaluation*. Academic Press; 2019. p. 391–406. <https://doi.org/10.1016/B978-0-12-805052-1.00024-3>.
- [9] Fogassy G, Thegarid N, Toussaint G, van Veen AC, Schuurman Y, Mirodatos C. Biomass derived feedstock co-processing with vacuum gas oil for second-generation fuel production in FCC units. *Appl Catal B Environ* 2010;96(3–4):476–85. <https://doi.org/10.1016/j.apcatb.2010.03.008>.
- [10] El-Sawy MS, Hanafi SA, Ashour F, Aboul-Fotouh TM. Co-hydroprocessing and hydrocracking of alternative feed mixture (vacuum gas oil/waste lubricating oil/waste cooking oil) with the aim of producing high quality fuels. *Fuel* 2020;269:117437. <https://doi.org/10.1016/j.fuel.2020.117437>.
- [11] De Rezende Pinho A, de Almeida MB, Mendes FL, Casavechia LC, Talmadge MS, Kinchin CM, et al. Fast pyrolysis oil from pinewood chips co-processing with vacuum gas oil in an FCC unit for second-generation fuel production. *Fuel* 2017;188:462–73. <https://doi.org/10.1016/j.fuel.2016.10.032>.
- [12] Mahmoudabadi ZS, Rashidi A, Panahi M. Controlled growth of graphene on γ -Al₂O₃ as highly efficient nanocomposite support of NiMoW catalysts by engineering approaches of chemical vapor deposition technique for hydrotreating of vacuum gas oil. *Fuel* 2023;350:128778. <https://doi.org/10.1016/j.fuel.2023.128778>.
- [13] Mahmoudabadi ZS, Rashidi A. Hydrogen creation and carbon sequestration by fracking carbon dioxide. Sustainable utilization of carbon dioxide: from waste to product. Singapore: Springer Nature Singapore; 2023. p. 111–35. https://doi.org/10.1007/978-981-99-2890-3_5.
- [14] Titov EY, Bodrikov IV, Vasiliev AL, Ivanova AG, Golovin AL, Shirokov DA, et al. Low-carbon pyrolysis of vacuum gas oil by non-thermal plasma. *Plasma Process Polym* 2024:e240061. <https://doi.org/10.3390/fire7100344>.
- [15] Pinto FE, Silva CF, Tose LV, Figueiredo MA, Souza WC, Vaz BG, et al. Evaluation of adsorbent materials for the removal of nitrogen compounds in vacuum gas oil by positive and negative electrospray ionization Fourier transform ion cyclotron resonance mass spectrometry. *Energy Fuels* 2017;31(4):3454–64. <https://doi.org/10.1021/acs.energyfuels.6b02566>.
- [16] Amemiya M, Korai Y, Mochida I. Catalyst deactivation in distillate hydrotreating (part 2) Raman analysis of carbon deposited on hydrotreating catalyst for vacuum gas oil. *J Jpn Pet Inst* 2003;46(2):99–104. <https://doi.org/10.1627/jpi.46.99>.
- [17] Bai X, Zhai Y, Zhang Y. Green approach to prepare graphene-based composites with high microwave absorption capacity. *J Phys Chem C* 2011;115(23):11673–7. <https://doi.org/10.1021/jp202475m>.
- [18] Zhou S, Yin J, Ma Q, Baihetiyaer B, Sun J, Zhang Y, et al. Montmorillonite-reduced graphene oxide composite aerogel (M–rGO): a green adsorbent for the dynamic removal of cadmium and methylene blue from wastewater. *Sep Purif Technol* 2022;296:121416. <https://doi.org/10.1016/j.seppur.2022.121416>.
- [19] Li Y, Sun J, Liu L, Yang F. A composite cathode membrane with CoFe₂O₄–rGO/PVDF on carbon fiber cloth: synthesis and performance in a photocatalysis-assisted MFC-MBR system. *Environ Sci Nano* 2017;4(2):335–45. <https://doi.org/10.1039/C6EN00454G>.
- [20] Tewari BB. Critical reviews on engineered nanoparticles in environmental remediation. *Curr J Appl Sci Technol* 2019;36(4):1–21. <https://doi.org/10.9734/cjast/2019/v36i430242>.
- [21] Elhenawy S, Khraisheh M, AlMomani F, Hassan MK, Al-Ghouti MA, Selvaraj R. Recent developments and advancements in graphene-based technologies for oil spill cleanup and oil–water separation processes. *Nanomaterials* 2021;12(1):87. <https://doi.org/10.3390/nano12010087>.
- [22] Zoghi AM, Allahyari S. Multifunctional magnetic C₃N₄–rGO adsorbent with high hydrophobicity and simulated solar light-driven photocatalytic activity for oil spill removal. *Sol Energy* 2022;237:320–32. <https://doi.org/10.1016/j.solener.2022.04.005>.
- [23] Ai Y, Liu Y, Huo Y, Zhao C, Sun L, Han B, et al. Insights into the adsorption mechanism and dynamic behavior of tetracycline antibiotics on reduced graphene oxide (rGO) and graphene oxide (GO) materials. *Environ Sci Nano* 2019;6(11):3336–48. <https://doi.org/10.1039/C9EN00866G>.
- [24] Liu X, Li X, Liu X, He S, Jin J, Meng H. Green preparation of Ag–ZnO–rGO nanoparticles for efficient adsorption and photodegradation activity. *Colloids Surf A Physicochem Eng Asp* 2020;584:124011. <https://doi.org/10.1016/j.colsurfa.2019.124011>.

- [25] Rahnama F, Ashrafi H, Akhond M, Absalan G. Introducing Ag₂O-Ag₂CO₃/rGO nanoadsorbents for enhancing photocatalytic degradation rate and efficiency of Congo red through surface adsorption. *Colloids Surf A Physicochem Eng Asp* 2021; 613:126068. <https://doi.org/10.1016/j.colsurfa.2020.126068>.
- [26] Kaptanoğlu İG, Yuşan S. Adsorption performance of Pb (II) ions on green synthesized GO and rGO: isotherm and thermodynamic studies. *Environ Res Technol* 2022;5(3):257–71. <https://doi.org/10.35208/ert.1110373>.
- [27] Minitha CR, Lalitha M, Jeyachandran YL, Senthilkumar L, RK RT. Adsorption behaviour of reduced graphene oxide towards cationic and anionic dyes: Co-action of electrostatic and π - π interactions. *Mater Chem Phys* 2017;194:243–52. <https://doi.org/10.1016/j.matchemphys.2017.03.048>.
- [28] Thakur A, Kumar S, Rangra VS. Synthesis of reduced graphene oxide (rGO) via chemical reduction. *AIP Conf Proc* 2015;1661(1). <https://doi.org/10.1063/1.4915423>.
- [29] Sharma N, Sharma V, Jain Y, Kumari M, Gupta R, Sharma SK, et al. Synthesis and characterization of graphene oxide (GO) and reduced graphene oxide (rGO) for gas sensing application. *Macromol Symp* 2017;376(1):1700006. <https://doi.org/10.1002/masy.201700006>.
- [30] Sadhukhan S, Ghosh TK, Rana D, Roy I, Bhattacharyya A, Sarkar G, et al. Studies on synthesis of reduced graphene oxide (RGO) via green route and its electrical property. *Mater Res Bull* 2016;79:41–51. <https://doi.org/10.1016/j.materresbull.2016.02.039>.
- [31] Fathy M, Gomaa A, Taher FA, El-Fass MM, Kashyout AEHB. Optimizing the preparation parameters of GO and rGO for large-scale production. *J Mater Sci* 2016;51:5664–75. (<https://link.springer.com/article/10.1007/s10853-016-9869-8>).
- [32] Sadhukhan S, Ghosh TK, Rana D, Roy I, Bhattacharyya A, Sarkar G, et al. Studies on synthesis of reduced graphene oxide (RGO) via green route and its electrical property. *Mater Res Bull* 2016;79:41–51. <https://doi.org/10.1016/j.materresbull.2016.02.039>.
- [33] Dalsania R, Gajera H, Savant M. Exploration of graphitic carbon from crude oil vacuum residue. *Carbon Trends* 2024 Dec 1;17:100424. <https://doi.org/10.1016/j.cartre.2024.100424>.
- [34] Jayachandiran J, Yesuraj J, Arivanandhan M, Raja A, Suthanthiraraj SA, Jayavel R, et al. Synthesis and electrochemical studies of rGO/ZnO nanocomposite for supercapacitor application. *J Inorg Organomet Polym Mater* 2018;28:2046–55. (<https://link.springer.com/article/10.1007/s10904-018-0873-0>).
- [35] Monthioux M. Describing carbons. *Carbon Trends* 2024;14:100325. <https://doi.org/10.1016/j.cartre.2024.100325>.
- [36] Gnanamoorthy G, Yadav VK, Latha D, Karthikeyan V, Narayanan V. Enhanced photocatalytic performance of ZnSnO₃/rGO nanocomposite. *Chem Phys Lett* 2020; 739:137050. <https://doi.org/10.1016/j.cplett.2019.137050>.
- [37] Ikram M, Raza A, Imran M, Ul-Hamid A, Shahbaz A, Ali S. Hydrothermal synthesis of silver decorated reduced graphene oxide (rGO) nanoflakes with effective photocatalytic activity for wastewater treatment. *Nanoscale Res Lett* 2020;15: 1–11. <https://doi.org/10.1186/s11671-020-03323-y>.
- [38] Xu Y, Lin Z, Huang X, Liu Y, Huang Y, Duan X. Flexible solid-state supercapacitors based on three-dimensional graphene hydrogel films. *ACS Nano* 2013;7(5):4042–9. <https://doi.org/10.1021/nn400715d>.
- [39] Sadiq MMJ, Shenoy US, Bhat DK. Novel RGO–ZnWO₄–Fe₃O₄ nanocomposite as high performance visible light photocatalyst. *RSC Adv* 2016;6(66):61821–9. <https://doi.org/10.1039/C6RA13002J>.
- [40] Sharma N, Vyas R, Sharma V, Rahman H, Sharma SK, Sachdev K. A comparative study on gas-sensing behavior of reduced graphene oxide (rGO) synthesized by chemical and environment-friendly green method. *Appl Nanosci* 2020;10:517–28. <https://doi.org/10.1007/s13204-019-01138-7>.
- [41] Zhao Y, He J. Superfast microwave synthesis of hierarchically porous rGO by graphite ignited reduction propagation. *Carbon* 2021;178:734–42. <https://doi.org/10.1016/j.carbon.2021.03.048>.



Advanced Analytical Techniques for Comprehensive Characterization of Vacuum Residue Oil (VRO): A State-of-the-Art Review

^{1,2 *} Ravi Dalsania, ¹ Hasmukh Gajera, ² Mahesh Savant

¹ Reliance Industries Limited, Village Motikhavdi, Jamnagar 361140, Gujarat, India.

² Department of Chemistry, Atmiya University, Rajkot-360005, Gujarat, India.

(Received: 26 February 2025

Revised: 30 March 2025

Accepted: 22 April 2025)

KEYWORDS

Analytical
Techniques,
Comprehensive
Characterization,
Vacuum Residue Oil

ABSTRACT:

The characterization of vacuum residue oil (VRO) presents substantial challenges due to its complex and diverse composition, including a wide range of heavy hydrocarbons and high molecular weight compounds. Existing literature has extensively documented various advanced analytical techniques for assessing VRO, yet the complexity of this material continues to pose difficulties in fully understanding its properties and optimizing its industrial applications. This review builds on prior research by providing a comprehensive overview of the latest characterization methods, categorizing them into three primary areas: physical and chemical bulk property analysis, saturates, aromatics, resins, and asphaltenes (SARA) fractionation, and molecular modeling approaches. The report highlights global standards and variations in VRO properties, with particular focus on the intricate correlations between physical properties such as refractive index and density, and the molecular weight of specific fractions. By compiling and synthesizing these advancements, this review not only underscores the significant diversity within VROs but also clarifies the crucial role of advanced techniques, such as FTIR, NMR spectroscopy, and chromatographic methods, in enhancing our understanding and optimizing the processing of VROs in industrial applications. The insights provided here aim to bridge the gap between existing characterization methods and their practical application in optimizing conversion processes in commercial residual oil units.

1. Introduction

Vacuum residue oil (VRO) is a byproduct of the vacuum distillation process in petroleum refining. Its complex composition, characterized by a high boiling point and substantial viscosity, makes it an essential feedstock in various industrial applications [1,2]. VRO is indispensable in producing heavy fuel oil (HFO), asphalt, bitumen, and lubricants, and serves as a base material for creating solvents, detergents, and specialty chemicals [41]. Understanding and optimizing the use of VRO is crucial for the transportation, construction, manufacturing, and chemical sectors, highlighting the need for advanced characterization techniques to exploit its potential fully shown in (refer Fig 1.) VRO is composed of a myriad of hydrocarbons and non-hydrocarbons, including resins, asphaltenes, and a variety of aromatic compounds [4]. This complexity presents significant challenges in its analysis and utilization. The detailed characterization of VRO involves understanding its physical and chemical properties, the distribution of its molecular components,

and the effects of various extraction and processing conditions on its composition [36].

Traditional methods of analyzing VRO, while useful, often fall short in providing comprehensive insights into its intricate structure. Consequently, sophisticated analytical methods have been created and improved to provide a more thorough and precise characterization. These methods include SARA (Saturates, Aromatics, Resins, and Asphaltenes) analysis molecular modeling, and a range of sophisticated spectroscopic and chromatographic techniques [123]. SARA analysis is a cornerstone for characterizing VRO [5,37]. It fractionates the oil into four main components: saturates, aromatics, resins, and asphaltenes [28,6]. This segregation allows for a clearer understanding of the oil's composition, facilitating targeted applications and processing methods. By determining the proportions of these fractions, researchers can predict the behavior of VRO in different industrial processes and improve the efficiency of its conversion into valuable products [38]. Molecular modeling procedures simulate the activity of VRO at the molecular level, providing an alternative



method to empirical investigation. These simulations can forecast VRO's behavior in a variety of scenarios, offering challenging insights to obtain through experimental methods alone. Molecular modeling is particularly useful in optimizing the refining process, enhancing the quality of the final products, and reducing the environmental impact of VRO utilization. To fully understand the molecular structure of VRO, spectroscopic techniques like GCMS, FTIR NMR are essential [2]. NMR spectroscopy provides detailed information on the hydrogen and carbon frameworks of VRO molecules, providing information about the different kinds of chemical bonds and atom arrangements [96]. On the other hand, functional groups in the oil can be found using FTIR spectroscopy, which helps to determine the chemical makeup of the oil. The accurate examination of the volatile components of VRO is made possible by GCMS, which combines the identification power of mass spectrometry with the separation capabilities of gas chromatography. Chromatographic methods are necessary for a thorough examination of VRO. TLC-FID is effective for confirming the purity of the oil and detecting impurities that might affect its performance [37]. GPC is employed for molecular weight analysis, providing insights into the size distribution of the oil's molecular components. Because it has a major influence on the oil's overall characteristics, the characterisation of the heavy oil aromatic portion within VRO is particularly important [15,123]. PAHs are isolated and quantified using methods like HPLC, which are crucial in determining the reactivity and stability of VRO [85]. Molecular fragmentation analysis and API-Mass Spectra Examination further aid in identifying the specific aromatic compounds present, enabling more precise control over the refining process.

The composition of VRO is also influenced by enhanced oil recovery (EOR) techniques, which are used to extract more oil from reservoirs. The application of thermal, chemical, and gas injection methods alters the molecular structure and properties of the oil [91]. Understanding these changes is essential for optimizing the refining process and improving the quality of the end products. This review explores the impact of various EOR techniques on VRO composition, providing insights into the evolving nature of this complex feedstock.

This review aims to deliver an in-depth analysis of advanced techniques employed in VRO characterization, emphasizing their critical role in enhancing the understanding and optimization of VRO applications across diverse industrial sectors. This review aims to provide guidance for future research and development efforts in the field of VRO analysis by analyzing the advantages and disadvantages of each method. The integration of traditional and advanced analytical techniques promises to enhance the efficiency and sustainability of VRO processing, contributing to the development of higher-quality and more environmentally friendly products.

At the atomic level, NMR spectroscopy is a potent method for clarifying the structural specifics of VRO. NMR provides information on the hydrogen and carbon environments within the oil, enabling the identification of various functional groups and the types of chemical bonds present [97]. This technique is particularly useful in distinguishing between different types of hydrocarbons, such as alkanes, alkenes, and aromatics, and in detecting heteroatoms like sulfur, nitrogen, and oxygen. To determine the functional groups in VRO, FTIR spectroscopy is frequently utilized. By measuring the absorption of infrared light at different wavelengths, FTIR provides a fingerprint of the molecular vibrations within the oil. This information is critical for understanding the chemical composition of VRO and for identifying specific compounds that contribute to its overall properties. FTIR is especially useful for detecting polar compounds and heteroatomic species, which are often present in significant quantities in VRO. GCMS is a combination of mass spectrometry's identifying power and gas chromatography's separation capability. This method works very well for examining the volatile parts of VRO and precise yield details about the molecular weight and structure of each individual chemical. GCMS is invaluable for identifying trace components and impurities that can affect the performance and quality of VRO-derived products. The high sensitivity and specificity of GCMS make it a cornerstone technique for VRO analysis. A chromatographic method called TLC-FID is used to evaluate the purity of VRO and find contaminants. According to their affinity for the stationary and mobile phases, TLC divides the components of VRO, whereas FID provides quantitative detection of the separated components. This technique is



particularly useful for monitoring the refining process and ensuring the consistency and quality of VRO-derived products.

The molecular weight study of VRO is performed using GPC. GPC offers a distribution profile of the molecular weights within the oil by sorting molecules according to their size. This information is critical for understanding the rheological properties of VRO and for optimizing its processing and utilization. GPC is especially useful for characterizing high-molecular-weight fractions, such as asphaltenes, which significantly influence the viscosity and stability of VRO [35].

HPLC isolates and quantifies specific components within VRO, such as PAHs. HPLC offers high resolution and sensitivity, allowing for the precise identification and quantification of aromatic compounds. This technique is crucial for assessing the quality and reactivity of VRO, because PAHs have a big influence on how the oil behaves when it's processed and used.

The utilization of enhanced oil recovery techniques aims to optimize oil extraction from depleted oil reservoirs [92]. These techniques, including thermal, chemical, and gas injection methods, significantly impact the composition and properties of VRO. Understanding the changes induced by EOR is essential for optimizing the refining process and improving the quality of the end products. This review examines the effects of various EOR techniques on VRO composition, providing insights into the evolving nature of this complex feedstock.

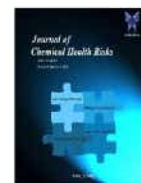
Thermal EOR techniques, such as steam injection and in-situ combustion, increases the temperature of the reservoir to reduce the viscosity of the oil and enhances its flow. These methods can alter the molecular structure of VRO, leading to the formation of lighter fractions and the degradation of heavier components. Understanding these changes is crucial for optimizing the refining process and improving the quality of VRO-derived products.

Chemicals including polymers, alkalis, and surfactants are injected during chemical EOR procedures in order to increase the oil's displacement efficiency. The content and characteristics of VRO are changed by these chemicals' interactions with the oil and the reservoir rock. For instance, whereas polymers raise the viscosity

of the injected water, surfactants can lower the interfacial tension between oil and water. To maximize the refining process and raise the caliber of the finished products, it is crucial to comprehend how these chemicals affect VRO. Gas injection EOR techniques, such as carbon dioxide (CO₂) injection, involve the injection of gases to increase the reservoir pressure and improve oil recovery. CO₂ injection, in particular, can significantly alter the composition of VRO by dissolving in the oil and reducing its viscosity. The interaction between CO₂ and VRO can lead to the formation of new compounds and the modification of existing ones. Understanding these changes is crucial for optimizing the refining process and improving the quality of VRO-derived products.

For specific characterizations such as NMR and FTIR, numerous studies highlight their efficacy in analyzing vacuum residue oil [46,43]. NMR spectroscopy is a powerful tool used to determine the molecular structure, composition, and chemical bonding in residual oils, providing detailed insights into the aromatic and aliphatic content as well as other functional groups. FTIR spectroscopy, on the other hand, offers a comprehensive characterization of the chemical composition and functional groups in VRO, enabling the identification of various chemical moieties including hydrocarbons, aromatics, aliphatics, and heteroatoms. These techniques collectively enhance the understanding of VRO's structural and functional properties, making them indispensable in the study and application of vacuum residue oils.

The characterization of vacuum residue oil is essential for optimizing its utilization across various industries. Advanced analytical techniques, including spectroscopic and chromatographic methods, provide detailed insights into the complex composition of VRO [16,120] combined with molecular modeling and SARA analysis, these techniques provide a thorough comprehension of the chemical and physical characteristics of VRO [49]. The application of enhanced oil recovery techniques further emphasizes the need for such advanced characterization methods. EOR processes can alter the composition of VRO, making it crucial to understand these changes to optimize recovery and processing strategies. By integrating traditional and advanced analytical techniques, researchers can improve the efficiency and sustainability of VRO processing,



contributing to the development of higher-quality and more environmentally friendly products.

2. Methods for Characterization of Residual Oils

2.1 Characterization Techniques

The characterization of vacuum residue oil is essential for optimizing its utilization across various industries. Advanced analytical techniques provide detailed insights into the complex composition of VRO [121]. These techniques can be segregated into physical characterization and chemical property characterization methods to provide a systematic understandings shown in Fig 2 and discussed in Table 1.

2.1.1 Physical Characterization Techniques

SARA analysis is a cornerstone for characterizing VRO. It fractionates the oil into four main components, allowing for a clearer understanding of the oil's composition. This segregation shown in (refer Fig 5a, b, c) is essential for predicting the behavior of VRO in different industrial processes and improving the efficiency of its conversion into valuable products [49].

Molecular modelling procedures simulate the activity of VRO at the molecular level. These simulations can forecast VRO's behavior in a variety of scenarios, offering insights that are challenging to obtain through experimental methods alone. This technique helps in understanding the interactions and stability of various components within the VRO, leading to better process optimization [16].

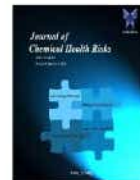
The graph shown in Fig 5a, depicts the hydrocarbon composition of the sample, detailing the weight percentages of Saturates, Aromatics, Resins, and C7-asphaltenes. Saturates, comprising slightly over 90%wt, are the predominant fraction, indicating a sample with a high concentration of non-polar, saturated hydrocarbons. This high level of saturates suggests a material with enhanced stability and lower reactivity, which is favorable for applications requiring resistance to chemical breakdown. Aromatics, constituting approximately 60%wt, represent hydrocarbons containing one or more aromatic rings, known for their greater chemical reactivity and potential impact on the thermal and oxidative stability of the sample. Resins account for around 70%wt, reflecting the presence of heavier, polar molecules that can significantly influence

the viscosity and surface properties of the material. Lastly, C7-asphaltenes make up about 40%wt of the sample, indicating a considerable portion of the heaviest and most complex molecules, which are often associated with challenges such as precipitation, fouling, and increased viscosity in petroleum-derived products. The composition suggests a complex interplay of stable and reactive hydrocarbon species, with implications for processing, handling, and end-use applications.

Graph 5b, presents the boiling point distribution of hydrocarbon fractions in the sample, highlighting a range from light naphtha to vacuum gas oil. The light naphtha fraction, boiling between 30°C and 100°C and composed of C5 to C7 hydrocarbons, represents the lightest and most volatile components, but it constitutes a relatively small portion of the sample. Moving up the boiling range, the heavy naphtha fraction, between 100°C and 180°C (C7 to C10), shows a significant increase in content, indicating a substantial presence of hydrocarbons suitable for gasoline production or petrochemical feedstock. The kerosene fraction, boiling between 180°C and 240°C (C11 to C14), reflects a moderate level of hydrocarbons commonly used in jet fuel, showcasing the sample's potential for aviation fuel production.

The diesel fraction, which boils between 240°C and 360°C and consists of C15 to C22 hydrocarbons, is the most prominent in the sample, indicating a high potential for diesel production. This suggests that the sample is rich in middle distillates, making it particularly valuable for producing diesel fuel. Finally, the vacuum gas oil fraction, boiling between 360°C and 540°C (C23 to C46), represents the heavier components of the sample. This fraction is crucial for further processing in catalytic cracking units to yield lighter, more valuable products such as gasoline and diesel. Overall, the distribution emphasizes the sample's suitability for refining processes aimed at maximizing the yield of diesel and other middle distillates.

The chart shown in 5c) illustrates the elemental composition of the sample in terms of weight percentage (%wt). Carbon is the dominant element, constituting 87%wt of the total composition, which is typical for hydrocarbon-based materials. This high carbon content indicates that the sample is primarily made up of organic compounds, contributing to its energy-rich nature.



Hydrogen is the second most abundant element, making up 14%wt of the sample. The carbon-to-hydrogen ratio suggests a structure rich in hydrocarbons, which are crucial for energy production and chemical processing. Sulfur is present at 9%wt, indicating a significant level of heteroatoms that may require removal during refining to meet environmental regulations and to prevent corrosion in processing equipment. Nitrogen and oxygen are present in smaller amounts, at 3%wt and 1.5%wt, respectively. These elements can impact the stability and reactivity of the sample, with nitrogen contributing to the formation of NO_x emissions and oxygen potentially leading to oxidative instability.

2.1.2 Chemical Property Characterization Techniques

NMR spectroscopy is a powerful tool used to determine the molecular structure, composition, and chemical bonding in residual oils. It provides detailed information on the hydrogen and carbon frameworks of VRO molecules, revealing the different kinds of chemical bonds and atom arrangements. This technique is crucial for understanding the aromaticity, aliphaticity, and the presence of functional groups in heavy oils [10].

FTIR spectroscopy serves as a powerful tool for comprehensive characterization of the chemical composition and functional groups in VRO. It identifies and quantifies various chemical moieties, including hydrocarbons, aromatics, aliphatics, and heteroatoms (see Fig 5a, b, c). FTIR provides essential data on the functional groups present, such as carbonyl, hydroxyl, and sulfide groups, by offering a fingerprint of the molecular vibrations within the oil.

GC-MS combines the identification power of mass spectrometry with the separation capabilities of gas chromatography to analyze the volatile components of VRO. This technique is invaluable for identifying and quantifying the various hydrocarbons and other compounds present in the oil. It enhances the resolution and identification of complex mixtures in heavy oils, making it possible to detect sulfur compounds and polycyclic aromatic hydrocarbons [116].

The application of enhanced oil recovery techniques further emphasizes the need for such advanced characterization methods. EOR processes can alter the composition of VRO, making it crucial to understand

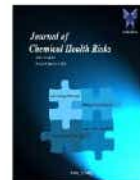
these changes to optimize recovery and processing strategies. By integrating traditional and advanced analytical techniques, researchers can improve the efficiency and sustainability of VRO processing, contributing to the development of higher-quality and more environmentally friendly products. This review highlights the significance of these methodologies in advancing VRO analysis and optimizing its utilization across various industrial applications.

2.2 SARA Analysis for Characterizing Residual Oils

SARA analysis is a fundamental technique employed to characterize the composition of crude and residual oils by separating them into four distinct fractions shown in Fig 3, Saturates, Aromatics, Resins, and Asphaltenes [52]. This method capitalizes on the differences in the polarizability and polarity of the oil components, enabling a detailed understanding of the oil's makeup, which is crucial for refining processes and predicting the behavior of oils in various applications [7]. The primary techniques for performing TLC, HPLC, and gravity-driven chromatographic separation are examples of SARA analytical techniques. Every approach has unique benefits and drawbacks that may influence the outcomes and how they are interpreted.

[53] complex mixture of hydrocarbon and non-hydrocarbon components that makes up residue oil has a boiling point range of about 760°C (for methane) and carbon numbers varying from 1 to over 100 atoms. [30,12] The final boiling temperatures of several types of residual oil have been observed to vary between 1000 and 2000°C using TBP distribution models. The number of acyclic alkane isomers that are feasible is about 36.7 million at a carbon atom number of 25 (boiling point = 402°C), and 5920 trillion at a carbon atom number of 100 (boiling point = 708°C). Although the precise count of constituents in a leftover oil mixture is uncertain, it is likely to surpass one million. For instance, just 5% of the components in the heaviest proportion of oil—vacuum residue—that boils at 540°C are known, and the other 95% are still unknown. The analysis of this intricate mixture poses considerable difficulties for experts in the petrochemical and refining sectors.

The complex combination is divided into fractions according to their chemical similarities in order to make the chemical characterization and comprehension of leftover oil easier. Using a variety of solvents, eluents,



and adsorbents, this separation into saturates, aromatics, resins, and asphaltenes (SARA) is based on the polarity of these fractions. [39,17]. Using n-heptane or n-pentane, the asphaltenes are precipitated from the oil mixture as the initial stage in the SARA fractionation process. [28,17] After the leftover oil combination has been de-asphalted, techniques like ASTM D2007, ASTM D4124, high-performance liquid chromatography (HPLC), or thin-layer chromatography with flame ionization detection (TLC-FID; IATROSCAN) can be used to check for saturates, aromatics, and resinous fractions [54].

Due to variances in the methodologies, the type of eluent, and the molecular weight of the solvents, which have a substantial impact on the relative proportions of each fraction, there have been documented considerable disparities between SARA results obtained by ASTM, HPLC, or TLC-FID procedures. [8] have predicted different qualities of residual oil, coke production, asphaltene stability, and other characteristics using the SARA composition results [19,29]. Many equations of state rely on the group hydrocarbon composition of residue oil as input data, and thermodynamic models that forecast sediment formation during residue oil extraction and refining are built upon this foundation [73]. Furthermore, the group hydrocarbon makeup of the feedstock used in different conversion processes to produce lighter, higher-value products offers important insights on how these processes work.

Consequently, there is a great deal of practical interest in researching techniques for determining the SARA composition of residual oil and its derivatives. Comparisons are difficult since different researchers analyze the SARA composition of residual oil and its byproducts using different analytical methodologies. The group hydrocarbon composition of extra light, light, medium, heavy, and extra heavy residue oil types, oil sands, and natural bitumen obtained using various techniques is covered in this review, which compiles a substantial body of data published in the literature [87]. It investigates the connections between SARA composition, residue oil's physicochemical characteristics, and several indicators that describe how residue oil behaves during extraction and refining. In this study, SARA composition in 308 residue oil samples that represented the following categories: extra light (specific gravity (SG) < 0.8017), light (0.8017 < SG < 0.855),

medium (0.8600 < SG < 0.9220), heavy (0.9220 < SG < 1.000), and ultra-heavy (SG > 1.000). The specific gravity, aromatic structure content (which is the total of all fractions containing aromatic carbon, such as aromatics, resins, and asphaltenes), and group composition data (SARA) of the 308 residue oil samples are summarized in (refer Table 2) [20,65]. The percentage distribution of the five methodologies utilized for the SARA analysis of residue oil composition for a database including 308 residue oils from published sources.

According to the data cited, the HPLC method is the one that is most frequently used for SARA residue oil composition analysis. It has been used to analyze the group hydrocarbon composition of oil sands and natural bitumens, as well as extra light, light, medium, heavy, and extra heavy residue oil types [40,41]. The ASTM D2007 method, which applies to all types of residual oil, is the second most used approach. The liquid chromatography approach comes next and has also been employed to ascertain the SARA composition of each residual oil group. In terms of SARA technique application, TLC-FID (Iatroscan) comes in fourth place [54]. It has been used to analyze light, medium, and heavy residue oil types using SARA. The modified ASTM D4124 method, which has also been utilized for SARA analysis of light, medium, and heavy grades of residual oil, is the least applied in terms of applicability.

Gravity-Driven Chromatographic Separation:

This traditional method, often guided by ASTM D2007, utilizes large sample volumes and significant quantities of solvents. The process involves sequential adsorption on clay and silica columns to fractionate the oil into its SARA components. During this process, the oil sample is first treated to precipitate asphaltenes, which are then filtered and weighed [26]. The remaining maltenes are subjected to further separation on adsorption columns. However, a major limitation of this method is the potential loss of volatile materials during the separation, which can lead to inaccuracies in the final composition analysis. This method is labor-intensive and time-consuming, but it remains widely used due to its established protocol and ability to handle large sample sizes.



Thin Layer Chromatography (TLC):

Compared to gravity-driven techniques, TLC with flame ionization detection (TLC-FID) offers a quicker and less solvent-intensive solution [55]. This method uses quartz rods coated with silica for separation; the separated fractions are then detected and quantified using flame ionization. To characterize AR maltene and its MPLC fractions, MK-6S (Misthuibish, Japan) and silica chromarods (Misthuibish, Japan) were employed. To guarantee data repeatability, several silica rods were examined concurrently. Initially, methylene chloride was used to dilute each MPLC phase and AR maltene. A small volume of each diluted sample was then spotted onto the TLC silica rods for analysis. After a brief drying period for the dilution solvents, hexane was eluted to a specified distance and dried to remove residual solvent. Subsequently, toluene was eluted to a shorter distance and dried. Finally, methylene chloride with a small percentage of methanol was eluted to an even shorter distance and dried for a brief period.

High-Pressure Liquid Chromatography (HPLC):

HPLC stands out for its ability to provide faster and more reproducible results compared to traditional chromatographic methods shown in Fig 4. Utilizing NH_2^- bonded columns, HPLC effectively separates the oil components without the need for prior removal of asphaltenes. This method minimizes the loss of volatile materials, ensuring more accurate quantification of the fractions. HPLC's precision and efficiency make it particularly useful for detailed compositional analysis and research applications where high accuracy is required. Its reproducibility and reduced solvent usage further enhance its appeal for modern analytical laboratories.

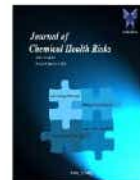
The SARA study of three distinct crude oil types is shown in Fig 4 utilizing ASTM, HPLC, and TLC-FID analytical techniques. The proportion of volatiles, saturates, aromatics, resins, and asphaltenes varies significantly amongst the crude oil samples according to each method. [10,7] For A-95 crude oil, the ASTM method indicates a high saturate content of approximately 60 wt%, with low volatile content around 10 wt%, and minimal amounts of aromatics, resins, and asphaltenes. The HPLC method, however, shows a more balanced profile with moderate volatiles at about 25 wt% and saturates at roughly 35 wt%, while the amounts of

aromatics and resins remain low. The TLC-FID method reveals a significantly higher volatile content of about 50 wt%, with moderate saturates around 20 wt% and similarly low levels of aromatics, resins, and asphaltenes. C-LH-99 crude oil follows a similar trend. The ASTM method reports high saturates (~55 wt%) and low volatiles (~15 wt%), with minimal aromatics and resins. HPLC results show increased volatiles (~30 wt%) and reduced saturates (~25 wt%). TLC-FID indicates high volatiles (~45 wt%) and moderate saturates (~25 wt%). C-R-00 crude oil demonstrates substantial variation among methods [54]. ASTM shows high saturates (~60 wt%), low volatiles (~15 wt%), and negligible aromatics and resins. HPLC and TLC-FID methods reveal moderate volatiles and saturates (~35 wt% and ~25 wt%, respectively) [55].

S-Ven-39 crude oil exhibits high saturates (~50 wt%) and low volatiles (~20 wt%) according to ASTM. HPLC and TLC-FID indicate increased volatiles (~35 wt%) and moderate saturates (~30 wt%). [55] SQ-95 crude oil shows high saturates (~55 wt%) and low volatiles (~20 wt%) with ASTM. HPLC and TLC-FID reveal higher volatiles (~40 wt%) and moderate saturates (~25 wt%). Tensleep-99 crude oil follows the trend of high saturates (~60 wt%) and low volatiles (~15 wt%) with ASTM. HPLC and TLC-FID show moderate volatiles (~30 wt%) and saturates (~25 wt%).

2.3 Advanced Analytical Techniques for Residual Oil Characterization

Advanced analytical techniques have catalyzed a paradigm shift in residual oil characterization, transcending the limitations of conventional methodologies. Amidst the vast array of traditional approaches, HRMS has emerged as a transformative force, similar to mass spectrometry and gas chromatography. HRMS's capacity for accurate mass measurement facilitates the discernment of intricate molecular structures within residual oil matrices, offering unparalleled resolution and sensitivity. In addition, two-dimensional gas chromatography (2D-GC) has become a powerful instrument for deciphering residual oil compositions. By its comprehensive separation capabilities, 2D-GC enables the dissection of highly intricate mixtures, surpassing the limitations of conventional GC techniques. Complementing these advancements, NMR stands out for its non-destructive



probing of molecular architectures and functional groups present in residual oils [46,56]. Leveraging the inherent magnetic properties of nuclei, NMR affords unprecedented insights into the chemical bonding and composition of residual oil constituents [22,23]. Pyrolysis gas chromatography-mass spectrometry (Py-GC/MS), on the other hand, provides a unique thermal decomposition-based method, facilitating the identification and characterization of biomarkers and heteroatoms within residual oil samples [66]. These advanced techniques find versatile applications across diverse sectors, including petroleum refining, environmental monitoring, and biofuel production [79,88]. Their integration not only enhances process efficiency and product quality but also fosters strides towards environmental sustainability. As the trajectory of analytical innovation continues unabated, ongoing advancements in instrumentation and interdisciplinary collaborations hold the promise of further revolutionizing residual oil characterization, driving the frontiers of knowledge in this critical domain.

UV-Visible Spectroscopy (UV-VIS) is used for structural analysis, identifying asphaltenes, mono- and bicyclic hydrocarbons, and metal binding within the oil [67]. Infrared Spectroscopy (IR) focuses on molecular characterization, assessing the degree of aromaticity, identifying hydrocarbon compounds, and dividing the oil into SARA fractions. It also measures API gravity, viscosity, density, and sulfur speciation. Oil shale and additives, asphaltenes, hydrocarbon chemicals, and molecular vibrations can all be examined using GC-MS. Molecular vibrations, the structural state of carbon in bitumen and kerogens, distillation fractions, mono- and bicyclic hydrocarbons, and asphaltene dimensions are all examined using TLC-FID. Viscosity, asphaltenes, hydrocarbon compounds, soluble fractions, molecular structures, and atom counts can all be precisely determined using NMR. Together, these methods provide a thorough characterization of crude oils, aiding in their analysis and processing.

HRMS is an analytical technique that provides accurate mass measurement of ions, which is essential for identifying complex molecular structures and characterizing trace components in residual oils. This high level of precision allows for the detailed analysis of minute constituents within a sample. 2D-GC offers comprehensive separation of components, making it

highly effective for resolving complex mixtures in residual oils. Its enhanced peak capacity facilitates a more detailed analysis compared to traditional gas chromatography, allowing for the identification of individual compounds within a complex matrix. NMR detects NMR signals from nuclei, enabling the determination of molecular structure, composition, and chemical bonding in residual oils [46]. The process of pyrolysis Py-GC/MS, or gas chromatography mass spectrometry, uses heat to break down samples in order to identify biomarkers, heteroatoms, and important constituents in leftover oils [50] as discussed in Table 3. By breaking down the sample into smaller fragments, Py-GC/MS can reveal detailed information about the chemical makeup and origins of the oil components, making it a powerful tool for oil analysis. Together, these techniques offer a comprehensive suite of methods for the detailed analysis and characterization of residual oils, providing insights into their composition, structure, and chemical properties.

2.4 Residual Oil Characterization through Molecular Modelling Processes

Residual oil characterization via molecular modeling processes represents a sophisticated approach leveraging computational techniques to elucidate the structural and chemical properties of residual oil components. Molecular modeling methods encompass a diverse array of computational tools, comprising molecular dynamics (MD), quantum mechanics (QM), and molecular mechanics (MM), each of which provides a different perspective on the behavior and interactions of molecules inside residual oil matrix. Techniques rooted in quantum mechanics, like density functional theory (DFT) and ab initio computations, provide precise electronic structure and energetics prediction shedding light on the molecular-level mechanisms underlying various chemical processes within residual oils [71]. Molecular mechanics approaches, on the other hand, employ simplified empirical force fields to simulate the conformations and interactions of complex molecular assemblies, facilitating the exploration of conformational landscapes and intermolecular forces governing residual oil behavior. Molecular dynamics simulations further augment these capabilities by providing a dynamic perspective on molecular motion and kinetics, enabling the study of phenomena such as diffusion, phase transitions, and reaction pathways in residual oil systems



[3]. The integration of molecular modeling techniques with experimental data, such as spectroscopic analyses and chromatographic profiles, allows for the refinement and validation of computational models, enhancing their predictive accuracy and reliability. Through the synergy of computational and experimental approaches, molecular modeling processes play a pivotal role in advancing our understanding of residual oil composition, reactivity, and behavior, with profound implications for applications spanning petroleum refining, environmental remediation, and renewable energy production [50,88].

3. Investigating the Impact of Enhanced Oil Recovery (EOR) Techniques on Residual Oil Composition

Enhanced Oil Recovery methods significantly influences both the molecular and macroscopic properties of residual hydrocarbons in oil reservoirs [9,93]. This investigation evaluates the effects of various EOR techniques, including thermal methods like steam flooding and in-situ combustion. These reduce oil viscosity and cause thermal cracking of long-chain hydrocarbons into lighter fractions, potentially affecting asphaltene stability [73,79]. Chemical EOR techniques, such as polymer flooding, surfactant flooding, and alkaline flooding, involve injecting chemicals that improve oil mobility and alter the wettability of the reservoir rock, leading to changes in molecular composition, emulsification, and interfacial tension. Gas injection methods, like CO₂ and nitrogen injection, cause oil swelling, reduce viscosity, and alter phase behavior, enhancing oil displacement. These EOR techniques induce specific changes in the residual oil's molecular structure, including variations in hydrocarbon chain lengths, aromaticity, and asphaltene precipitation, as well as alterations in physical properties like viscosity, density, and interfacial tension [51].

4. Characterization of Heavy Oil Aromatic Fraction

4.1. High-Performance Liquid Chromatography (HPLC)

Analyzing vacuum residue oil using HPLC involves a detailed process to separate and identify its complex mixture of high-boiling point hydrocarbons [107,81]. Initially, the vacuum residue oil sample is diluted in an appropriate solvent, typically toluene, to facilitate

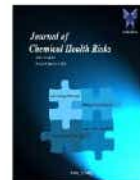
injection into the HPLC system. To remove particulates, the sample may undergo additional clean-up steps, such as filtration or centrifugation. In the HPLC system, the sample is injected into a column packed with a suitable stationary phase. The choice of stationary and mobile phases is critical, often utilizing reverse-phase HPLC due to the non-polar nature of many components in vacuum residue oil. As the sample components are transported through the column by the mobile phase, they are divided into groups according to how they interact with the stationary phase. Detection is typically achieved using a UV-Vis or refractive index detector, capable of identifying and quantifying the various fractions. The resulting chromatogram provides detailed information on the composition of the vacuum residue oil, including the presence and concentration of asphaltenes, resins, aromatics, and saturates, facilitating a comprehensive analysis of its chemical properties [101].

4.2. Identification and Quantification of Polynuclear Aromatic Hydrocarbons (PAHs)

The main theme of the survey on the latest in-depth techniques for the analysis of vacuum residue oil focuses on the identification and quantification of polynuclear aromatic hydrocarbons within this complex matrix. PAHs are significant due to their environmental impact and health risks, necessitating precise analytical methods. In order to fully characterize PAHs in vacuum residue oil, the survey assesses sophisticated techniques as FTIR, GC-MS, and HPLC. [57,58] These techniques provide high sensitivity and specificity, enabling the detection of trace levels of PAHs amidst a background of heavy hydrocarbons [59]. The study focuses on the developments in sample preparation techniques that improve the effectiveness and precision of PAH analysis, such as solid-phase extraction (SPE) and accelerated solvent extraction (ASE). Additionally, the survey examines the integration of hyphenated techniques, like HPLC-MS and GC-MS/MS, offering comprehensive insights into the molecular composition of vacuum residue oil [60]. This technical evaluation aims to inform the development of more effective analytical protocols, ensuring better environmental monitoring and risk assessment of PAHs in heavy oil fractions [47].

4.3. Molecular Fragmentation Analysis

molecular fragmentation analysis emerges as a pivotal tool for elucidating the complex molecular composition



of this heavy oil fraction [74]. By subjecting vacuum residue oil samples to mass spectrometry and analyzing the resulting fragmentation patterns, researchers can gain crucial insights into the structural characteristics and chemical constituents present in the oil. This method makes it possible to identify and measure a wide range of substances, such as species that contain heteroatoms, polynuclear aromatic hydrocarbons, and other complicated organic molecules, which are often challenging to characterize using conventional analytical methods. The ability to precisely determine the molecular composition of vacuum residue oil is paramount for understanding its properties, behavior, and environmental impact [60]. As such, molecular fragmentation analysis stands as an indispensable component of the analytical toolkit for investigating vacuum residue oil and developing strategies for its efficient utilization and environmental management [60].

4.4. API-Mass Spectra Examination

The examination of API-mass spectra holds significant relevance within the context of the survey on the latest in-depth techniques for the analysis of vacuum residue oil. Vacuum residual oil contains complex chemical components, and one effective analytical method for determining their molecular makeup is atmospheric pressure ionization mass spectrometry, or API mass spectrometry. By subjecting the oil samples to API-mass spectrometry, researchers can obtain detailed information about the mass-to-charge ratios of ions generated from the oil's molecular components. Numerous substances, such as heteroatom-containing species, polynuclear aromatic hydrocarbons, and other organic molecules found in the vacuum residue oil, can be identified and measured using this technique. The examination of API-mass spectra enables the elucidation of structural features, functional groups, and molecular fragments within the oil, providing crucial insights into its chemical composition and properties. Therefore, API-mass spectra examination serves as a vital technique in the comprehensive analysis of vacuum residue oil, contributing to our understanding of its complex molecular makeup and facilitating informed decision-making in various industrial and environmental applications.

5. Structural Analysis of Vacuum Residue

5.1. Nuclear Magnetic Resonance (NMR) Spectroscopy

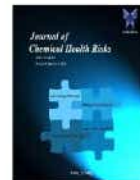
NMR spectroscopy is a powerful analytical tool used to gain detailed structural insights into the molecular composition of vacuum residue oil [32]. NMR characterizes the chemical environment of nuclei within the oil's molecular structure, providing crucial information about aromaticity, aliphatic chains, and the presence of heteroatoms.

This detailed characterization discussed in Table 4. is essential for understanding the complex properties and behavior of vacuum residue oil, which in turn informs the development of more efficient processing methods.

Additionally, NMR spectroscopy offers insights into molecular connectivity, stereochemistry, and conformational dynamics, revealing the intricate molecular architecture of vacuum residue oils. This ability to dissect the molecular structure has significant implications for industrial applications, such as improving refining processes, enhancing environmental management strategies, and optimizing quality control measures. Specifically, NMR analysis has shown that understanding the distribution and interaction of various chemical functionalities within vacuum residue oil can lead to more targeted and effective processing techniques, reducing environmental impact and improving product quality.

5.2. FTIR

FTIR spectroscopy is intricately linked to the survey on advanced techniques for analyzing vacuum residue oil [34]. In this survey, FTIR spectroscopy serves as a powerful tool for the comprehensive characterization of the chemical composition and functional groups present in vacuum residue oil [94]. By subjecting oil samples to FTIR analysis, researchers can obtain detailed information about the vibrational modes of molecular bonds present in the oil [76]. This technique allows for the identification and quantification of various chemical moieties, including hydrocarbons, aromatics, aliphatics, and heteroatoms. Moreover, FTIR spectroscopy provides valuable insights into the presence of functional groups such as carbonyl, hydroxyl, and sulfide groups, which are essential for understanding the reactivity and properties of vacuum residue oil. Examination of FTIR spectra



enables researchers to elucidate the molecular structure, composition, and properties of vacuum residue oil, thereby facilitating the development of efficient processing methods, environmental management strategies, and quality control measures in various industrial applications [43] (see Table 5.)

FTIR spectroscopy is a crucial analytical tool for characterizing the chemical composition and functional groups in vacuum residue oils [33]. Studies have shown that FTIR provides detailed information about the vibrational modes of molecular bonds, enabling the identification and quantification of various chemical moieties, including hydrocarbons, aromatics, aliphatics, and heteroatoms [94]. This capability is essential for understanding the reactivity of these oils, particularly in identifying functional groups such as carbonyl, hydroxyl, and sulfide, which play a significant role in oil processing and stability.

Moreover, FTIR has proven effective in detecting trace contaminants and offering enhanced sensitivity to minute compositional changes during oil processing, making it invaluable for quality control and environmental assessments. The correlation between FTIR data and physical properties like viscosity and density allows for a more comprehensive understanding of oil behavior, which is critical for optimizing processing methods and ensuring environmental compliance. However, challenges remain in fully leveraging FTIR for real-time monitoring and in developing standardized protocols for its application across different types of heavy oils [72].

5.3. GCMS

GC-MS serves as a cornerstone for the comprehensive characterization of the complex molecular composition of vacuum residue oil discussed in Table 6 [92]. GC-MS allows the isolation and identification of specific components within the oil sample based on their mass spectra and retention times by combining gas chromatography and mass spectrometry. This method makes it possible to identify and measure a wide range of substances, such as heteroatom-containing species, polynuclear aromatic hydrocarbons (PAHs), and other organic molecules present in vacuum residue oil. Additionally, GC-MS provides valuable insights into the molecular weight distribution, structural features, and chemical functionalities of the oil constituents. The examination of GC-MS spectra enables researchers to

unravel the intricate molecular architecture of vacuum residue oil, facilitating the development of efficient processing methods, environmental management strategies, and quality control measures in various industrial applications.

GC-MS techniques have significantly enhanced the analysis of vacuum residue oils, enabling the development of methods for detailed hydrocarbon profiling. discuss new GC-MS techniques that provide comprehensive data on vacuum residues, leading to a deeper understanding of their composition [103]. The resolution and identification have improved capabilities of GC-MS for complex mixtures in heavy oils, essential for accurate characterization of these challenging materials [99]. The application of GC-MS in oil refinery product analysis, which enhances the detection of sulfur compounds and polycyclic aromatic hydrocarbons, thus aiding in quality control and refining processes [100]. The use of comprehensive two-dimensional GC-MS (GC×GC-MS) by facilitates the separation and identification of high-boiling compounds in vacuum residues, providing detailed compositional insights [98]. Focus on the optimization of GC-MS techniques, introducing new methodologies for sample preparation and chromatographic conditions, which improve the analysis of petrochemical products [112]. A detailed study provided on the biomarker composition of vacuum residues, offering insights into their origins and chemical characteristics, vital for geochemical and environmental studies [35]. Research by reveals the chemical complexity and molecular weight distribution in oil sands vacuum residue, contributing to a better understanding of these resources. A Review on recent advancements in GC-MS instrumentation and techniques, highlighting significant improvements in analyzing heavy oil fractions and reflecting the ongoing evolution in this field [59]. The application of GC-MS for sulfur compound analysis in vacuum residues, allowing for the identification and quantification of various sulfur-containing compounds, important for both environmental and industrial applications [31]. Finally, provided a comprehensive profiling of products obtained from heavy oil upgrading processes using GC-MS, offering valuable data for optimizing these processes and improving product quality [112].



6. Chromatographic Techniques

6.1. TLC-FID for Purity Confirmation

TLC-FID is highly relevant, particularly when discussing sophisticated methods of vacuum residue oil analysis. This method offers a rapid and effective means to confirm the purity of various compounds present in the oil sample. TLC separates individual components based on their affinity to the stationary phase, followed by visualization using a suitable detection method, in this case, Flame Ionization Detection. FID provides quantitative information about the separated compounds by measuring the ions generated upon combustion, thus enabling the determination of purity levels. In the analysis of vacuum residue oil, TLC-FID aids in confirming the absence of impurities or contaminants that may compromise the quality or performance of the oil. This technique is particularly valuable in quality control processes, ensuring that the oil meets specified purity standards for its intended application. Therefore, TLC-FID emerges as a crucial tool for purity confirmation within the realm of advanced analytical techniques for vacuum residue oil analysis, contributing to quality assurance and product integrity in various industrial sectors.

The evaluation of vacuum residue oil purity has seen significant advancements through improved TLC-FID methods, offering higher sensitivity and more accurate assessments of purity [104]. The development of advanced TLC-FID protocols has enabled precise purity measurements in heavy oil fractions, addressing the complexities inherent in these materials [121]. Enhanced resolution and quantification of various components in crude oil residues have been achieved using TLC-FID, as demonstrated in studies that optimize these methods for better analytical outcomes [102]. Novel approaches for purity confirmation in petrochemical products through optimized TLC-FID methods have provided more robust and reliable results, facilitating better quality control [97]. The continuous monitoring of purity levels during oil refinery processes has been improved by the application of TLC-FID, enabling real-time quality assessment and process optimization [113]. Detailed characterization of heavy oil fractions and their purity assessment using TLC-FID has provided critical insights into their composition, supporting more efficient utilization and processing of these resources discussed in

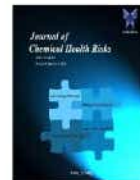
Table 7 [104]. Recent advancements in TLC-FID techniques have enhanced the analysis and purity confirmation of petrochemicals, reflecting ongoing improvements in this field [105]. For the purpose of separating and verifying the purity of crude oil components, high-resolution TLC-FID techniques have been developed, which provide increased accuracy and dependability [55]. The utilization of TLC-FID for purity confirmation in oil sands-derived vacuum residues has highlighted its effectiveness in handling complex matrices found in these materials [60]. Finally, comprehensive studies on the use of TLC-FID for analyzing and confirming the purity of vacuum residue oil have consolidated its role as a crucial tool in petrochemical analysis, providing detailed and accurate data essential for industry applications [59].

6.2. Molecular Weight Analysis using GPC

Molecular Weight Analysis using GPC is a vital technique within the scope of advanced analyses for vacuum residue oil. GPC is adept at determining the distribution of molecular weights present in the oil sample. Using this technique, molecules are separated according to size as they move through a porous gel matrix. Smaller molecules take longer to elute than larger molecules, which elute earlier. Detection methods such as refractive index or ultraviolet absorption allow for the quantification of the separated fractions. In the analysis of vacuum residue oil, GPC provides essential insights into the distribution of molecular sizes, helping to characterize the complexity of the oil's composition. By determining the average molecular weight and polydispersity index, GPC facilitates the assessment of the oil's suitability for various industrial applications [44]. Moreover, it aids in understanding the relationship between molecular size and properties such as viscosity, thermal stability, and solubility. Thus, molecular weight analysis using GPC stands as a critical technique for gaining a comprehensive understanding of vacuum residue oil, guiding formulation, processing, and quality control efforts in the petroleum industry [108].

7. Discussions

The published reviews on characterization of residual oils highlights significant differences in the methods and results. For instance, the study emphasizes the importance of SARA analysis in understanding the properties of vacuum residual oils [15]. It notes that the



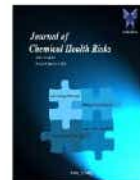
correlation between density and refractive index is strong, indicating a strong correlation between these properties. In contrast, other studies, focus on the use of advanced analytical techniques like petroleomics and molecular modeling to better understand the composition and properties of heavy petroleum mixtures [80]. Additionally, research explores the thermal cracking behavior and viscosity prediction of vacuum residues, highlighting the need for more comprehensive approaches to understanding residual oil properties [67] and [128]. These differences in focus and methodology underscore the complexity of residual oil characterization and the need for diverse approaches to fully understand these complex mixtures.

A comprehensive overview of the challenges in petroleum characterization [17]. The authors discuss the various methods used to analyze petroleum crude oils, highlighting the importance of understanding the chemical nature of these complex substances. The article emphasizes that petroleum properties vary widely, making it difficult to measure them using a single standard method. It highlights the importance of understanding these variations to optimize oil refining processes and improve profitability. The authors discuss the use of the SARA (Saturates, Aromatics, Resins, and Asphaltenes) characterization method to analyze petroleum crude oils, and examine the application of the additive rule to predict asphaltene content from vacuum residue and TBP yield, which was found to be effective. The article also discusses the importance of accurate TBP (True Boiling Point) distillation data in refining processes, as it affects refining margins, and highlights the need for reliable TBP analysis to avoid underestimation or overestimation of refining margins, which can lead to incorrect crude oil selection. The authors examine the use of various analytical techniques, including chromatography, spectroscopy, and mass spectrometry, as well as chemometric approaches and modeling methods. The article emphasizes the significant impact of petroleum characterization on oil refining processes and the need for innovative techniques to improve profitability, as well as the importance of environmental regulations and the need for oil refining processes to be environmentally friendly.

8. Summary

The thorough examination of residual oils in this review makes it clear that there has been a substantial evolution in the characterization of VRO complex substances over time. The field started out with simple measurements of chemical and physical properties and has since advanced to more complex methodologies including molecular modeling, SARA analysis, and instrumental procedures. These developments have made it possible to comprehend residual oils' composition and characteristics better, which is essential for maximizing their use in a variety of industrial applications. Among these developments, SARA analysis stands out as a key technique that makes it easier to separate residual oils into four fractions: saturate, aromatic, resin, and asphaltene. The behavior and possible uses of these oils are significantly influenced by each fraction. The molecular weight ranges for the various SARA fractions are as follows: saturates ($350 \leq \text{MW} \leq 870$) < aromatics ($440 \leq \text{MW} \leq 1100$) < resins ($790 \leq \text{MW} \leq 1850$) < asphaltenes ($990 \leq \text{MW} \leq 2950$). These variations highlight the complexity and diversity of residual oils. These ranges demonstrate the wide variety of molecule structures that are present and their important influence on the characteristics of oil.

Crucially, the origin of the vacuum residual oil affects the composition of SARA fractions, which in turn affects attributes like density, hydrogen content, and Conradson carbon concentration. This diversity suggests that in addition to SARA analysis, careful consideration of the residual oils' provenance and the particular analytical techniques used are also necessary for a complete characterization of the oils. The observed differences in molecular weight among various oils highlight the necessity of customized analytical methods to completely understand their makeup and function. Beyond SARA analysis, sophisticated analytical methods have become essential for gaining molecular-level understanding of heavy oils, such as FT-ICR Mass Spectrometry. These methods are critical for creating comprehensive kinetic models that are necessary for industrial residue conversion process optimization. Despite these developments, the high viscosity, low volatility, and melting point of vacuum residual oils continue to pose difficulties for reliable analysis, frequently producing unexpected results in simple physical property evaluations. Although residual oil



characterization has advanced significantly, more study and technical advancement are needed to solve lingering issues and deepen our understanding. For chemical engineers working in commercial residual oil conversion units, further developments in analytical methodologies are essential to their ability to efficiently optimize conversion operations. In the end, thorough residual oil characterisation promotes the efficient and sustainable use of these priceless resources in the global energy landscape in addition to improving industrial applications.

9. Future Directions and Challenges

Future directions and challenges in the analysis of vacuum residue oil present exciting opportunities for advancement in the field.

- One promising direction involves the integration of advanced spectroscopic and chromatographic methods that improve data analysis and interpretation using artificial intelligence and machine learning algorithms. This interdisciplinary approach holds the potential for more accurate and efficient characterization of complex oil matrices, enabling deeper insights into their chemical composition and properties.
- Additionally, further research efforts could focus on developing novel analytical methods capable of addressing specific challenges associated with vacuum residue oil analysis, such as the characterization of high molecular weight compounds and the detection of trace-level impurities. Moreover, the exploration of greener and more sustainable analytical approaches, such as green chromatography and spectroscopy, could contribute to reducing the environmental footprint of oil analysis processes. However, several challenges remain, including the development of standardized protocols for vacuum residue oil analysis, the optimization of analytical techniques for real-time monitoring in industrial settings, and the interpretation of complex data obtained from advanced analytical instruments.

References:

1. Iliyan Kolev, Dicho Stratiev, Ivelina Shishkov, Effect of Crude Oil Quality on Properties of Hydrocracked Vacuum Residue and Its Blends with Cutter Stocks to Produce Fuel Oil Processes 2023, 11(6), 1733;
2. Zhu, X.C., Shi, Q.A., Zhang, Y.H., Pan, N., Xu, C.M., Chung, K.H., Zhao, S., Characterization of nitrogen compounds in Coker heavy gas oil and its subfraction by liquid chromatographic separation followed by Fourier transform ion cyclotron resonance mass spectrometry. *Energy Fuel*. 2011; 25, 281–287.
3. Wiehe, I.A., A solvent-resid phase diagram for tracking resid conversion. *Ind. Eng. Chem. Res.* 1992; 31, 530–536.
4. Wiehe, I.A., Asphaltene solubility and fluid compatibility. *Energy Fuels* 2012; 26, 4004–4016.
5. Wiehe, I.A., *Process Chemistry of Petroleum Macromolecules*. Taylor & Francis Group. CRC Press, Boca Raton. 2008.
6. Wiehe, I.A., Liang, K.S., Asphaltenes, resins, and other petroleum macromolecules. *Fluid Phase Equilib* 1996; 117, 201–210.
7. Woods, J., Kung, J., Kingston, D., Kotlyar, L., Sparks, B., McCracken, T., Canadian crudes: a comparative study of SARA fractions from a modified HPLC separation technique. *Oil Gas Sci. Technol.* 2008; 63, 151–163.
8. Wu, Y., Zhang, N., Molecular management of gasoline streams. *Chem Eng Trans* 2009; 18, 749–754.
9. D., Hou, J., Doda, A., Trivedi, J., Application of organic alkali for heavy-oil enhanced oil recovery (EOR), in comparison with inorganic alkali. *Energy Fuels* 2016; 30, 4583–4595.
10. Xu, C., Gao, J., Zhao, S., Lin, S., Correlation between feedstock SARA components and FCC product yields. *Fuel* 2005; 84, 669–674.
11. Xu, H.H., Okazawa, N., Moore, R.G., Mehta, S.A., Laureshen, C.J., Ursenbach, M.G., Mallory, D., In situ upgrading of heavy oil. *J CAN PETROL TECHNOL* 2001; 40.
12. Vargas, F.M., Chapman, W.G., Application of the One-Third rule in hydrocarbon and crude oil systems. *Fluid Phase Equilib.* 2010; 290, 103–108.
13. Verstraete, J.J., Revellin, N., Dulot, H., Hudebine, D., Molecular reconstruction of vacuum gasoils. *Prep Am Chem Soc Div Fuel Chem* 2004; 49, 20–21.



14. Verstraete, J.J., Schnongs, Ph, Dulot, H., Hudebine, D., Molecular reconstruction of heavy petroleum residue fractions. *Chem. Eng. Sci.* 2010; 65, 304–312.
15. Verkoczy, B., Factors affecting cooking in heavy oil cores, oils and SARA fractions under thermal stress. *J. Can. Pet. Technol.* 1993; 32, 7.
16. Stratiev, D., Shishkova, I., Marinov, I., Nikolaychuk, E., Nedelchev, A., Ivanova, H., Yordanov, D., Tankov, I., Mitkova, M., Stanulov, K., Toteva, V., Paramonov, P.V., Chernyshova, E.A., Obryvalina, A.N., Effect of feedstock origin on conversion and yields of products from the ebullated bed vacuum residue hydrocracker. *Neftepererabotka i neftechimia* 2017; 10, 3–13.
17. Stratiev, D.S., Shishkova, I.K., Nikolaychuk, E., Sharafutdinov, I.M., Vely, A., Mitkova, M., Yordanov, D., Rudnev, N., Relationship of the aromatic structural types in vacuum gas oil to empirical correlations based on bulk properties. *Petrol. Sci. Technol.* 2016; 34 (9), 860–865.
18. Stratiev, D., Shishkova, I., Nikolova, R., Tsaneva, T., Mitkova, M., Yordanov, D., Investigation on precision of determination of SARA analysis of vacuum residual oils from different origin. *Pet. Coal.* 2016; 58, 109–119.
19. Murgich, J., Abanero, J.A., Molecular recognition in aggregates formed by asphaltene and resin molecules from the Athabasca oil sand. *Energy Fuels* 1999; 13, 278–286.
20. Nassar, N.N., Hassan, A., Pereira-Almao, P., Application of nanotechnology for heavy oil upgrading: catalytic steam gasification/cracking of asphaltenes. *Energy Fuels* 2011; 25, 1566–1570.
21. Nazar, A.R.S., Bayandory, L., Investigation of asphaltene stability in the Iranian crude oils. *Iranian Journal of Chemical Engineering* 2008; 5 (1), 3–12.
22. Nedelchev, A., Stratiev, D., Stoilov, G., Dinkov, R., Lepidis, K., Sharpe, R., Russell, C.A., Petkova, N., Petkov, P., Visbreaker performance improvement by optimisation of process conditions and application of chemical additive treatment program. *OG* 2013; 3, 147–153.
23. Negin, C., Ali, S., Xie, Q., Application of nanotechnology for enhancing oil recovery: a review. *Petroleum* 2016; 2, 324–333.
24. Stratiev, D., Shishkova, I., Tsaneva, T., Mitkova, M., Yordanov, D., Investigation of relations between properties of vacuum residual oils from different origin, and of their deasphalted and asphaltene fractions. *Fuel* 2016; 170, 115–129.
25. Stratiev, D.S., Sotirov, S., Shishkova, I., Nedelchev, A., Sharafutdinov, I., Veli, A., Mitkova, M., Yordanov, D., Sotirova, E., Atanassova, V., Atanassov, K., Stratiev, D.D., Rudnev, N., Ribagin, S., Investigation of relationships between bulk properties and fraction properties of crude oils by application of the Intercriteria Analysis. *Petrol. Sci. Technol.* 2016; 34, 1113–1120. 2016.1188114.
26. Strausz, O.P., Mojelsky, T.W., Lown, E.M., The molecular structure of asphaltene: an unfolding story. *Fuel* 1992; 71, 1355–1363. 90206-4.
27. Li, Y., Deng, X., Yu, W., Group-type analyses of heavy petroleum fractions by preparative liquid chromatography and synchronous fluorescence: analyses of aromatics by ring number of Liaohe vacuum gas oil, coker gas oil and heavy cycle oil. *Fuel* 1998; 77, 277–284.
28. Liang, W., Que, G., Chen, Y., Liu, C., Chemical Composition and Characteristics of Residues of Chinese Crude Oils, Asphaltenes and Asphalts. *Developments in Petroleum Science. Elsevier Science B.V.* 2000; 40, 280-304.
29. Liao, Z., Zhao, J., Creux, P., Yang, C., Discussion on the structural features of asphaltene molecules. *Energy Fuels* 2009; 23, 6272–6274.
30. Liguras, D.K., Allen, D.T., Structural models for catalytic cracking 1. Model compound reactions. *Ind. Eng. Chem. Res.* 1989; 28, 674–683.
31. Liu, C., Que, G., Chen, Y., Liang, W., Characterization of vacuum residues by adsorption chromatography and ¹H-NMR spectroscopy. *Fuel Sci. Technol. Int.* 1988; 6, 449–469.
32. Ch, Zhu, Ch, Jin, L., Shen, R., Liang, W., Step by step modeling for thermal reactivities and chemical compositions of vacuum residues and their SFEP asphalts. *Fuel Process. Technol.* 1999; 59, 51–67.
33. Liu, H., Wang, Z., Guo, A., Lin, C., Chen, K., The distribution of Ni and V in resin and asphaltene subfractions and its variation during thermal processes. *Petrol. Sci. Technol.* 2015; 33, 203–210.
34. , P., Shi, Q., Chung, K.H., Zhang, Y., Pan, N., Zhao, S., Xu, C., Molecular characterization of sulfur



- compounds in Venezuela crude oil and its SARA fractions by electrospray ionization Fourier transform ion cyclotron resonance mass spectrometry. *Energy Fuels* 2010; 24, 5089–5096.
35. Maity, S.K., Ancheyta, J., Marroquin, G., Catalytic aquathermolysis used for viscosity reduction of heavy crude oils: a review. *Energy Fuels* 2010; 24, 2809–2816.
36. Matsushita, K., Marafi, A., Hauser, A., Stanislaus, A., Relation between relative solubility of asphaltenes in the product oil and coke deposition in residue hydroprocessing. *Fuel* 2004; 83, 1669–1674.
37. Marques, L.C.C., Pereira, J.O., Bueno, A.D., Marques, V.S., Lucas, E.F., Mansur, C.R.E., Machadod, A.L.C., González, G., A study of asphaltene-resin interactions. *J. Braz. Chem. Soc.* 2012.; 23, 1880–1888.
38. Marques, S., Maget, J., Verstraete, M.J.J., Improvement of ebullated-bed effluent stability at high conversion operation. *Energy Fuels* 2011; 25, 3867–3874.
39. Martens, G.G., Marin, G.B., Kinetics for hydrocracking based on structural classes: model development and application. *AIChE J.* 2001; 47, 1607–1622.
40. McDermott, J.B., Libanati, C., LaMarca, C., Klein, M.T., Quantitative use of model compound information: Monte Carlo simulation of the reactions of complex macromolecules. *Ind. Eng. Chem. Res.* 1990; 29, 22–29.
41. McKenna, A.M., Marshall, A.G., Rodgers, R.P., Heavy petroleum composition. 4. Asphaltene compositional space. *Energy Fuels* 2013; 27, 1257–1267.
42. McKenna, A.M., Williams, J.T., Putman, J.C., Aeppli, C., Reddy, C.M., Valentine, D.L., Lemkau, K.L., Kellermann, M.Y., Savory, J.J., Kaiser, N.K., Marshall, A.G., Rodgers, R.P., Unprecedented ultrahigh resolution FT-ICR mass spectrometry and parts-per-billion mass accuracy enable direct characterization of nickel and vanadyl porphyrins in petroleum from natural seeps. *Energy Fuels* 2014; 28, 2454–2464.
43. Melendez, L.V., Lache, A., Orrego-Ruiz, J.A., Pachon, Z., Mejia-Ospino, E., Prediction of the SARA analysis of Colombian crude oils using spectroscopy and chemometric methods. *J. Pet. Sci. Eng.* 2012, 90–9, 56–60.
44. Merdignac, I., Espina, D., Physicochemical characterization of petroleum fractions: the state of the art. *Oil Gas Sci Technol-Rev IFP.* 2007; 62, 8–29.
45. Merino-Garcia, D., Andersen, S.I., Thermodynamic characterization of asphalteneresin interaction by microcalorimetry. *Langmuir* 2004; 20, 4559–4565.
46. Molina, D.V., Uribe, U.N., Murgich, J., Correlations between SARA fractions and physicochemical properties with ¹H NMR spectra of vacuum residues from Colombian crude oils. *Fuel* 2010; 89, 185–192.
47. , R.G., Laureshen, C.J., Mehta, S.A., Ursenbach, M.G., Belgrave, J.D.M., Weissman, J.G., Kessler, R.V., A downhole catalytic upgrading process for heavy oil using in situ combustion. *Journal petrol technol* 1999; 38.
48. Morgan, T.J., Alvarez-Rodriguez, P., George, A., Herod, A.A., Kandiyoti, R., Characterization of Maya crude oil maltenes and asphaltenes in terms of structural parameters calculated from nuclear magnetic resonance (NMR) spectroscopy and laser desorption-mass spectroscopy (LD-MS). *Energy Fuels* 2010; 24, 3977–3989.
49. Moy, F., Mangani, F., Hofhine, T.R., A novel petrochemistry solution: SARA fractionation of crude oil using an adaptable Gilson MPLC system. 2013.
50. Karimi, A., Qian, K., Olmstead, W.N., Freund, H., Yung, C., Gray, M.R., Quantitative evidence for bridged structures in asphaltenes by thin film pyrolysis. *Energy Fuels* 2011. ; 25, 3581–3589.
51. , M.R., Correlation between Refractive Indices and Other Fuel-Related Physical/chemical Properties of Pyrolysis Liquids Derived from Coal. 2017.
52. Kharrat, A.M., Zacharia, J., Cherian, V.J., Anyatonwu, A., Issues with comparing SARA methodologies. *Energy Fuels* 2007; 21, 3618–3621.
53. Khorasheh, F., Khaledia, R., Gray, M.R., Computer generation of representative molecules for heavy hydrocarbon mixture. *Fuel* 1998; 77, 241–253.
54. Kim, E., Cho, E.J., Moon, S., Park, J.I., Kim, S., Characterization of petroleum heavy oil fractions prepared by preparatory liquid chromatography



- with thin-layer chromatography, high-resolution mass spectrometry, and gas chromatography with an atomic emission detector. *Energy Fuels* 2016; 30 (4), 2932–2940.
55. Kim, J.G., Kim, J.H., Song, B.J., Jeon, Y.P., Lee, ChW., Lee, Y.S., Im, J.S., Characterization of pitch derived from pyrolyzed fuel oil using TLC-FID and MALDITOF. *Fuel* 2016; 167, 25–30.
56. Klee, T., Masterson, T., Miller, B., Barrasso, E., Bell, J., Lepkowitz, R., West, J., Haley, J.E., Schmitt, D.L., Flikkema, J.L., Cooper, T.M., Ruiz-Morales, Y., Mullins, O.C., Triplet electronic spin states of crude oils and asphaltenes. *Energy Fuels* 2011; 25, 2065–2075.
57. Koots, G.C., Angstrom, A., Rodgers, R.P., Marshall, A.G., Use of saturates/aromatics/resins/asphaltenes (SARA) fractionation to determine matrix effects in crude oil analysis by electrospray ionization Fourier transform, ion cyclotron resonance mass spectrometry. *Energy Fuel*. 2006; 20, 668–672.
58. Koots, J.A., Speight, J.G., Relation of petroleum resins to asphaltenes. *Fuel* 54, 179–184. Kuo, C.J., 1984. Effects of crude types on visbreaker conversion. *Oil Gas J.* 1975; 82 (39), 100–103.
59. Lee, S., Speight, J.G., Loyalka, S.K., *Handbook of Alternative Fuel Technologies*. CRC Press, Florida. 2007.
60. , A.Y., Parra, M.J., Determination of molecular weight of vacuum residue and their SARA fractions. *C.T. F Ciencia, Tecnol., Futuro* 2010; 4, 101–112.
61. Leon, O., Contreras, E., Rogel, E., Dambakli, G., Acevedo, S., Carbognani, L., Espidel, J., Adsorption of native resins on asphaltene particles: a correlation between adsorption and activity. *Langmuir* 2002.; 18,5106–5112.
62. Li, D.D., Greenfield, M.L., Chemical compositions of improved model asphalt systems for molecular simulations. *Fuel* 2014; 115, 347–356.
63. Hashemi, R., Nassar, N.N., Almao, P.P., Enhanced heavy oil recovery by in situ prepared ultradispersed multimetallic nanoparticles: a study of hot fluid flooding for athabasca bitumen recovery. *Energy Fuels* 2013; 27, 2194–2201.
64. Hashmi, S.M., Firoozabadi, A., elf-assembly of resins and asphaltenes facilitates asphaltene dissolution by an organic acid. *J. Colloid Interface Sci.* 2013; 394, 115–123.
65. Hayes, M.H., Stacey, M., Standley, J., Studies on bitumen: Part 1. Characterization of bitumen by use of physical methods. *Fuel* 1972; 51, 27–31.
66. Hauser, A., Alhumaidan, F., Al-Rabiah, H., Absi Halabi, M., Study on thermal cracking of Kuwaiti heavy oil (vacuum residue) and its SARA fractions by NMR spectroscopy. *Energy Fuels* 2014; 28 (7), 4321–4332.
67. , A.A., Bartle, K.D., Kandiyoti, R., Molecular size and weight of asphaltene and asphaltene solubility fractions from coals, crude oil sand bitumen. *Reply. Fuel*. 2007; 86, 309–312.
68. Herod, A.A., Bartle, K.D., Kandiyoti, R., Characterization of heavy hydrocarbons by chromatographic and mass spectrometric methods: an overview. *Energy Fuels* 2007; 21, 2176–2203.
69. Herod, A.A., Bartle, K.D., Morgan, T.J., Kandiyoti, R., Analytical methods for characterizing high-mass complex polydisperse hydrocarbon mixtures: an overview. *Chem. Rev.* 2012; 112, 3892–3923.
70. Hertkorn, N., Ruecker, C., Meringer, M., Gugisch, R., Frommberger, M., Perdue, E.M., Witt, M., Schmitt-Kopplin, P., High-precision frequency measurements: indispensable tools at the core of the molecular-level analysis of complex systems. *Anal. Bioanal. Chem.* 2007; 389, 1311–1327.
71. Hinkle, A., Shin, E.J., Liberatore, M.W., Herring, A.M., Batzle, M., Correlating the chemical and physical properties of a set of heavy oils from around the world. *Fuel* 2008.; 87, 3065–3070.
72. E., Watkinson, P., A study of asphaltene solubility and precipitation. *Fuel* 2004; 83,1881–1887.
73. Hong, E., Watkinson, P., Precipitation and fouling in heavy oil–diluent blends. *Heat Transf. Eng.* 2009; 30 (10–11), 786–793.
74. Hongfu, Y., Xiaoli, C., Haoran, L., Yupeng, X., Determination of multi-properties of residual oils using mid-infrared attenuated total reflection spectroscopy. *Fuel* 2006; 85, 1720–1728.
75. , S.R., Zhang, L., Z., Bennett, C.A., Klein, M.T., Zhao, S., Molecular level kinetic modeling of resid pyrolysis. *Ind. Eng. Chem. Res.* 2015; 54, 4226–4235.
76. Hou, Z., Zhang, L., , S.R., Shi, Q., Zhao, S., Xu, C., Klein, M.T., Molecular level composition and



- reaction modeling for heavy petroleum complex system, 2015.
77. Xu, C., Shi, Q. (Eds.), *Structure and Modeling of Complex Petroleum Mixtures. Structure and Bonding*, Springer, Cham, vol. 168, pp. 93–119.
78. C.S., Hendrickson, C.L., Rodgers, R.P., McKenna, A.M., Marshall, A.G., *Petroleomics: advanced molecular probe for petroleum heavy ends. J. Mass Spectrom.* 2011; 46, 337–343.
79. Hsu, C.S., Lobodin, V.V., Rodgers, R.P., McKenna, A.M., Marshall, A.G., *Compositional boundaries for fossil hydrocarbons. Energy Fuels* 2011; 25, 2174–2178.
80. Hsu, C.S., McLean, M.A., Qian, K., Aczel, T., Blum, S.C., Olmstead, W.N., Kaplan, L.H., Robbins, W.K., Schulz, W.W., *Online liquid-chromatography mass-spectrometry for heavy hydrocarbon characterization. Energy Fuels* 1991; 5, 395–398.
81. Liñan, L.Z.; Lima, N.M.N.; Maciel, M.R.W.; Filho, R.M.; Medina, L.C.; Embiruçu, M. Correlation for predicting the molecular weight of Brazilian petroleum residues and cuts: An application for the simulation of a molecular distillation process. *J. Pet. Sci. Eng.* 2011, 78, 78–85.
82. Rodriguez, A.L.C.; Tovar, L.P.; Maciel, M.R.W.; Filho, R.M. Optimizing the Polynomial to Represent the Extended True Boiling Point Curve from High Vacuum Distillation Data Using Genetic Algorithms. *Chem. Eng. Trans.* 2015, 43, 1561–1566.
83. Sbaite, P.; Batistella, C.B.; Winter, A.; Vasconcelos, C.J.G.; Maciel, M.R.W.; Filho, R.M.; Gomes, A.; Medina, L.; Kunert, R. True Boiling Point Extended Curve of Vacuum Residue Through Molecular Distillation. *Pet. Sci. Technol.* 2006, 24, 265–274.
84. Haynes, H.W.; Matthews, M.A. Continuous-Mixture Vapor-Liquid Equilibria Computations Based on True Boiling Point Distillations. *Ind. Eng. Chem. Res.* 1991, 30, 1911–1915.
85. Lopes, M.S.; Watanabe, E.R.L.D.R.; Lopes, E.S.; Gomes, V.M.; Medina, L.C.; Filho, R.M.; Maciel, M.R.W. Extending the true boiling point curve of heavy crude oil utilizing molecular distillation and characterization of the products obtained. *Pet. Sci. Technol.* 2017, 35, 1523–1529.
86. Coronel-García, M.; de la Torre, A.R.; Domínguez-Esquivel, J.; Melo-Banda, J.; Martínez-Salazar, A. Heavy oil hydrocracking kinetics with nano-nickel dispersed in PEG300 as slurry phase catalyst using batch reactor. *Fuel* 2021, 283, 118930.
87. J.S. Buckley, Y. Some mechanisms of crude oil/brine/solid interactions, *Journal of Petroleum Science and Engineering*; 20, 155–160.
88. Hemmingsen, P.V.; Silset, A.; Hannisdal, A.; Sjöblom, J. Emulsions of Heavy Crude Oils. I: Influence of Viscosity, Temperature, and Dilution. *J. Dispers. Sci. Technol.* 2005, 26, 615–627.
89. D.; Nenov, S.; Shishkova, I.; Georgiev, B.; Argirov, G.; Dinkov, R.; Yordanov, D.; Atanassova, V.; Vassilev, P.; Atanassov, K. Commercial Investigation of the Ebullated-Bed Vacuum Residue Hydrocracking in the Conversion Range of 55–93%. *ACS Omega* 2020, 5, 33290–33304.
90. Yarranton, H. Prediction of Crude Oil Saturate Content from a SimDist Assay. *Energy Fuels* 2022, 36, 8809–8817.
91. Stratiev, D.; Shishkova, I.; Dinkov, R.; Petrov, I.; Kolev, I.; Yordanov, D.; Sotirov, S.; Sotirova, E.; Atanassova, V.; Ribagin, S.; et al. Empirical Models to Characterize the Structural and Physiochemical Properties of Vacuum Gas Oils with Different Saturate Contents. *Resources* 2021, 10, 71.
92. Abutaqiya, M. Advances in Thermodynamic Modeling of Nonpolar Hydrocarbons and Asphaltene Precipitation in Crude Oils. Ph.D. Thesis, Rice University, Houston, TX, USA, 2019.
93. Abutaqiya, M.I.L.; Alhammadi, A.A.; Sisco, C.J.; Vargas, F.M. Aromatic Ring Index (ARI): A Characterization Factor for Nonpolar Hydrocarbons from Molecular Weight and Refractive Index. *Energy Fuels* 2021, 35, 1113–1119.
94. Stratiev, D.S.; Marinov, I.M.; Shishkova, I.K.; Dinkov, R.K.; Investigation on feasibility to predict the content of saturate plus mono-nuclear aromatic hydrocarbons in vacuum gas oils from bulk properties and empirical correlations. *Fuel* 2014, 129, 156–162.
95. Zheng, Y., Liu, H., & Zhang, J. Structural analysis of heavy oils via NMR and mass spectrometry. *Energy & Fuels*, 2023, 37(2), 2345-2356.



96. Lee, S., & Kim, H. NMR spectroscopy for characterization of petrochemical residues. *Fuel*, 2022, 250, 123-130.
97. Brown, A., Davis, P., & Williams, R. Insights into residual oils using NMR techniques. *Journal of Petroleum Science*, 2021, 60(4), 789-798.
98. Kumar, R., & Sharma, M. NMR spectroscopic investigation of heavy oil residues. *Chemical Engineering Journal*, 2020, 380, 1223-1230.
99. Chen, Q., Wang, L., & Li, F. Characterization of vacuum residue oil components. *Industrial & Engineering Chemistry Research*, 2019, 58(14), 5567-5574.
100. Zorzenão, P. C. S., Mariath, R. M., & Pinto, F. E. Klein subfractions extracted from Brazilian vacuum residue: Chemical characterization and stabilization of model water-in-oil (W/O) emulsions. *Journal of Petroleum Science*, 2018, 160, 1-11.
101. Zhao, Y., & Li, J. NMR analysis of heavy oil fractions. *Fuel Processing Technology*, 2017, 159, 45-52.
102. , T., Harris, R., & White, P. NMR spectroscopic studies on vacuum residues. *Petroleum Chemistry*, 2016; 56(6), 789-795.
103. Garcia, M., & Lopez, A. Comprehensive NMR study of petrochemical residues. *Applied Petrochemical Research*, 2015; 5(4), 231-240.
104. Wang, X., Zhang, Y., & Liu, Q. NMR and FT-ICR analysis of residual oils. *Journal of Fuel Chemistry*, 2014; 92(5), 412-421.
105. Verstraete, J.J., Revellin, N., Dulot, H., Hudebine, D., Molecular reconstruction of vacuum gasoils. *Prep Am Chem Soc Div Fuel Chem* 2004; 49, 20-21.
106. Verstraete, J.J., Schnongs, Ph, Dulot, H., Hudebine, D., Molecular reconstruction of heavy petroleum residue fractons. *Chem. Eng. Sci.* 2010; 65, 304-312.
107. Wang, Y., J., Miller, G., Harris, T., Moore, R. Optimization of GC-MS techniques for petrochemical analysis. *Analytical Methods*. 2022.
108. Wilson, A.; White, J.; Green, D. TLC-FID method for monitoring oil refinery processes. *Anal. Chem.* 2022; 94, 6271-6278.
109. Wiehe, I.A., Asphaltene solubility and fluid compatibility. *Energy Fuels* 2012; 26, 4004-4016.
110. I.A., Process Chemistry of Petroleum Macromolecules. Taylor & Francis Group. CRC Press, Boca Raton. 2008.
111. Wiehe, I.A., Liang, K.S., Asphaltenes, resins, and other petroleum macromolecules. *Fluid Phase Equilib* 1996; 117, 201-210.
112. Xie, D., Hou, J., Doda, A., Trivedi, J., Application of organic alkali for heavy-oil enhanced oil recovery (EOR), in comparison with inorganic alkali. *Energy Fuels* 2016; 30, 4583-4595.
113. Xu, C., Gao, J., Zhao, S., Lin, S., Correlation between feedstock SARA components and FCC product yields. *Fuel* 2005; 84, 669-674.
114. Xu, H.H., Okazawa, N., Moore, R.G., Mehta, S.A., Laureshen, C.J., Ursenbach, M.G., Mallory, D., In situ upgrading of heavy oil. *J CAN PETROL TECHNOL* 40. 2014.
115. Youtcheff, J. Automated high-performance liquid chromatography saturate, aromatic, resin, and asphaltene separation. Technical Report FHWA-HRT-15-055, Turner-Fairbank Highway Research Center, McLean, VA, USA. 2016; HRDI-10, (202) 493-3090.
116. Zhou, S.L., Zhou, Z.S., Wen, M.B., Lieh, C.L., Keqia, C.H., 1999. Research study on complex reaction of vacuum residual oil. *ACTA PetroleiSinica (Petroleum Processing Section)* 2011; 15, 73.
117. Alomair, O., Jumaa, M., Alkorie, A., Hamed, M., Heavy oil viscosity and density prediction at normal and elevated temperatures. *J. Petrol. Explor. Prod. Technol.* 2015; 6(2) 253-236.
118. Schabron, F., Gardner, G.W., Hart, J.K., Niss, N.D., Miyake, G., Netzel, D.A., The Characterization of Petroleum Residua, Report to Mobil Research and Development Corp. And DOE. 1993; 11076-3539.
119. Akbarzadeh, K., Alboudwarej, H., Svrcek, W.Y., Yarranton, H.W., A generalized regular solution model for asphaltene precipitation from n-alkane diluted heavy oils and bitumens. *Fluid Phase Equilib.* 2005; 232, 159-170.
120. Dinkov, R., Stratiev, D., Stanulov, K., Mitkova, M., Georgiev, K., Veli, A., Investigation on relationship between physicochemical properties of vacuum residual oils and their content of aromatic constituents. *Erdol ErdGas Kohle* 2014; 130, 195-199.



121. Ternan, M., Kriz, J.F., Effects of H/C ratio and molecular weight on microcarbon residue of vacuum resid subfractions. *Petrol. Sci. Technol.* 1998; 16, 167–168.

122. Fletcher, T.H., gasification fundamentals. In: *Integrated Gasification Combined Cycle (IGCC) Technologies*. Brigham Young University, 2017; pp. 223–256.

Figures and Tables

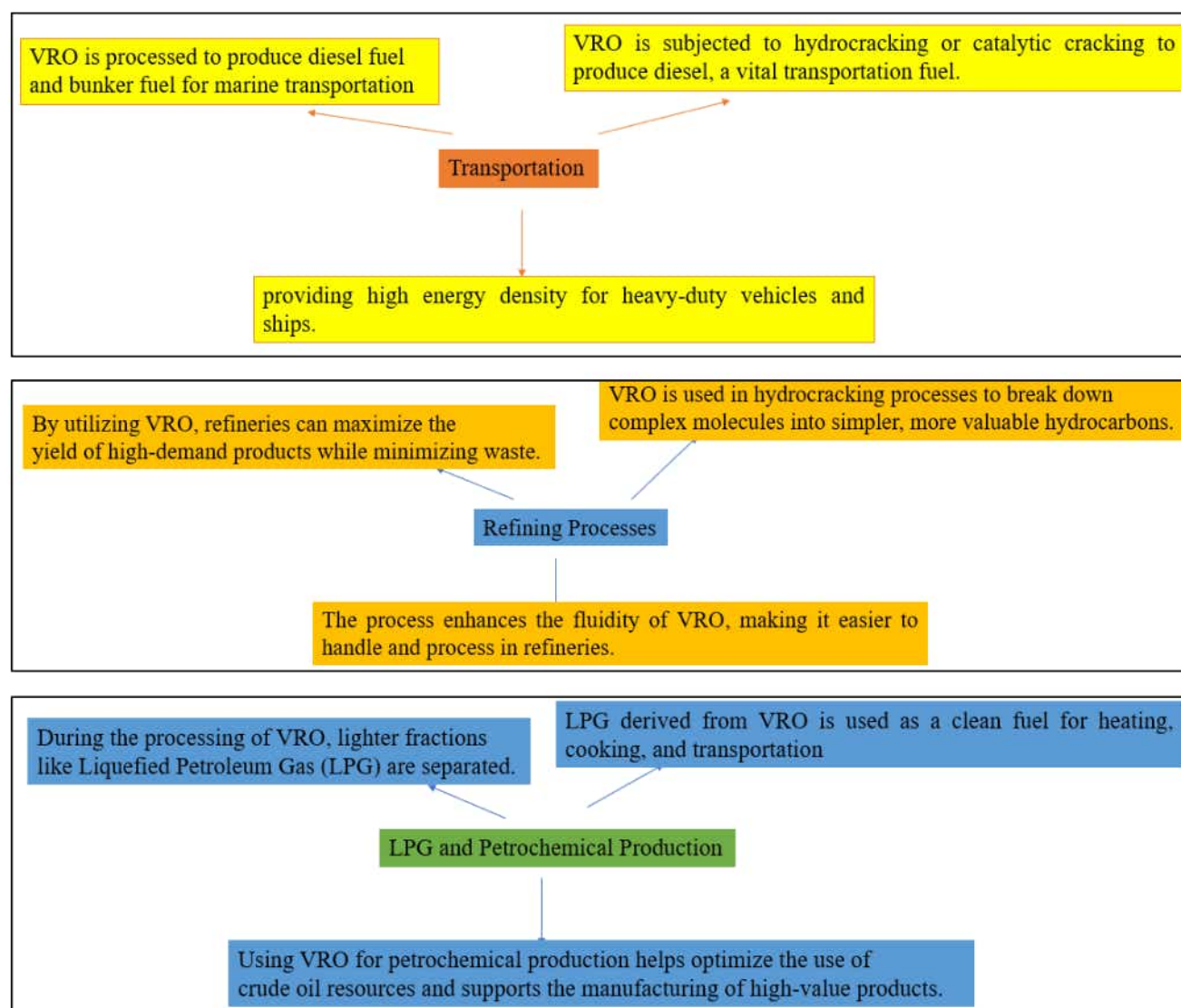


Figure 1. Positive perspectives for utilization of VRO

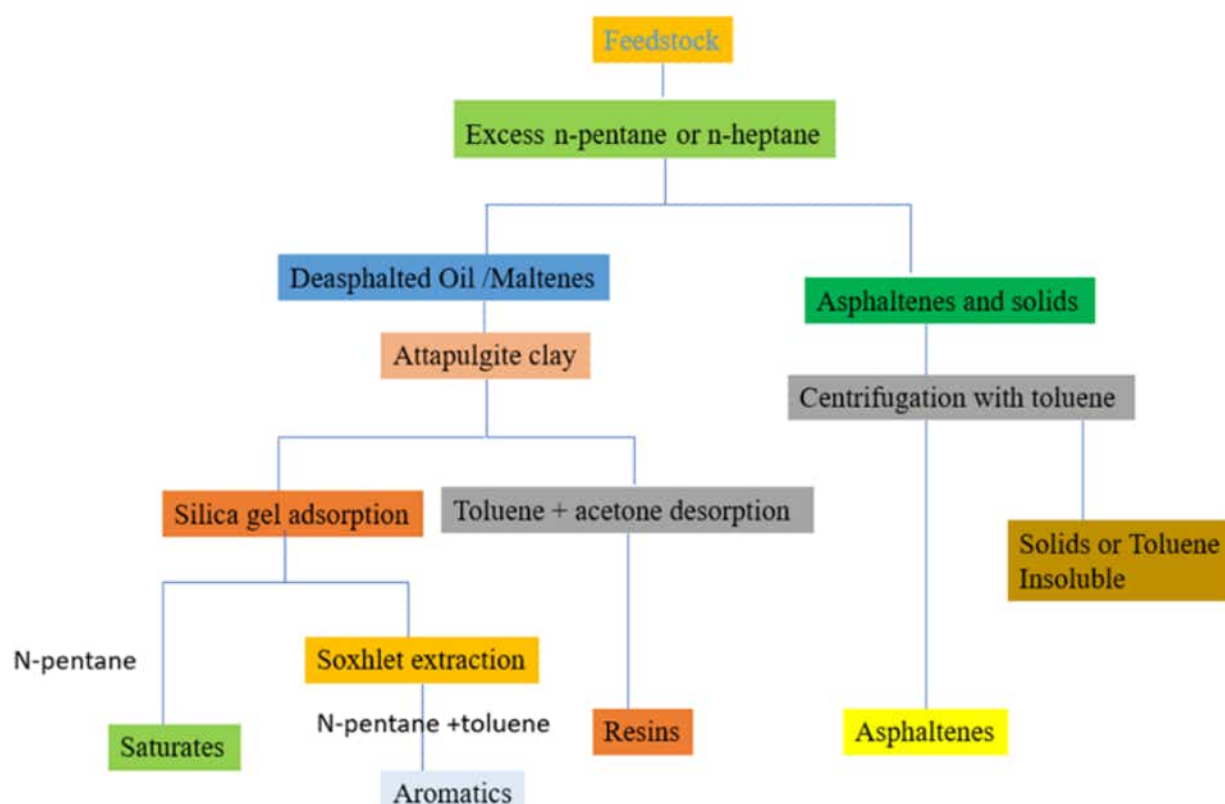
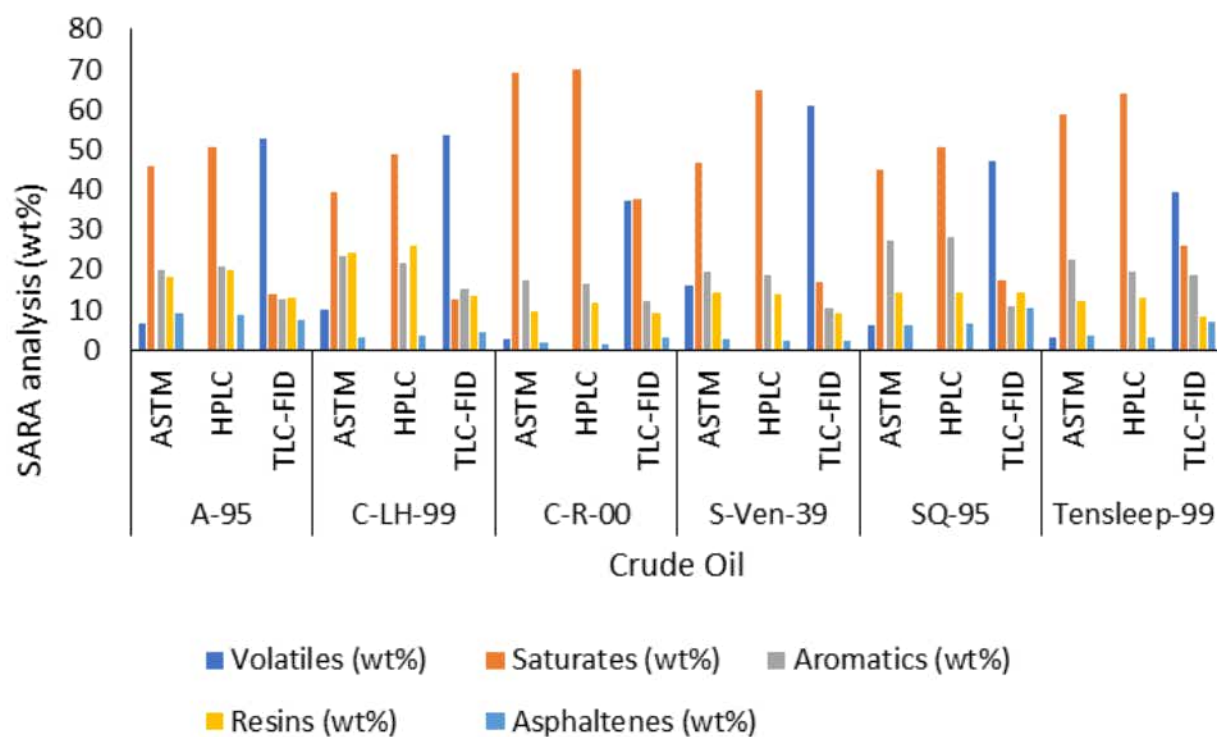
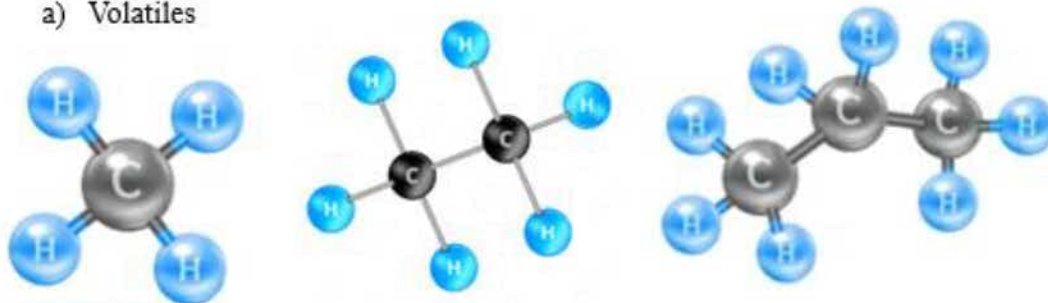


Figure 2. Schematic Procedure for SARA fractionation.

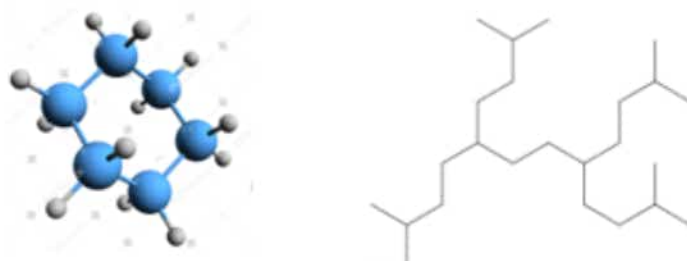




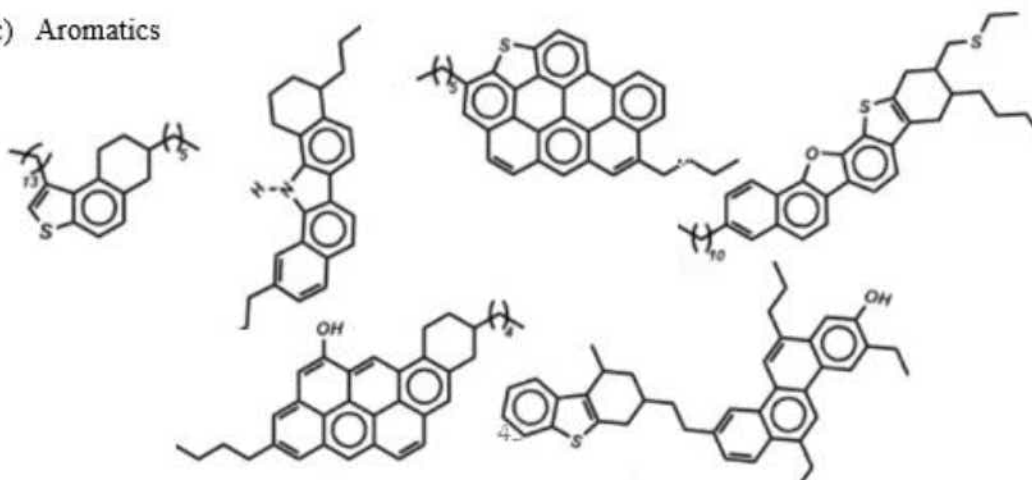
a) Volatiles



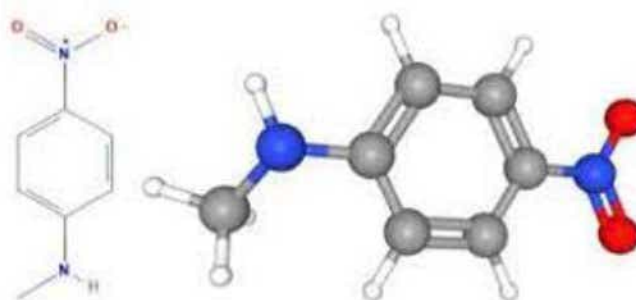
b) Saturates



c) Aromatics



e) Resins





f) Asphaltenes

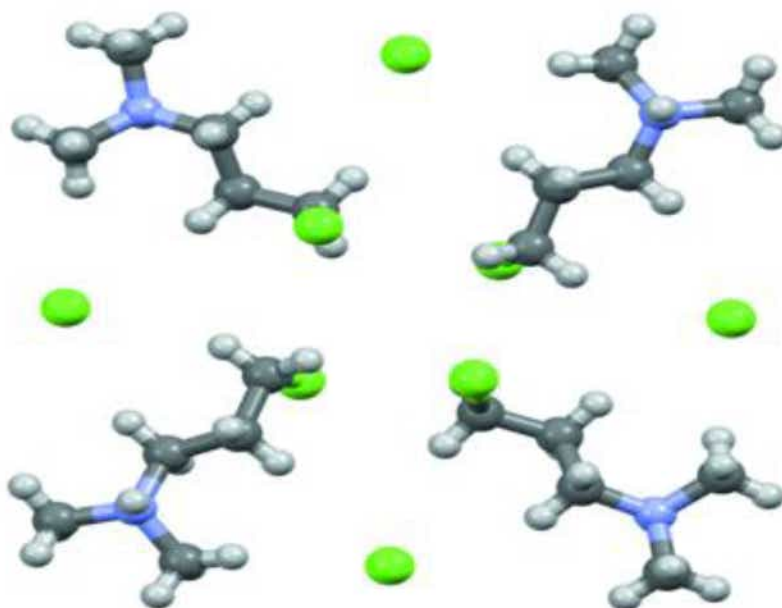


Figure 3. a. SARA analysis of various crude oils b. Fractions presents in the respective analysis.

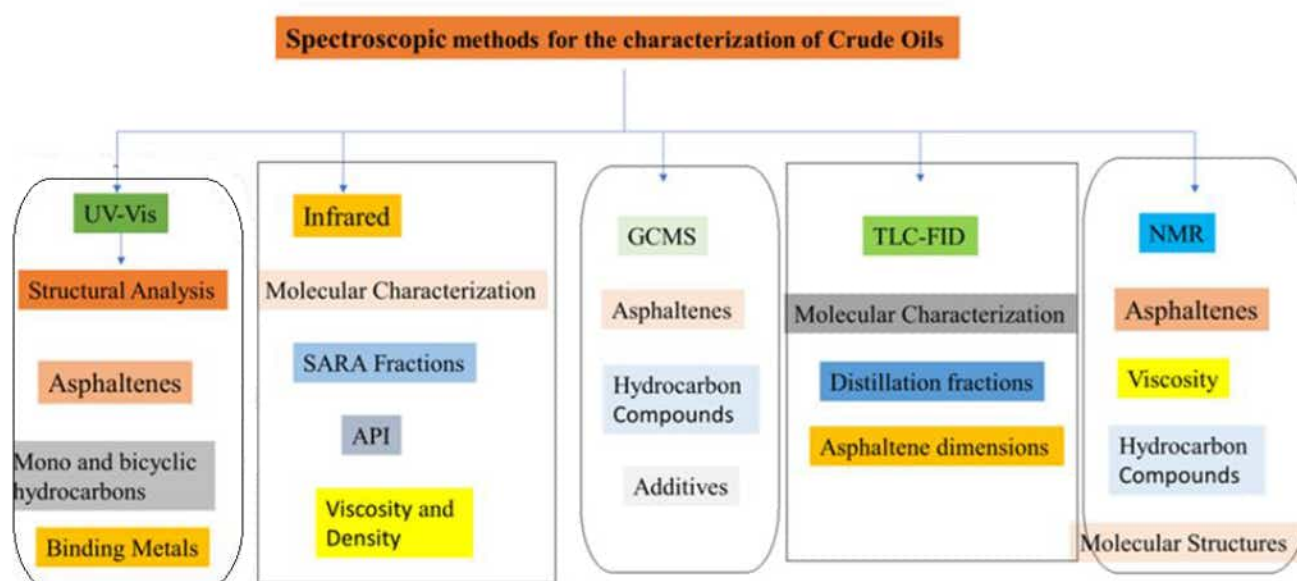
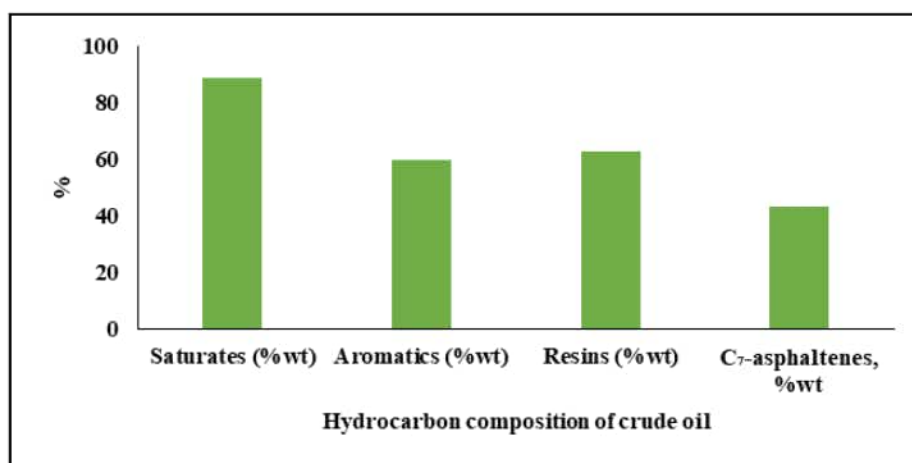
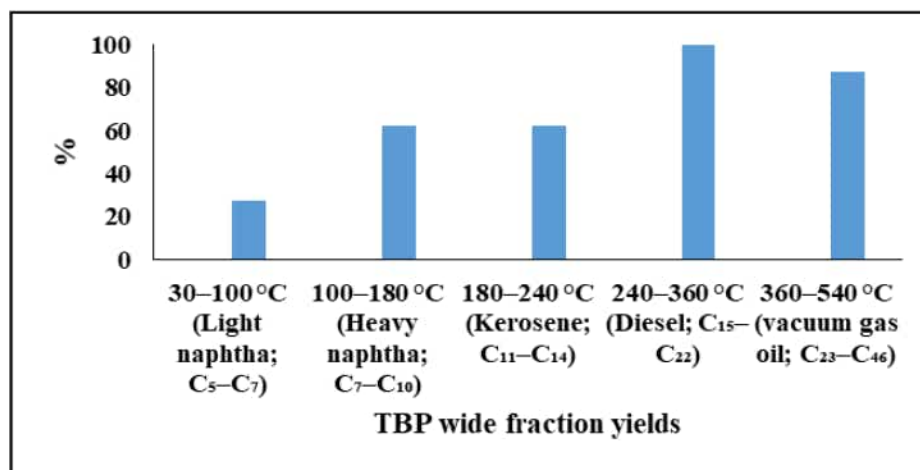


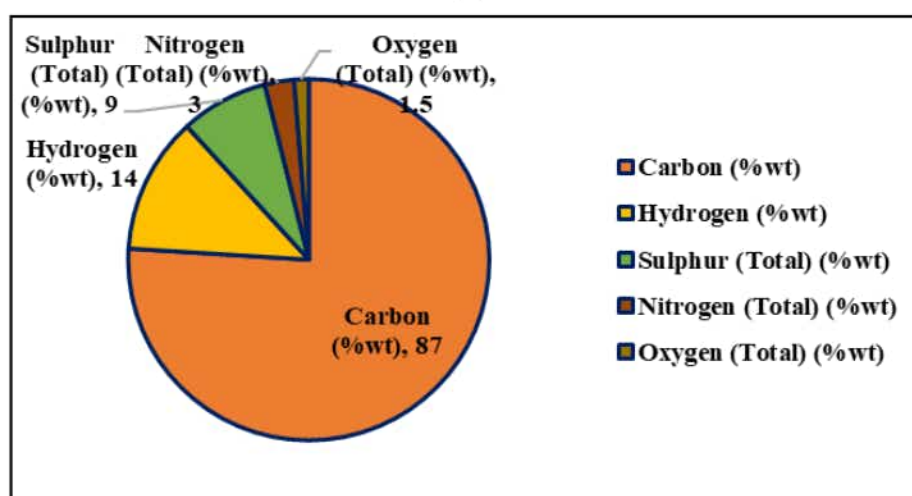
Figure 4. Spectroscopic methods for crude oil properties.



(a)



(b)



(c)

Figure 5. a) Hydrocarbon values of VRO; b) Maximum values of fractions in VRO; c) Group hydrocarbon composition of crude oil



Exploration of graphitic carbon from crude oil vacuum residue

Ravi Dalsania^{a,b,*}, Hasmukh Gajera^a, Mahesh Savant^b

^a Reliance Industries Limited, Village Motikhavdi, Jamnagar 361140, Gujarat, India

^b Department of Chemistry, Atmiya University, Rajkot, Gujarat 360005, India

ARTICLE INFO

Keywords:

ARA analysis
Characterization
¹H and ¹³C NMR
Vacuum residue
Graphitic carbon

ABSTRACT

Preparation of graphitic carbon from low value refinery waste has captivated immense interest in past years owing to its low cost and abundant nature. Successful utilization of petroleum vacuum residue is a major challenge in the petroleum industry. In this study pyrolysis of vacuum residue fractions has been carried out for the preparation of graphitic carbon like material. The vacuum residue fractions were obtained from three different crude oils originated from Middle East, Canada and South America. The purity of the Aromatic, Resin and Asphaltene (ARA) fractions were confirmed using TLC-FID which denoted complete separation. The chemical composition were determined using elemental analysis and it revealed ARA fractions to be carbon rich regardless of its origin. Further, sulphur content was found to be high in ARA fractions from Heavy Crude oil (HCO). The degree of polymerization and molecular weight measured using GPC specify that asphaltene has high accumulation with high molecular weight compared with aromatic and resins. ARA derived carbon and heat-treated materials were analysed by TGA, XRD and Raman spectroscopy to study microstructural changes in formation of graphite like material. Thermogravimetric analysis of all ARA samples revealed the different decomposition stages for pyrolyzed, calcined and graphitized samples. The results of XRD demonstrated that the distance between the planes (d-spacing) is above 3.35 Å for all high temperature treated ARA derived carbon materials irrespective of its origin, indicating formation of graphite like structure. In Raman analysis, the nature and intensity of G and D bands evolution during each step of pyrolysis is supporting XRD results for formation of highly ordered graphitic carbon material. Furthermore, understanding feed quality has direct influence on high efficiency, low costs and sustainability, the major issues for oil refinery business.

1. Introduction

Oil reserves play a vital role in uplifting overall economy and hence petroleum is a key element of modern civilization. Its constant demand has increased the cost of refinery in world. The refineries major cost comes from crude oil procurement. Investigating innovative method to refine heavy oil to highly sought light oil is one promising way to cut down refinery costs. Though there are sophisticated methods a clear knowledge is still not achieved to understand the elaborate chemistry of petroleum. In general, it is understood that a diverse oil characterization is required to confront the challenge of crude oils complex nature [1]. In this regard numerous characterization studies on bulk physical and chemical properties; and on SARA analysis for crude oil have attracted more attention [2–5].

GPC is a common method for the estimation of molecular weight

distributions of asphaltene [6]. Gel permeation chromatography of the crude oil provides the benefit of short analysis time and offers reliable data on molecular weight distribution and its evaluation [7]. N. Alawani et al. [1] have used gel permeation chromatography to obtain chemically well-defined fractions on the separation of crude oils. B. Azinfar et al. [8] used both simulated distillation and GPC for a better insight of the molecular weight distributions of complex mixtures. Likewise, fractionation technique with combined separation power of TLC and a universal detector FID accompanied with the simplicity, short duration and low demand for hazardous solvents has made TLC-FID superior for the investigation of a wide spectrum of organic compounds [9,10]. TLC-FID is used extensively for measuring aromatic and saturated hydrocarbons, and asphaltene/resin extracts in solvent fractions of crude oils, petroleum source rocks, and reservoir rocks [11,12].

Furthermore, carbon, hydrogen, nitrogen, sulfur and oxygen

Abbreviation: ARA, aromatic resin and asphaltene; EHCO, extra heavy crude oil; LCO, light crude oil; HCO, heavy crude oil; TLC-FID, Thin layer chromatography and flame ionization detection; GPC, Gel Permeation Chromatography; FT-ICR, Fourier transform ion cyclotron resonance mass spectrometry.

* Corresponding author.

E-mail addresses: ravi.dalsania@ril.com (R. Dalsania), Hasmukh.Gajera@ril.com (H. Gajera).

<https://doi.org/10.1016/j.cartre.2024.100424>

Received 12 August 2024; Received in revised form 4 November 2024; Accepted 4 November 2024

Available online 5 November 2024

2667-0569/© 2024 The Author(s). Published by Elsevier Ltd. This is an open access article under the CC BY-NC-ND license (<http://creativecommons.org/licenses/by-nc-nd/4.0/>).

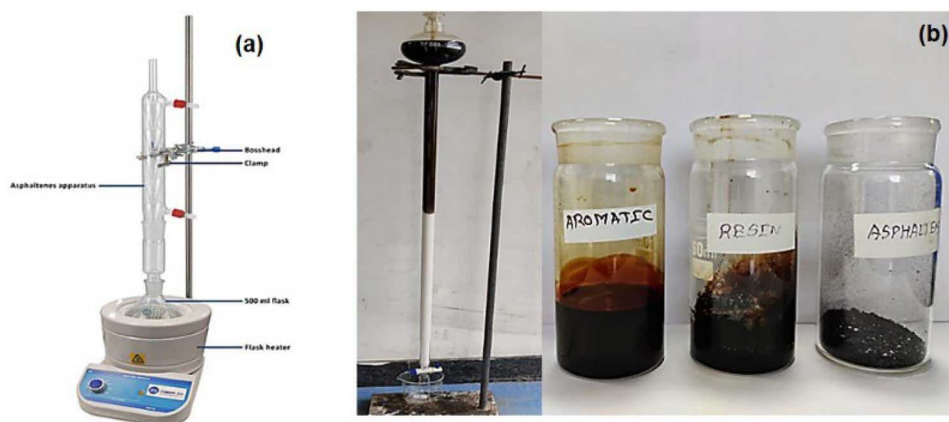


Fig. 1. a) Schematic of Soxhlet extractor for asphaltene separation and b) ARA fraction characterized in this study.

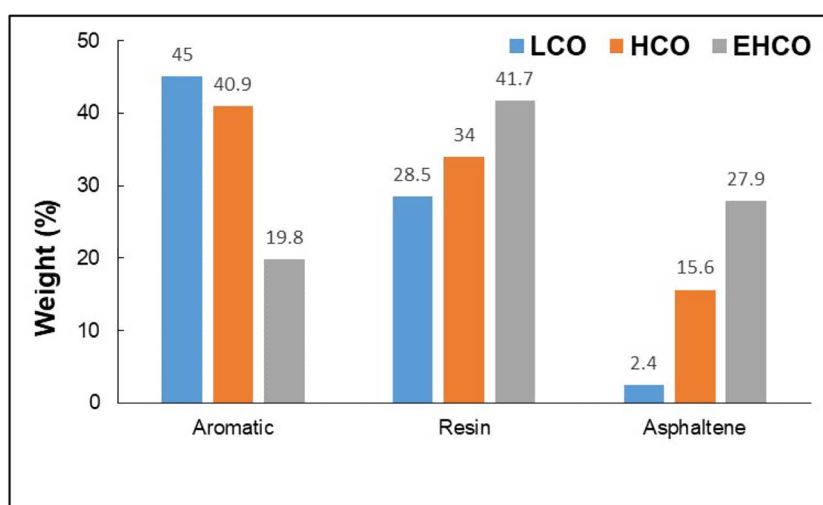


Fig. 2. Weight distribution of aromatic, resin and asphaltene (ARA) fractions for the three vacuum residues.

Table 1

Properties of vacuum residue fractions extracted from the crude oils under investigation.

Characteristics	LCO	HCO	EHCO
Pour point (wt. %)	60	118	139
CCR (wt. %)	22.7	29.3	35.1
Density (g/ml)	1.0339	1.0801	1.0856
Total carbon (wt. %)	83.8	82.87	85.06
Total Hydrogen (wt. %)	11.2	9.38	10.04
Total Nitrogen (wt. %)	0.66	0.77	1.01
Total Sulphur (wt. %)	3.68	6.17	3.54
Total Oxygen (wt. %)	0.66	0.81	0.35
Heteroatoms (wt. %)	5.00	7.75	4.90
C/H ratio	7.48	8.83	8.47
Total Metals (wt. ppm)	137	718	1464

(CHNSO) are few of the usually identified elements in crude oil which influence the fuel product properties. For example, sulfur content is one of the significant corrosive media in crude oil [13]. Similarly, nitrogen-containing compounds create problem such as deactivation and inhibition of acid catalyst, corrosion related to acid-base pair, and metal complexation [14]. Therefore, it is a common practice of elemental analysis for determination of CHNSO content in petroleum products. In the same way organometallic complexes are formed by the presence of metallic particles which tends to be significant precursors in the asphaltenes precipitation during the refining processes. ICP-OES is

broadly implemented in the petrochemical industry for the examination of trace elements during refining of crude oil [15,16]. Ash content a measure of inorganic impurities in the crude oil which affects boiler efficiency is also determined by ICP-OES [17,18].

In recent years, mass spectrometry serves as a basic approach for the accurate analysis of mass and structure of crude oil components [19–21]. J.M. Santos et al. [19] have shown SARA fractionation analysis by FT-ICR MS has allowed the individual fraction and selective chemical of the crude oil components characterization. Likewise, P. Juan et al. [20] have established the usage of FT-ICR MS as a potential tool in combination with supercritical fluid extraction fractionation to study molecular composition of the vacuum residue. Similarly, Z. Farmani et al. [21] have gained a clear image of the neglected fractions in crude oil studies and the saturate fraction by ultrahigh resolution mass spectrometry. Due to the occurrence of significant amount of compounds in crude oil, various ionization methods such as atmospheric pressure chemical ionization, electrospray ionization are employed for complex mixture analysis [22,23]. API-MS delivers option to handle the complex nature of crude oil by grouping compounds on the basis of heteroatom content, and designating molecular formulae [24].

In the same manner nuclear magnetic resonance and fourier transform infrared spectroscopy are utilized widely for the compositional inspection of crude oil. FTIR has been applied broadly for the structural determination of asphaltene [25–27]. M. Asemani et al. [27] performed geochemical correlation of different oil samples from four oil fields by applying FTIR spectroscopy to identify and relate asphaltene structures.

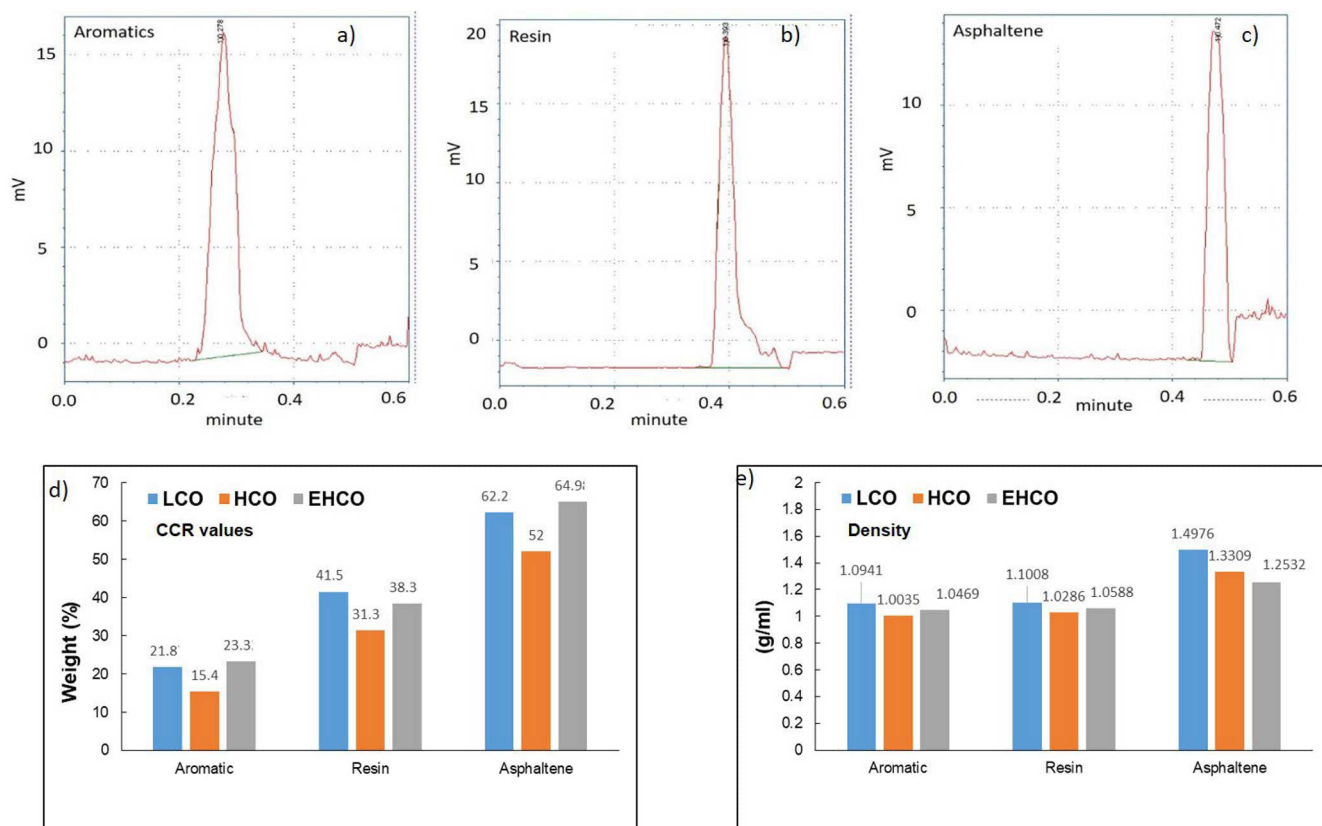


Fig. 3. TLC-FID chromatograms of the isolated a) aromatic, b) resin and c) asphaltene fractions, d) Conradson carbon residue prediction and e) density chart of ARA analysis.

Table 2

Origin based elemental analysis for extracted aromatic, resin and asphaltene.

Elemental Analysis	AROMATIC			RESIN			ASPHALTENE		
	LCO	HCO	EHCO	LCO	HCO	EHCO	LCO	HCO	EHCO
Total Carbon (wt. %)	85.24	83.11	85.41	84.91	82.88	85.09	84.51	82.20	86.71
Total Hydrogen (wt. %)	10.97	9.86	9.91	9.96	9.00	9.52	8.91	7.38	7.58
C/H ratio	7.77	8.43	8.62	8.53	9.21	8.94	9.48	11.14	11.44
H/C ratio	0.12	0.12	0.10	0.12	0.11	0.11	0.11	0.09	0.09
Total Nitrogen (wt. %)	0.41	0.39	0.72	0.97	1.09	1.32	1.56	1.36	1.65
Total Sulphur (wt. %)	2.7	5.78	3.18	3.06	6.25	3.34	3.53	8.34	3.97
Total Oxygen (wt. %)	0.61	0.86	0.78	1.10	0.78	0.73	1.49	0.72	0.09
Heteroatoms (wt. %)	3.72	7.03	4.68	5.13	8.12	5.39	6.58	10.42	5.71

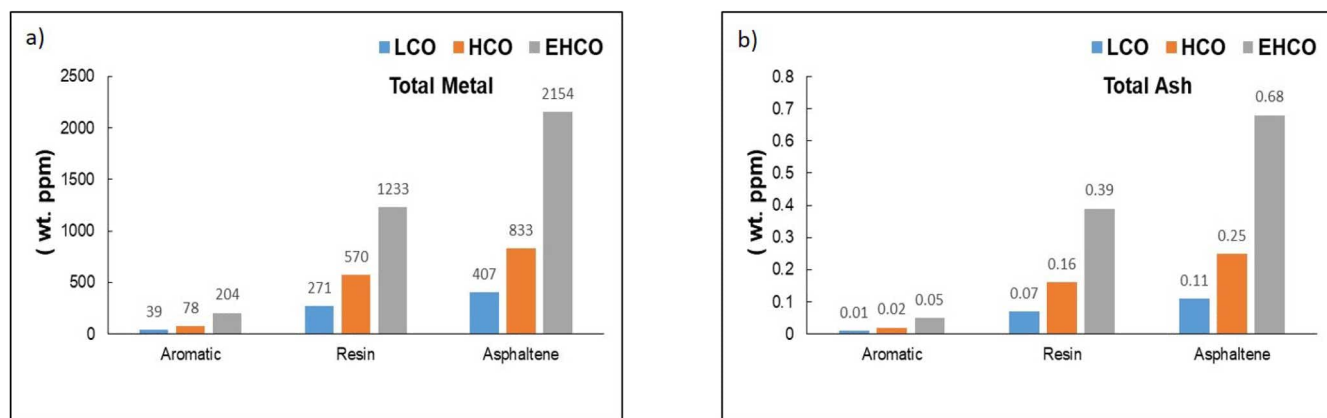


Fig. 4. Plot showing total metal and ash content in origin based ARA fractions.

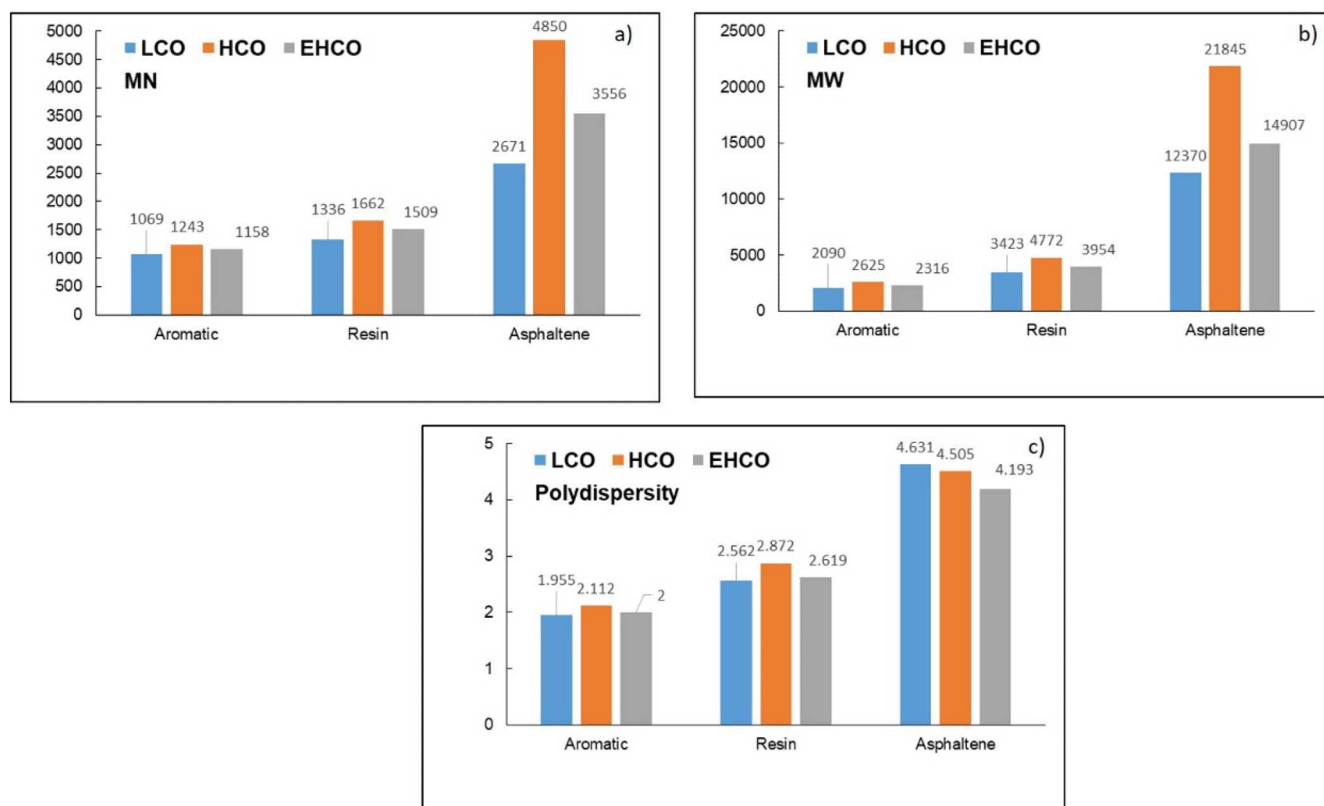


Fig. 5. Average molecular weight and polydispersity values by GPC.

Table 3
¹H NMR protons distribution of ARA fractions.

NMR	Types	δ position	AROMATIC			RESIN			ASPHALTENE		
			LCO	MCO	HCO	LCO	MCO	HCO	LCO	MCO	HCO
1H NMR	Hal; γ	0,1–1,1	18,08	22,59	21,63	17,14	18,39	17,98	33,42	17,15	22,25
	Hal; β	1,2–2,1	47,65	55,03	44,54	47,00	52,01	45,55	37,83	55,50	56,07
	Hal; α	2,2–4,0	18,00	10,82	23,29	22,59	18,68	20,70	13,35	17,81	13,29
	Har mono aromatic rings	6,0–7,1	7,87	6,22	5,16	5,03	4,99	4,96	9,22	4,65	3,46
	Har of di, tri and tetra aromatic rings	7,3–9,0	8,39	5,34	5,38	8,23	5,94	10,80	6,18	4,89	4,94
	Total aliphatic hydrogen	0,4–4,0	83,73	88,44	89,46	86,73	89,08	84,23	84,60	90,46	91,61
	Total aromatic hydrogen	6,0–9,0	16,26	11,56	10,54	13,26	10,93	15,76	15,40	9,54	8,40

Table 4
¹³C NMR protons distribution of ARA fractions.

NMR	Types	δ position	AROMATIC			RESIN			ASPHALTENE		
			LCO	MCO	HCO	LCO	MCO	HCO	LCO	MCO	HCO
¹³ C NMR	Methyl of carbon to aliphatic or alkyl chain	10–20	11,51	13,24	3,34	12,79	8,79	8,40	7,48	13,08	4,76
	Methylene of carbon to aliphatic or alkyl chain	20–25	11,51	8,68	13,04	9,30	9,56	13,20	7,48	8,41	9,52
	Methylene group attached to aromatic ring	25–40	9,71	36,53	42,14	41,67	49,35	50,80	33,18	35,98	71,43
	CH of aromatic compounds	110–160	67,27	41,55	41,47	36,24	32,30	27,60	51,87	42,52	14,29
	Total aliphatic carbon	10–40	32,73	58,45	58,52	63,76	67,70	72,40	48,14	57,47	85,71
	Total aromatic carbon	110–160	67,27	41,55	41,47	36,24	32,30	27,60	51,87	42,52	14,29

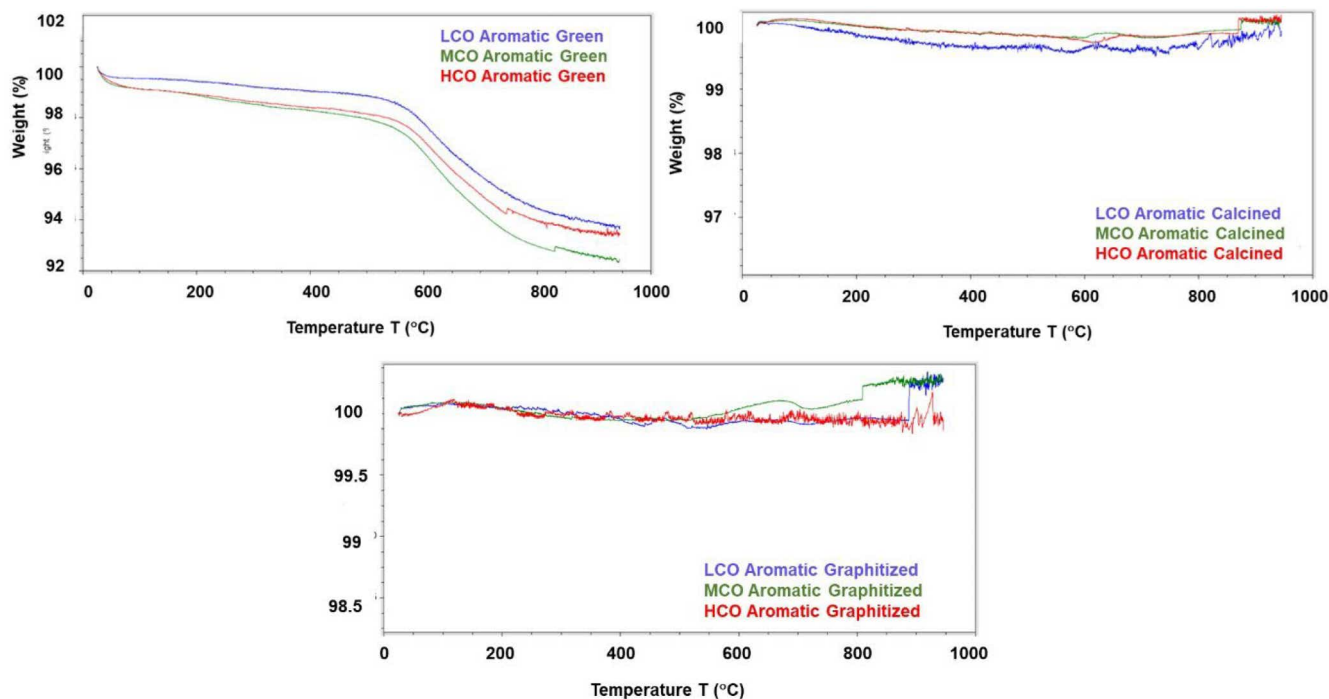
Table 5
Yield of carbon at different stages of pyrolysis.

SAMPLE	AROMATIC			RESIN			ASPHALTENE		
	LCO	HCO	EHCO	LCO	HCO	EHCO	LCO	HCO	EHCO
Green Carbon	21.9	15.4	23.3	41.5	31.4	38.4	62.3	52.0	65.0
Calcined Carbon	85.0	79.4	82.4	83.9	82.4	80.4	75.7	75.6	71.5
Graphitized carbon	96.2	96.0	99.3	92.5	95.8	97.7	94.5	99.5	98.0

Table 6

Elemental proportions of carbon samples.

Origin	Sample	Total Carbon	Total Hydrogen	Total Nitrogen	Total Sulphur	Total Oxygen	Total Heteroatoms
Aromatic LCO	Green	89.39	2.43	0.69	5.39	2.10	8.18
	Calcined	98.21	0.07	0.21	1.51	0.00	1.72
	Graphitized	99.99	0.00	0.01	0.00	0.00	0.01
Aromatic HCO	Green	88.59	2.68	1.26	5.40	2.07	8.73
	Calcined	97.94	0.03	0.31	1.72	0.00	2.03
	Graphitized	99.99	0.00	0.01	0.00	0.00	0.01
Aromatic EHCO	Green	91.02	2.82	1.45	3.60	1.11	6.16
	Calcined	94.79	0.03	0.32	2.31	2.55	5.18
	Graphitized	99.99	0.00	0.01	0.00	0.00	0.01
Resin LCO	Green	88.17	2.10	1.18	6.69	1.86	9.73
	Calcined	96.82	0.04	0.34	2.81	0.00	3.14
	Graphitized	99.99	0.00	0.01	0.00	0.00	0.01
Resin HCO	Green	88.36	2.55	1.98	4.03	3.08	9.09
	Calcined	96.38	0.03	0.51	2.74	0.35	3.60
	Graphitized	99.99	0.00	0.01	0.00	0.00	0.01
Resin EHCO	Green	88.36	2.55	1.98	4.03	3.08	9.09
	Calcined	96.38	0.03	0.51	2.74	0.35	3.60
	Graphitized	99.99	0.00	0.01	0.00	0.00	0.01
Asphaltene LCO	Green	87.60	2.01	1.57	7.02	1.80	10.39
	Calcined	95.47	0.04	0.19	2.05	2.25	4.49
	Graphitized	99.99	0.00	0.01	0.00	0.00	0.01
Asphaltene HCO	Green	82.27	1.77	2.50	7.83	5.64	15.97
	Calcined	94.61	0.02	0.35	3.01	2.02	5.38
	Graphitized	99.99	0.00	0.01	0.00	0.00	0.01
Asphaltene EHCO	Green	87.19	2.16	2.36	4.69	3.60	10.65
	Calcined	94.93	0.01	0.43	3.48	1.15	5.06
	Graphitized	99.99	0.00	0.01	0.00	0.00	0.01

**Fig. 6.** TGA analysis of green, calcined and graphitized carbon from origin based ARA fractions.

S. B. Yang et al. [28] employed FTIR and data-driven methods to anticipate crude oil properties. In similar way, NMR studies furnish essential details on organic matter functional groups [29–31]. It also indicates the source rock sedimentary surroundings, and thermal maturity thus has distinctive advantage in geochemical assessment of crude oil [29]. The Low-field nuclear magnetic resonance based method has realistic utility like non-destructive, require minimum sample without hazardous solvents, analysis cost is economical, analysis is quick, whole method workflow is straightforward and easy to perform physical property determination [30]. Rakhmatullin et al. [31] present

the possibility of ^{13}C NMR spectroscopy for the quick analysis of heavy crude oil from physical characteristics to the arrangement of functional groups. It additionally highlights the capability of NMR to study both systematically and empirically the elemental configuration along with molecular composition of organic materials, its fractions, and aspired products. However, sophisticated analytical procedures are still required to enhance the performance of refinery conversion processes.

Moreover it is established that the chemical characteristics of crude oil vary based on its origin. Besides refinery usually use blend of crude oils [32]. Hence various groups have shown interest to study the

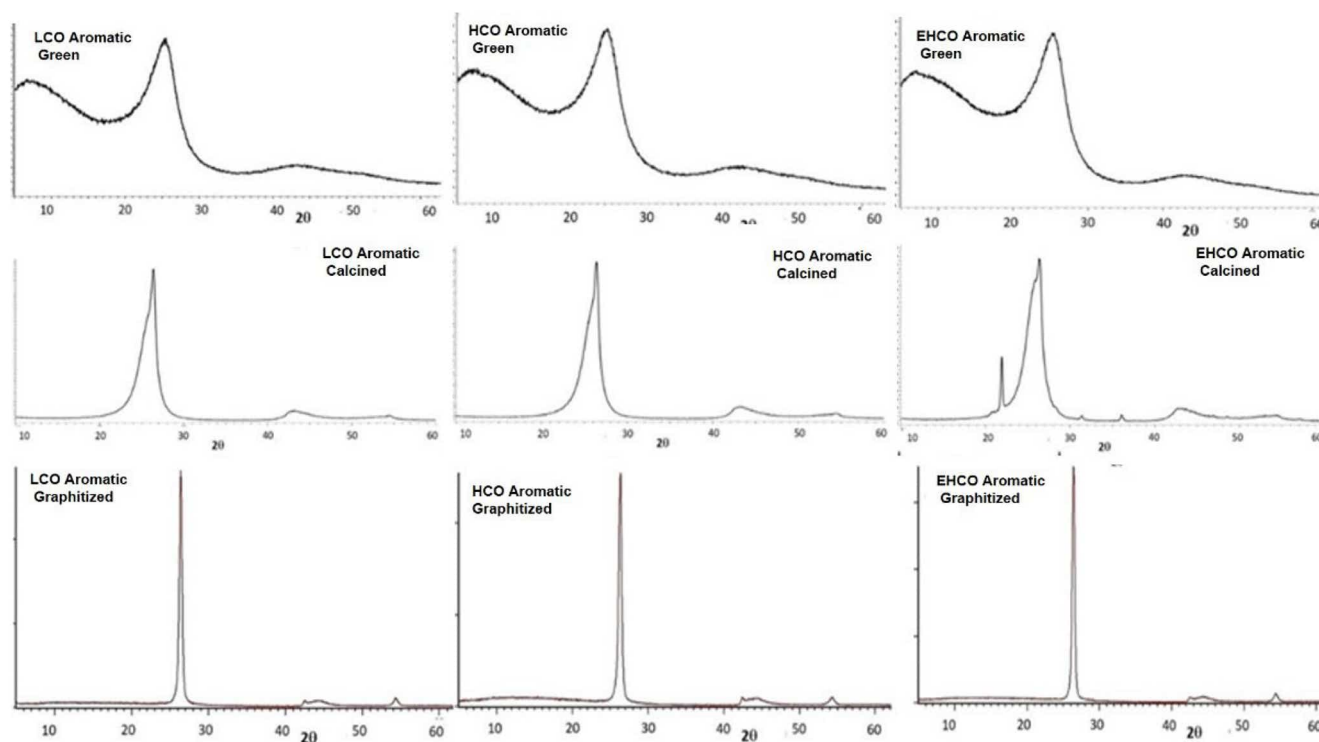


Fig. 7. XRD pattern of green, calcined and graphitized samples from aromatics.

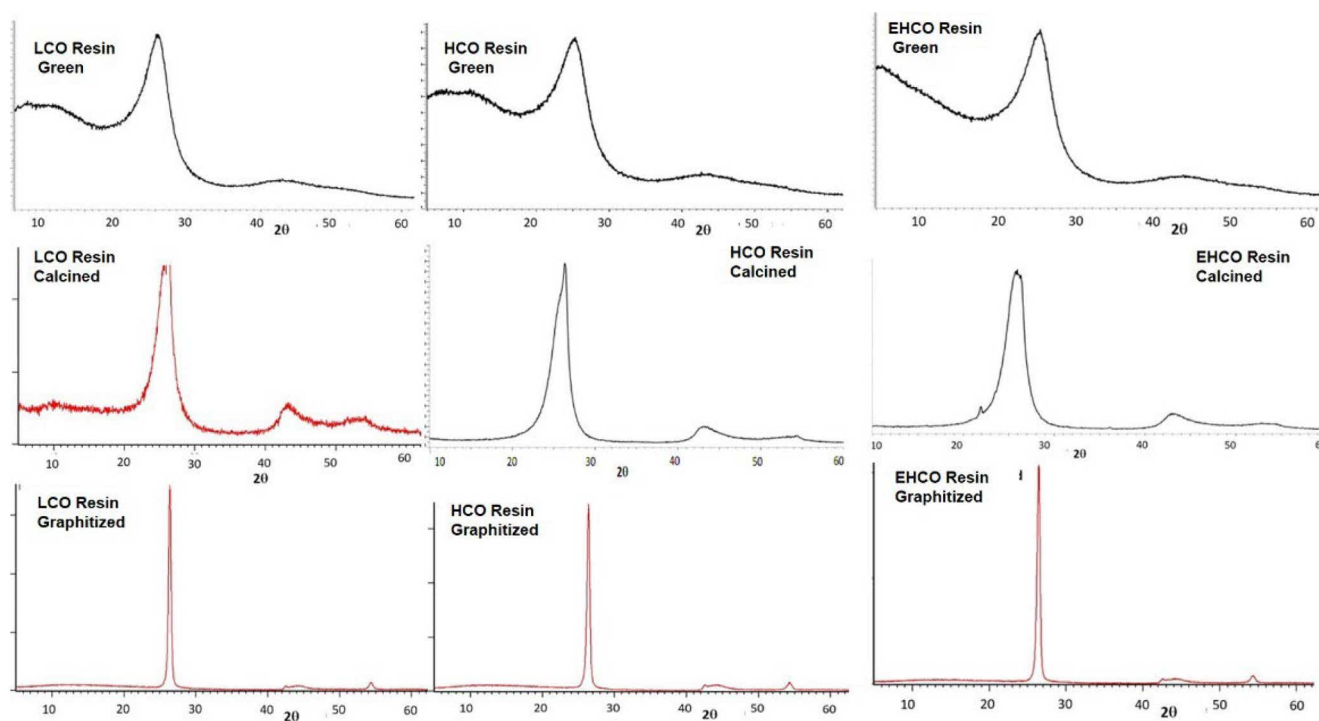


Fig. 8. XRD pattern of green, calcined and graphitized samples from resins.

characteristics of crude oil from different origin [33–35]. A. B. Gar-marudi et al. [33] used infrared spectrometry and chemometrics to successfully classify crude oils based on its origin. Similarly, O. Galtier et al. [34] utilized mid-infrared spectroscopy to classify crude petroleum oils according to their geographical origins. Likewise M. Salehzadeh et al. [35] carried profound investigation of light, medium and heavy oil asphaltenes and observed excess hydrogen content and

hydrogen/carbon atomic ratio in heavy oil asphaltene. Nevertheless, there is a significant anticipation for origin based studies on crude oil.

Additionally, in recent years there are few reports on effective use of petroleum vacuum residue as a raw material to convert into high value carbon based materials. Currently, with the constant growth in concern over management of natural resources the petrochemical industry have difficulties in efficiently managing petroleum vacuum residue. Besides,

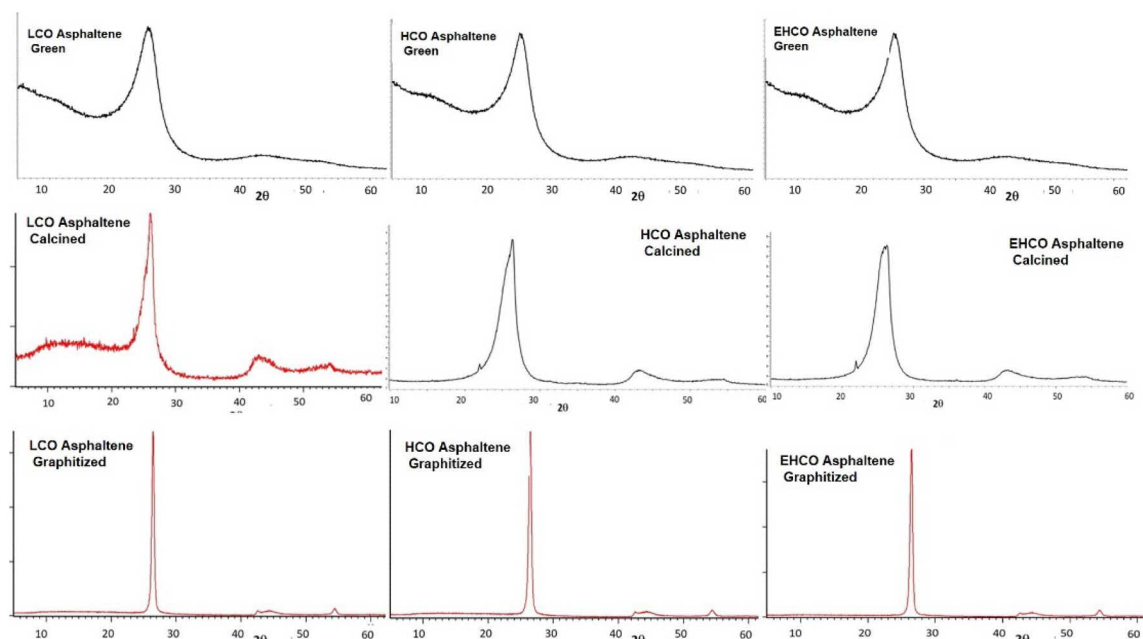


Fig. 9. XRD pattern of green, calcined and graphitized samples from asphaltenes.

Table 7

Data obtained for XRD analysis.

Sample	Origin	AROMATIC			RESIN			ASPHALTENE		
		d-spacing (Å ^o)	Lc (Å ^o)	La (Å ^o)	d-spacing (Å ^o)	Lc (Å ^o)	La (Å ^o)	d-spacing (Å ^o)	Lc (Å ^o)	La (Å ^o)
Green	LCO	3.515	21.30	16.90	3.518	22.60	21.90	3.505	22.80	18.10
Calcined	LCO	3.380	8.022	4.165	3.386	7.868	4.487	3.47	3.16	3.53
Graphitized	LCO	3.382	20.279	43.062	3.379	19.673	43.004	3.372	19.23	34.59
Green	HCO	3.528	20.70	19.70	3.538	20.90	24.10	3.524	19.90	25.30
Calcined	HCO	3.377	8.290	4.332	3.381	6.924	3.865	3.387	6.09	3.89
Graphitized	HCO	3.387	17.814	45.672	3.387	18.744	39.774	3.371	16.75	34.89
Green	EHCO	3.522	21.20	19.80	3.513	21.40	20.80	3.507	24.00	21.80
Calcined	EHCO	3.380	7.581	3.541	3.392	5.432	4.115	3.389	5.87	3.54
Graphitized	EHCO	3.380	24.579	36.645	3.362	20.712	33.085	3.371	18.49	38.04

the effective utilization of high value added petroleum vacuum residue is also economical. X. Zhai et al. [36] fabricated Fe₃N-codoped porous carbon-embedded Fe₃C nanoparticles from petroleum vacuum residue for highly efficient oxygen reduction. For Li-ion batteries anodic material, J. L. Tirado et al. [37] carried co-pyrolysis of petroleum residue to obtain Tin-carbon composites and SnO₂. Furthermore H. Chao et al. [38] reports of carbon with porous structure from vacuum residue for its implementation in Lithium ion capacitors.

The purpose of the research is to carry out an extensive characterization for aromatic, resin and asphaltene fractions from vacuum residue distillate of light, heavy and extra heavy crude oil. Furthermore, the purpose is also to convert ARA fractions into graphitic carbon like material and study co-relation of each type of vacuum residue on conversion of graphitic carbon material. For which heat treated samples at all stages are analysed to understand structural changes using TGA, XRD and Raman spectroscopy. All results are discussed in details in this article.

2. Materials and methods

2.1. Studies on vacuum residue and ARA analysis

2.1.1. Materials

Crude oils with distinct characteristics were selected and tested from three separate origins: Middle East, Canada and South America. Based

on their American Petroleum Institute values they are referred as Low (Middle East, API - 33.4), Heavy (Canada, API - 21.4) and Extra Heavy (South America, API - 9.5) crude oil throughout the study. The Low (LCO), Heavy (HCO) and Extra Heavy (EHO) exhibited Conradson Carbon Residue values of 5.1, 9.5 and 12.9, respectively.

2.1.2. Methods

To estimate the yield of fractions regular test methods for distillation of crude petroleum (ASTM D2892) and heavy hydrocarbon mixtures (ASTM D5236) were done. The resulting vacuum residues were considered as raw materials for this study. The determination of asphaltene in vacuum residue was carried out by following ASTM D6560 (Fig. 1a). The remaining maltenes were passed through column bed prepared by activated, alumina oxide with mesh size 100 and silica gel of FIA grade. The glass column length was 1150 mm, internal diameter 15 mm and bulb capacity 500 ml for 10 g sample weight. The saturates were obtained as first fraction which is soluble in n-heptane. Aromatic fraction was obtained next by addition of toluene in bulb. Finally, resin fraction was obtained by adding a mixture of toluene and methanol in 1:1 ratio. The fraction solvents were evaporated to get the pure SAR fractions. The ARA fractions studied in this study are represented in Fig. 1b.

The purity of the fractions isolated using the above described method was measured using TLC-FID on a latroscan MK-6S system. The hydrogen flow rate of the FID was 160 mL/min; the air flow rate was 2

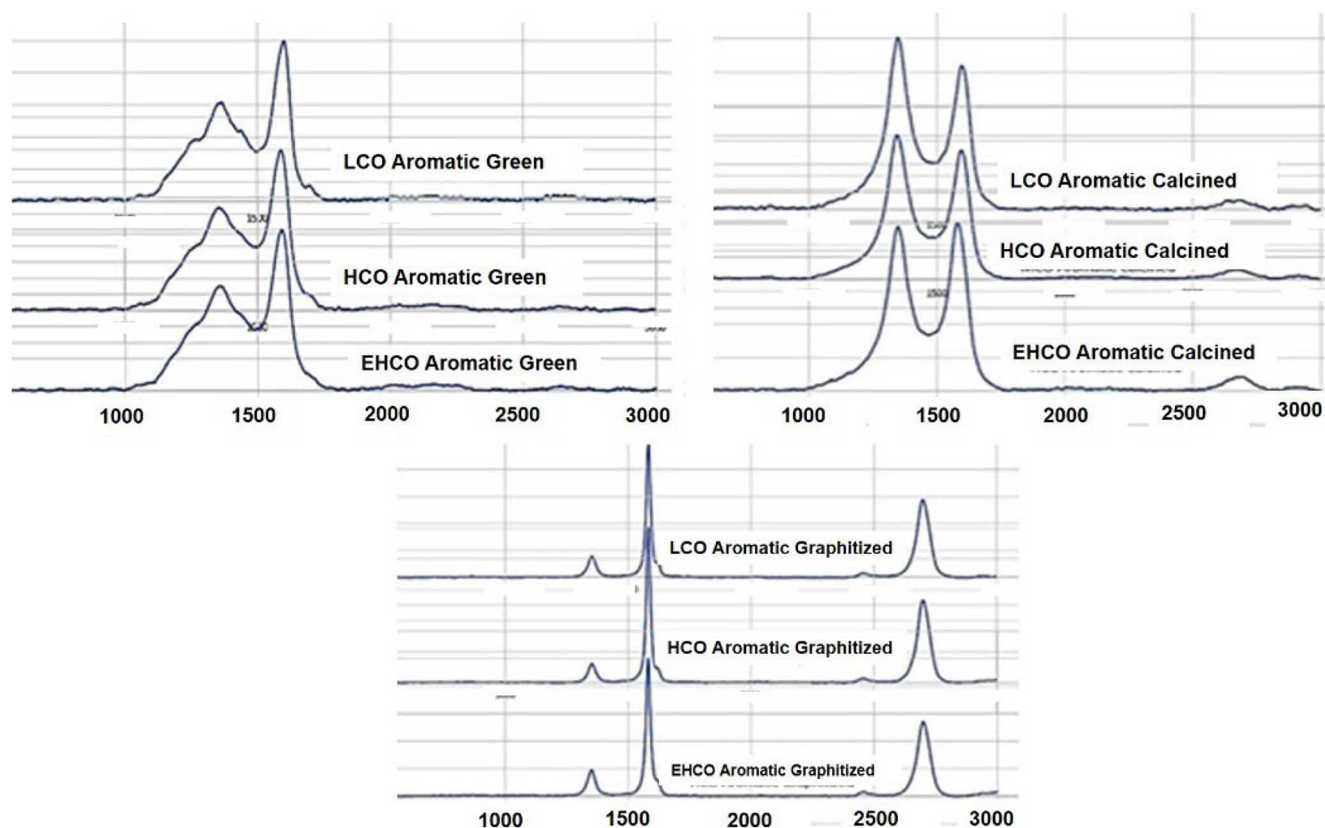


Fig. 10. Raman spectra of green, calcined and graphitized carbon of origin based aromatics.

L/min. A solution of approximately 1 % wt. /vol. of material in dichloromethane was prepared, of which 1 μ L drop was spotted on silica coated chroma rod. It was followed by drying at 80 $^{\circ}$ C in oven for 5 min after which the chromarod was eluted sequentially. The first chamber filled with n-hexane for saturates at 100 mm height.

However, the saturate were eliminated from this study due to their low carbon yield % following pyrolysis at 500 $^{\circ}$ C for 10 min. Second, it was heated once again at 80 $^{\circ}$ C for 5 min with known quantity of toluene for aromatic at 50 mm height was eluted. Finally for the last stage heating was carried for 10 min at 80 $^{\circ}$ C, chamber filled with methanol and DCM mixture for resin at 25 mm height was eluted. The data were collected with SIC-480 II software. This procedure was repeated for ARA fractions from different origin crude oil. ASTM D4530 method was used for the determination of the amount of carbon residue in ARA fraction. The relative density of the ARA fractions were measured by using pycnometer.

The CHNSO content was determined using the Elementary Vario Macro CUBE instrument. A known quantity of the sample was placed into a combustion tube at a temperature of 1150 $^{\circ}$ C. Under these circumstances, CHNS underwent quantitative conversion to their respective gases, namely CO₂, H₂O, NO_x, and SO_x. This conversion occurred during sample combustion at 850 $^{\circ}$ C in an oxygen-rich environment. The resulting gases were then directed into the reduction tube via a U-tube, where impurities such as excess oxides and halides were eliminated using copper and silver metals. Nitrogen content was directly measured using a TCD detector operating at 240 $^{\circ}$ C. Pure elemental oxide gases were trapped in a specific column and subsequently released at a designated temperature for analysis by the TCD detector, with helium serving as the carrier gas. Verification and calibration were conducted using various standards with different concentrations. Elemental analyses were performed on the VR sample and its fractions of ARA (Aromatic, Resins, and Asphaltene). In this process, samples weighing between 25 and 50 mg were prepared with double the quantity of

tungsten oxide and then injected directly into the column using an auto sampler. The instrument's operational range spanned from 0 to 100 %, with a minimum detection limit of 100ppm.

Metal and ash content in crude oil were determined by inductively coupled plasma optical emission spectrometry (ICP-OES). Perkin Elmer optima 8300 model with sulphur chemiluminescence detector (SCD) was employed. The carrier gases were argon and oxygen. 0.2 to 0.25 gm samples were dissolved in an industrial solvent, decalin. Diluted samples were carried through peristaltic pump, samples and argon were mixed in nebulizer and made an aerosol. This aerosol and extra oxygen mixed in plasma tube generated plasma. These charged elements photon passed through photon multiplier tube and emitted the energy at the end of path. Emitted energy covert in electric signal in detection system. Minimum detection limit of the detector is 0.1 ppm.

The 60 mg samples were diluted in 5 mL tetrahydrofuran (THF). GPC analysis was performed using a Perkin Elmer Turbo matrix-40 instrument with PLgel mixed-b columns packed with 5 μ m polystyrene gel beads with microporous stationary phase. The column length and diameter 300 * 7.5 mm with the flow rate of 1 mL min⁻¹ for a total run time of 15 min was followed. Refractive index detector was used. Polystyrene standards were used to calibrate for relative M_w and M_n .

Mass analysis was conducted on a Waters Alliance e2695 separations module with QDa detector. The samples were prepared by weighing approximately 0.2 g sample dissolved in 250 ml toluene. The injection volume was 10 μ L, total run time of 1 min. These samples were ran and recorded the data between 100 and 1000 Dalton mass and instrument limit is 50 to 1200 Dalton. The ¹H NMR and ¹³C NMR spectra acquisition were obtained on a Bruker Biospin Avance III 400 MHz liquid state NMR spectrometer along with 5 mm Broad Band observed probe with gradient coil along Z axis. The samples were prepared by diluting samples in deuterated chloroform (CDCl₃) solvent. Spectra were recorded using 16 scans, top spin 2.1 and the number of scans was 4000.

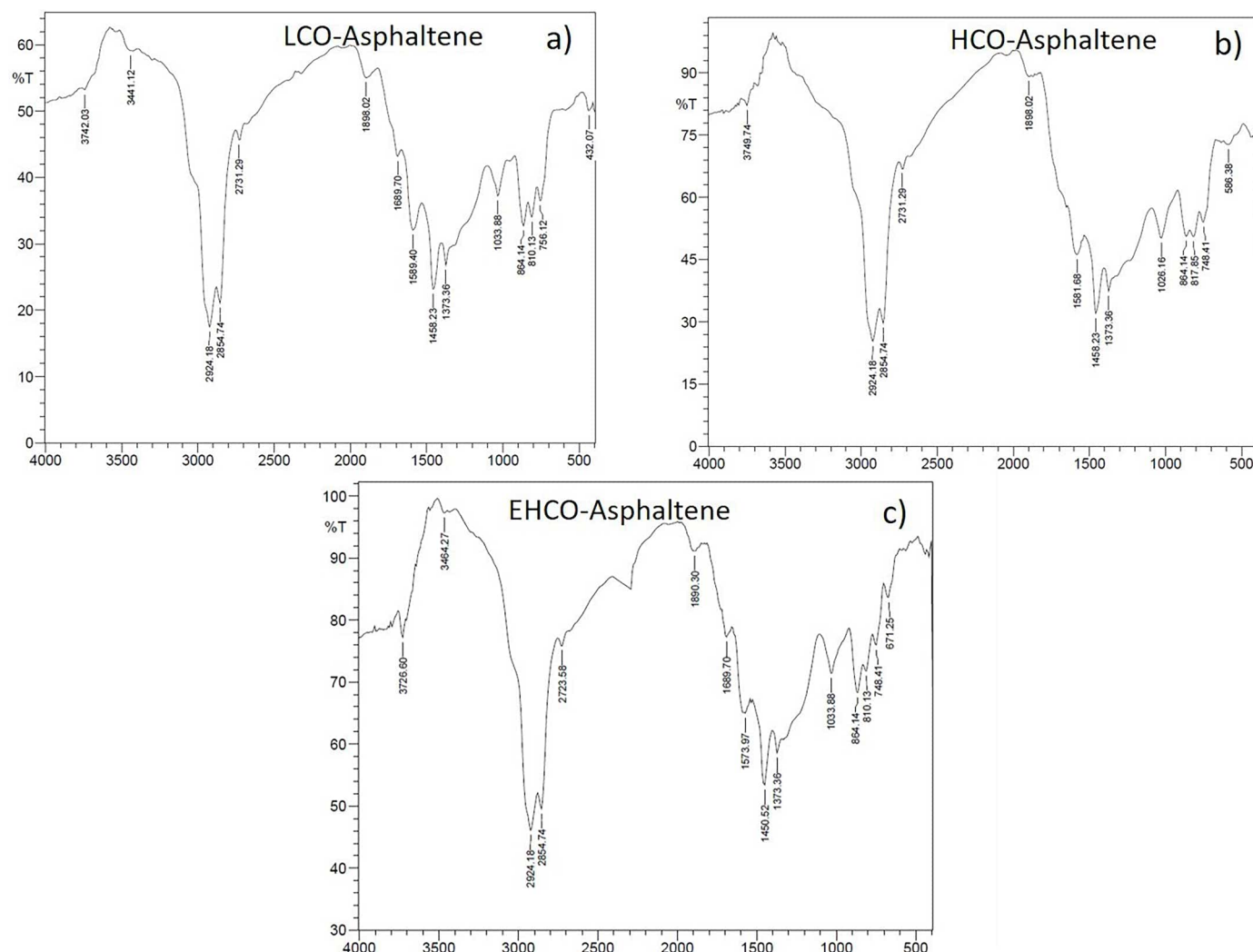


Fig. 11. FTIR spectra of the origin based asphaltenes.

2.2. Preparation of graphitic carbon like material

2.2.1. Materials

Aromatic, resin and asphaltene (ARA) fractions from three different vacuum residues (Light Crude oil, Heavy Crude oil and Extra Heavy Crude oil) were used as a raw material for preparation of green coke for this study.

2.2.2. Methods

The raw materials were pyrolyzed at 500 °C for 10 min under inert atmospheric condition as per ASTM D4530 resulting in the formation of green carbon. The obtained green carbon samples were further heat treated in two step, followed by heating at 900 °C with heating rate of 10 °C and 1350 °C with rate of 5 °C and held for 30 min and 5 hr respectively to produce calcined carbon. This was done to remove all volatile matters for further processing to get graphitized carbon. Graphitization was done at 2800 °C with heating rate of 15 °C and held for 2 hr.

The Raman spectra were recorded in Confocal Raman Microscope (LabRAM HR Evolution, HORIBA Scientific, Jobin Yvon Technology) at ambient temperature using the 532 nm laser in the wavenumber range 200–3000 cm^{-1} . The number of accumulations was 5 with time 2 s and the spectra were baseline corrected with the LabSpec6 software program. Multiple measurements were performed on powder of each individual sample and averaged spectra was represented. XRD measurements have been done on Panalytical's X'Pert Pro instruments.

The radiation source used is Cu K-alpha and nickel metal used in beta filter. It is equipped with x-Celerator solid-state detector. Instrument operated using the 40 mA and 45 kV at a scanning speed of 5°/min. Below 200 mesh carbon powder sample was taken on glass side and collected the spectra. Thermal stability investigation of carbon samples was done by using TA Instruments Q500 thermogravimetric analyzer. Samples were analyzed in the temperature range from 20 to 950 °C with a heating rate 10 °C/min under atmosphere. 10 mg each sample was taken in the crucible and placed in the instruments.

3. Results and discussion

3.1. Studies on vacuum residue and ARA analysis

The vacuum residues exhibit distinct characteristics and hence there is significant variation in various fractions as shown in Fig. 2 extra heavy and heavy crude oil have an abundant asphaltene and resin fractions. Fig. 2 shows the results of ARA analysis from different regions. The range of resin and asphaltene fractions between origin based vacuum residues are 41.7–28.5 % and 27.9–2.4 %. Aromatic fraction ranges from 45 to 19.8 %, highest being LCO (45 %), followed by HCO (40.9 %) and least in EHCO (19.8 %). ARA fractions from LCO is aromatic rich whereas EHCO has the highest resin and asphaltene fractions. The data in Table 1 indicate the characteristics of vacuum residue (VR) from LCO, HCO and EHCO. As anticipated, extra heavy crude oil has high CCR,

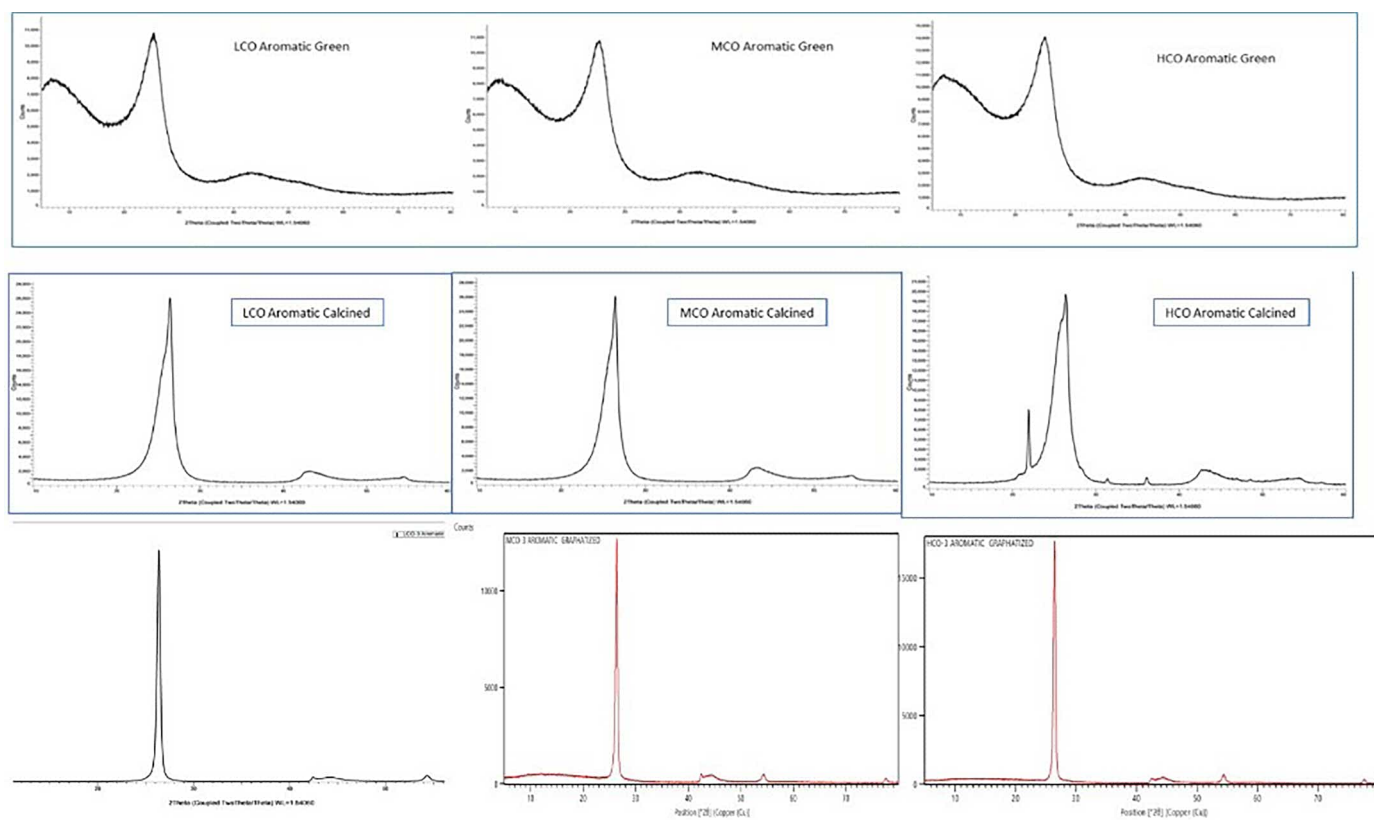


Fig. 12. XRD pattern of green, calcined and graphitized samples from aromatics.

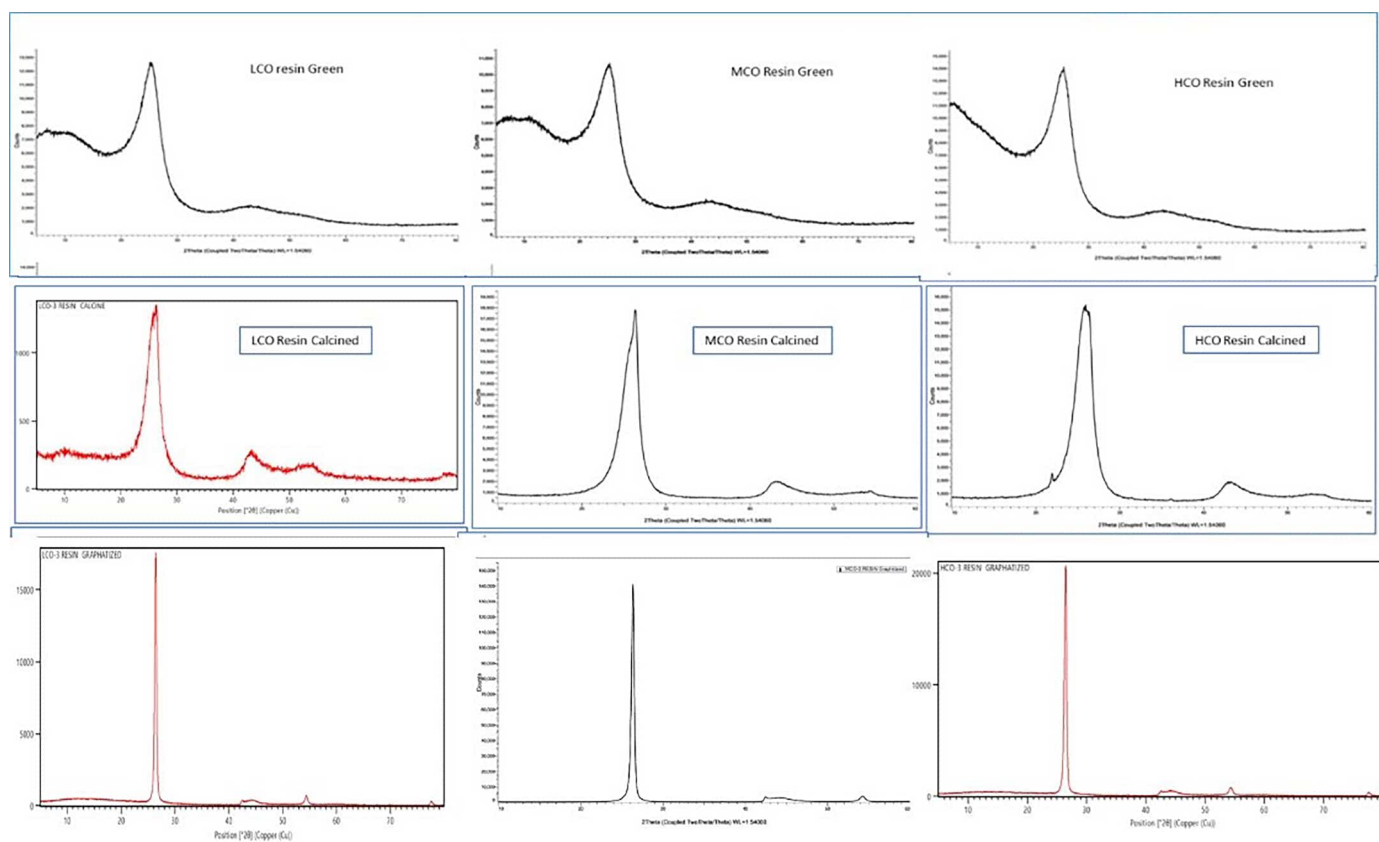


Fig. 13. XRD pattern of green, calcined and graphitized samples from resins.

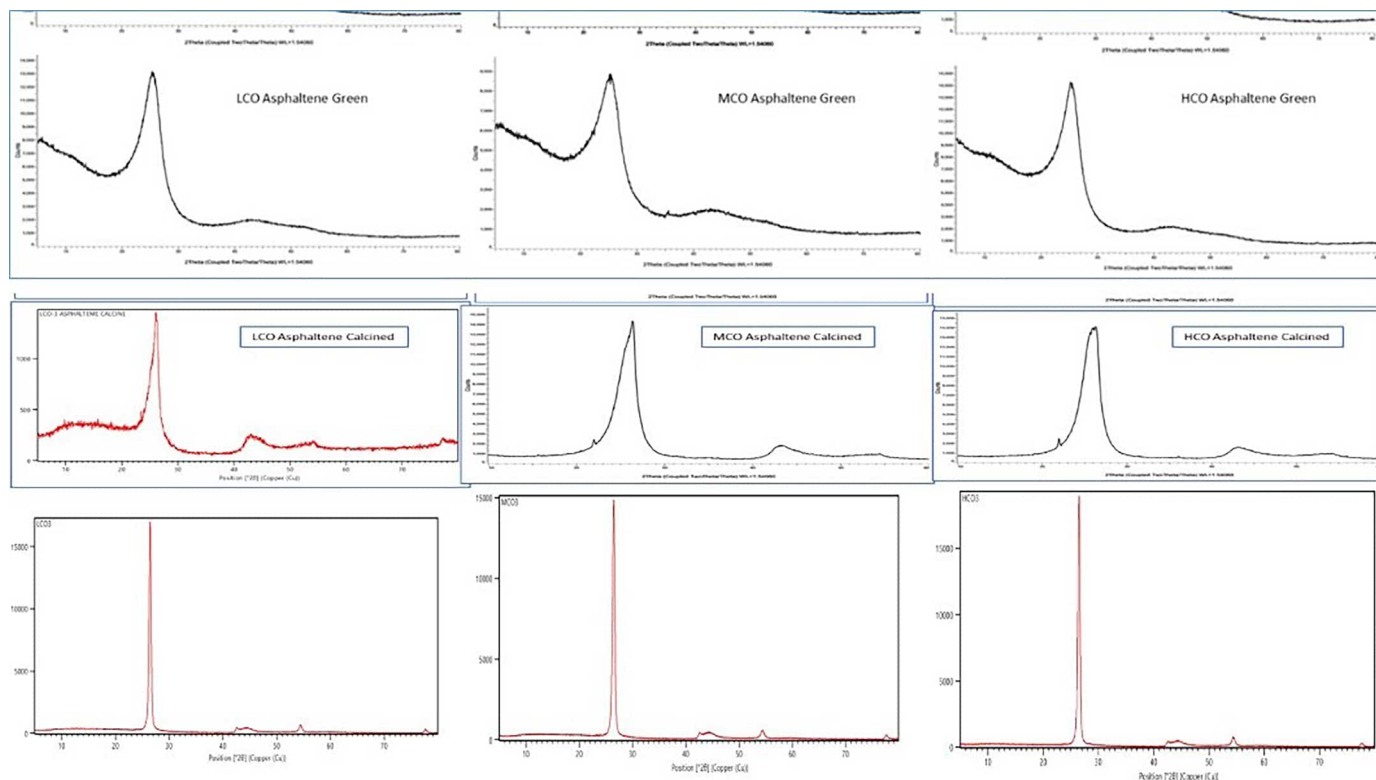


Fig. 14. XRD pattern of green, calcined and graphitized samples from asphaltenes.

pour point, density along with total carbon, nitrogen and metal. In contrast, heavy crude oil was found to be rich in total sulphur, oxygen, heteroatoms and high C/H ratio. Even though there is not any major dissimilarity in hydrogen content between origins, light crude oil has slightly high hydrogen content (11.2 %).

Fig. 3a to 3c shows TLC-FID chromatograms of the isolated ARA fraction from vacuum residue of (which sample LCO/HCO/EHCO). The chromatogram has distinct single peak representing 99 % purity and sufficient isolation. Density and CCR were used to predict ARA fractions of vacuum residues [39]. Fig. 3d summarizes the results of measurements of Conradson carbon content, which indicates the difference among the samples. For asphaltene and aromatic fraction, carbon content of EHCO dominates whereas that of LCO falls shortly behind EHCO. Further it is interesting to note that LCO preside over EHCO in resin fraction with slightly high carbon content. However, the carbon content of ARA fraction from HCO differs strongly with low value. Similarly, density is a key property for the assessment, simulation and expansion of petroleum reservoirs. Fig. 3e show the measured density for aromatic, resin and asphaltene from different origins. The light crude oil is a low-viscous material and is expected to have low density when compared to very viscous heavy/extra heavy oil with a high specific density [40]. However, it is interesting to note that the obtained value reflects the opposite trend (Fig. 3e). The density for LCO were found to be high in all the aromatic, resin and asphaltene fraction, respectively.

The elemental compositions of the investigated origin based ARA fraction are represented in Table 2. Regardless of the samples from different origin they are all carbon rich with more than 82 wt. % in ARA fractions. The carbon, hydrogen, C/H, nitrogen and oxygen composition of the aromatic fraction did not vary significantly irrespective of its origin. However, the sulfur and as a result the heteroatom content was high in aromatic fraction from HCO. The similar pattern was observed for the elemental composition in resin and asphaltene fractions. The elemental composition of carbon in the range of 80–90 % have been reported earlier for oils samples from south of Iran [27,4]. The H/C-ratio is an important guideline that indicates the degree of saturation and

determines the abundance ratio of aromatic and aliphatic compounds. This ratio decreases with the increase in aromatic proportion and decrease in the aliphatic proportion. The H/C values of ARA below unity indicates the samples are highly aromatic [4]. The heteroatom content reached a maximum of approx. 8 wt. % in Asphaltene. Anyhow, sulfur was high in content among heteroatom in all ARA fractions. Aromatic fraction from LCO has the lowest sulfur (2.7 %) and oxygen (0.61 %), whereas from HCO has lowest nitrogen (0.39 %) content. Likewise, the high content of nitrogen (1.65 %), oxygen (0.61) and sulfur (8.34 %) were identified in asphaltene from EHCO and LCO, and resin fraction from HCO.

Inductively coupled plasma optical emission spectrometry are regularly used for crude oil and products analysis [16,41]. The ICP-OES results of ARA fractions shown in Fig. 4, illustrate the presence of metal and ash concentration in ARA fractions along with its variation among different origin sample. The metal concentrations in aromatic, resin and asphaltene are in the range of 39–204 ppm, 271–1233 ppm and 400–2154 ppm (Fig. 4a), respectively. The excess metal contents were present in ARA fractions from EHCO. The low metal content in LCO against HCO and EHCO agrees with the facts that light crude oil usually contains relatively low metal. The presence of metallic particles are important as they might have a significant role in the asphaltene accumulation [42]. Correspondingly (Fig. 4b), the ash concentration in aromatic, resin and asphaltene are in the range of 0.01–0.05 ppm, 0.07–0.39 ppm and 0.11–0.68 ppm. Consequently, the difference in ash content follow the same pattern noticed for metal concentrations.

Estimating molecular weight distribution of ARA fractions could be important to anticipate the phase behaviour and prevent asphaltene depositions. Similarly molecular weight distribution influences the chemical composition which directly affects the combustion characteristics of fuel oil [7]. Hence determination of molecular weight distribution becomes mandatory which is analysed by Gel Permeation chromatography in the present study. The number-average molecular weight (M_N) is defined as the average based on the number of polymer chain molecules at a particular molecular weight, whereas the

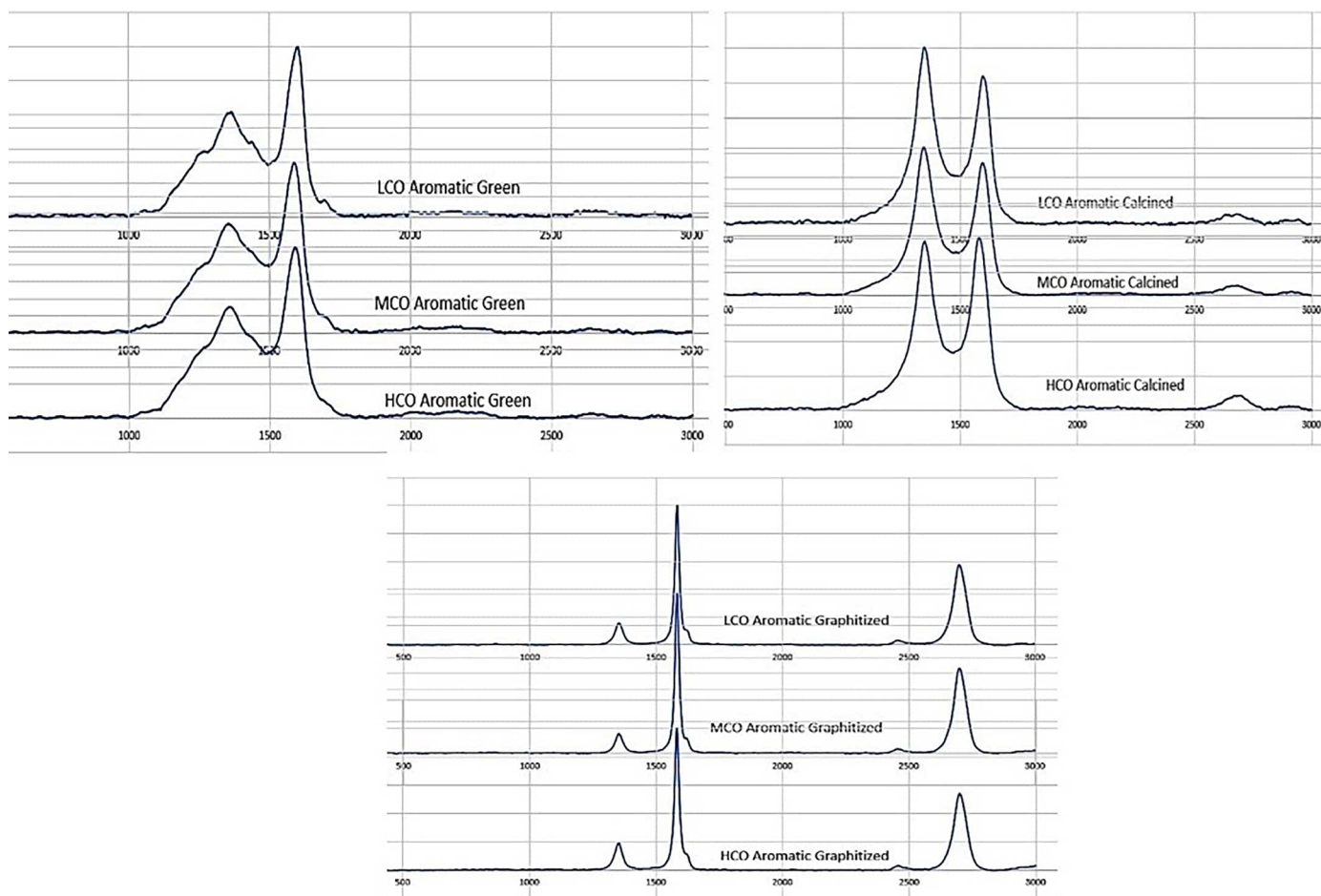


Fig. 15. Raman spectra of green, calcined and graphitized carbon of origin based aromatics.

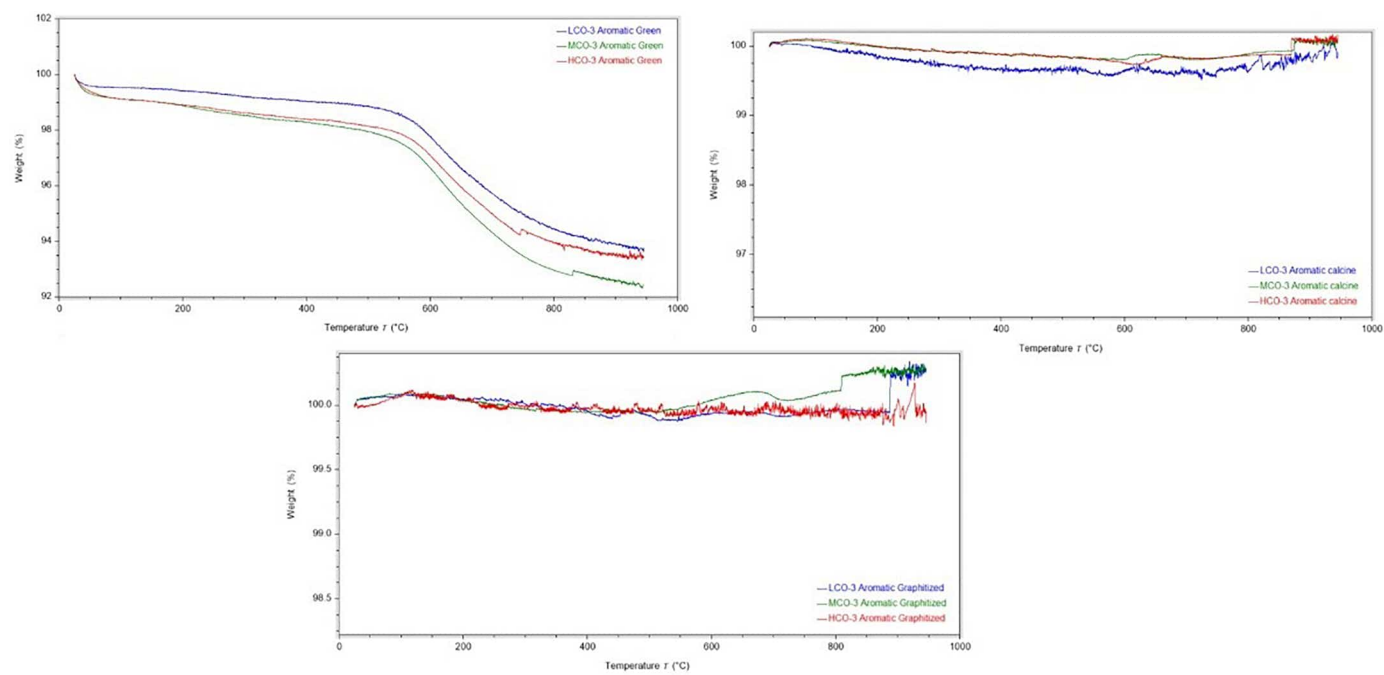


Fig. 16. TGA analysis of green, calcined and graphitized carbon from origin based ARA fractions.

Table 8

Data obtained for Raman analysis.

Sample	Origin	AROMATIC		RESIN		ASPHALTENE	
		I _D /I _G	La (nm)	I _D /I _G	La (nm)	I _D /I _G	La (nm)
Green	LCO	0.6164	31.19	0.6773	28.39	0.7175	26.79
	HCO	0.6424	29.92	0.6372	30.17	0.7454	25.79
	EHCO	0.6240	29.47	0.9220	27.77	0.6890	27.90
Calcined	LCO	1.1925	16.12	1.0112	19.01	1.2171	15.80
	HCO	1.1169	17.21	1.2641	15.21	1.2571	15.29
	EHCO	0.9812	19.59	1.2083	15.91	1.1948	16.09
Graphitized	LCO	0.1581	121.61	0.1241	154.95	0.1401	137.23
	HCO	0.1234	155.79	0.1552	123.84	0.4580	41.98
	EHCO	0.1902	101.07	0.1619	118.77	0.4149	46.34

weight-average molecular weight (MW) corresponds to the mass (or weight) of the polymer chain molecules at a particular molecular weight. Higher side poly dispersity indicates the broadness of molecule. As shown in Fig. 5a, the number-average molecular weight (M_N) of aromatics and resin were basically consistent with those of different origin. However, the M_N of asphaltenes derived from different origin were higher varying in the range of 2671–4850 (g.mol⁻¹). This proposed that the asphaltene especially derived from HCO had larger molecular weight with M_N value of 4850 (g.mol⁻¹). Likewise, the weight-average molecular weight (MW) for origin based ARA fractions based on GPC detection are shown in Fig. 5b. The results showed that there was great difference in MW for asphaltene compared with aromatic and resin fraction. The HCO-asphaltene had a high MW value of 21,845. Likewise the highest average molecular weight in asphaltene was presented by [6].

The polydispersity, an indication of heterogeneity of a sample based on size from the various fractions are illustrated in Fig. 5c. The values observed were very similar for the aromatic and resin fractions. Also it is has the same trend as its molecular weight distribution (Fig. 5a & b). G. A. Mansoori et al. [43] detected relative values of polydispersity for aromatic, resin and asphaltene from heavy fraction of crude oil by means of GPC. It is well reported fact that asphaltenes show a very large size polydispersity. The obtained results reflect the same result. Similarly, the asphaltene fraction has high polydispersity value as well it does not follow the trend noticed for molecular weight distribution. For instance, both mass and number molecular weight of asphaltene fraction follows the descending order of HCO, EHCO and LCO. But, for the polydispersity it follows a different order, where LCO has high value followed by HCO and EHCO. G. A. Mansoori et al. reports broad distribution of sizes and molecular characteristics for asphaltene [43]. D. Oldham et al. [44] investigated polydispersity of crude oil due to asphaltene oxidation and hypothesized that increased polydispersity affects viscosity.

Several researchers have published the application of NMR in the assessment of heavy petroleum fractions. The proton NMR spectroscopy is used for quantitative analysis of paraffinic and aromatic hydrogen, where carbon NMR spectroscopy is used for paraffinic and aromatic carbon atoms. For such complicated molecules, the aliphatic protons participation on a ¹H NMR spectrum emerges as a large signal with a continuous superimposing of numerous peaks and most strong compared to aromatics and are basically classified into three types of protons namely, a, b and c with reference to an aromatic core. The investigation of the range of every kind is not simple to attain but are commonly resolved from 0.1 to 1.1 ppm for d type protons, broad peak obtained at 1.2 to 2.1 ppm for c type protons, 6.0 to 7.1 ppm for b type protons and 7.0 to 9.0 for a type proton. Proton NMR provides type of hydrogen and its concentration in compound and also describe the nature of compound. Proton NMR attributed δ position of alkyl or paraffinic is 0.1 to 1.1 for methyl, 1.2 to 2.1 for aliphatic methylene and 2.2 to 4.0 for naphthenic or -CH₃, -CH₂ group proton. The aromatic proton resonance δ position for mono aromatic ring 6.0 to 7.1 and di. Tri and tetra or pera aromatic rings 7.3 to 9.0. Where CDCl₃ three peak appeared at 7.26 and TMS at 0. Table 3 shows the total aliphatic and aromatic

proton. In aromatic, total aliphatic hydrogen increased from light to heavy and total aromatic hydrogen decreased from light to heavy. However, the similar contribution did not found in resins, where heavy crude resin have less aliphatic hydrogen and more aromatic hydrogen as compare to other resins fraction. Asphaltene fraction have similarly to aromatic fraction aromatic proton increased from light to heavy and aromatic proton decreased from light to heavy. These results clearly signposted for aromatics and asphaltene were light to extra heavy aromatic proton decreased and aliphatic proton increased however the resins did not follow the similar trend also C/H ratio in elemental analysis similar trend was derived Table 4.

The carbon skeleton was justified by the ¹³C NMR which provided the structure information of carbon compound. For this reason, ¹³C NMR spectra has turned to be a typical choice for the analysis of crude oil fractions. When comparing ¹H and ¹³C NMR spectra it is plausible to distinguish many variation between them. For instance, ¹³C NMR spectra have huge chemical shifts scale (more than 220 ppm) that diminishes over lapping between peaks. The ¹³C NMR is insensible than ¹H NMR because of its reduced natural abundance and magnetogyric ratio of the ¹³C nucleus, but in the event of the ¹H decoupled ¹³C NMR spectra it is more straightforward when there is no peak splitting. The ¹³C NMR signals between 20.00 and 40.00 ppm come from aliphatic of -CH and -CH₂ associated to linear alkanes and cyclic compounds. The methyl group have ¹³C NMR signals have 10 to 20 with branches methyl group also appeared in this range. While aromatic carbon showed the signal in ¹³C NMR between 110 and 160 ppm. Above table represent the aromatic carbon increasingly pattern showing from light to heavy. However, the total carbon lowers side in HCO fractions matrix due to higher side hetero atoms.

3.2. Preparation of graphitic carbon like material

The heat treatment of ARA fractions were carried out in different stages. The products obtained at various stages of heat treatment of ARA fraction were referred as green (stage I), calcined (stage II) and graphitized carbon (stage III). In order to obtain green coke, the ARA fraction was used as raw material. Table 5 shows the yield of carbon at different stages of pyrolysis. The highest yield of green carbon for ARA fractions was noticed for EHCO, except for resin fractions where LCO has more yield. However the lowest yield of green carbon for ARA fractions was from MCO. The yield of green carbon was in the range of 15.4–23.3, 31.4–41.5 and 52–65 for aromatic, resin and asphaltene fractions. The yield of calcined carbon denotes more conversion has taken place for aromatic and resin fraction when compared to asphaltene. The yield of calcined carbon did not show much variation among ARA fraction and is in the range of 71.5–85. Moreover, the yield of graphitized carbon for all ARA fraction are above 90. Almost complete conversion has taken place for aromatic (EHCO) and asphaltene (HCO) which is 99.3 and 99.5.

The effect of pyrolysis temperature on elemental content is presented in Table 6. Table 6 shows that carbon content increases on calcination and graphitization of green carbon. At the same time, as expected there was a progressive decrease of hydrogen, nitrogen, sulphur and oxygen

with calcination and graphitization process corresponding to an increase of volatile and gases (CO , CO_2 , NO_2 , CH_4) loss [45]. The decrease of oxygen is anticipated to increase the sample basic nature [46]. Hence, the increased C/H and C/O ratios are indicative of dehydrogenative polymerization and dehydrative polycondensation during heat treatment [45]. Further, the relatively high quantities of heteroatoms in green carbon decreases on calcination and graphitization showing the loss of numerous functional groups [45]. The highest amount of carbon (99.99) in all ARA fractions after graphitization process indicates the complete graphitization.

Fig. 6 shows the thermogravimetric analysis of green, calcined and graphitized samples of ARA fractions. The TGA curve of green aromatic fraction represented three decomposition stages. However the overall weight loss was only 7 %. The first weight loss step started at about 27.8 °C, was related to adsorbed moisture and impurities. While the second weight loss step initiated at about 554.28 °C may be attributed to the reaction of carbon with oxygen leading to the release of CO_2 [47]. The third weight loss step at around 727 °C may be to the sublimation of carbon backbone [48]. The TGA curve of calcined and graphitized aromatic fraction shows negligible weight loss indicating the thermal stability of the formed graphite. The characteristics were identical for resin and asphaltene fractions.

The XRD patterns of the green, calcined and graphitized origin based aromatic fraction are shown in Fig. 7. A difference in XRD pattern was noticed, green carbon exhibited broad peak at approximately $2\theta = 25.46^\circ$ with low intense shoulder peak at around $2\theta = 43.24^\circ$. These corresponds to the (002) and (004) peaks indication presence of some less oriented graphitic carbon in samples. XRD patterns of calcined samples show increase in intensity of peak with shifting towards higher theta values this indicates more orientation of carbon atoms in graphitic manner. Further on graphitization the peak turns completely symmetric with a sharp peak representing the presence of only graphitic carbon like material in samples. This shows the formation of graphitic carbon like material from cured derived carbon at high temperature. The HCO and EHCO fractions (Figs. 8 and 9) for green, calcined and graphitized represents the same behavior comparative to aromatic fraction as shown in Fig. 7, except for a small change. In case of calcined HCO, there is an additional sharp peaks at $2\theta = 21.86^\circ$, 31.54° and 36.25° . Even for resin and asphaltene fraction, the XRD patterns show same behavior as observed in aromatic fraction for all green, calcined and graphitized process.

The interlayer spacing obtained from the XRD patterns are given in Table 7. The interlayer spacing of green carbon were around the range 3.505–3.538 Å, this indicates presences of less oriented graphitic carbon in starting material. Moreover, the interlayer spacing of calcined and graphitized carbon decreases to around 3.36 Å indicating the formation of highly ordered graphitic carbon after high temperature treatment to graphite like material. In addition the crystallite size L_a and L_c were calculated to assess the average size of the carbon atoms. In the green sample, the L_c and L_a were in the range 19.90–24 Å and 16.90–25.30 Å which shows a notable decrease on calcination indicating the increase of defects in the structure. Further, with graphitization there was once again a remarkable increase in L_c and L_a values suggesting the increase of order with the transformation to graphite like structure. There was not any distinguishable difference in interplanar spacing and crystallite size with feed quality variation due to ARA fraction from different origin Figs. 10–16.

The transformation to graphite like material in the samples has been further supported by Raman spectroscopy. In the recent years, pyrolysis of petroleum vacuum residue is procuring significant recognition with raising awareness on sustainability, the transformation and nature of carbonaceous substance were analyzed in depth with the aid of Raman spectroscopy [49]. As shown in Fig. 12, the Raman spectrum of carbon from origin based aromatics exhibits two peaks at 1355 cm^{-1} and 1575 cm^{-1} , which are designated to the D band and G band, correspondingly. These peaks grow sharp and intense on calcination, indicating the

orientation of carbon atoms in more ordered way. Additionally, a broad peak evolves around 2500 cm^{-1} denoting the coexistence of graphite phase. With the further increase in temperature during graphitization process, the Raman spectrum exhibits defect (D) and graphitic (G) bands at 1354 and 1584 cm^{-1} and an overtone 2D band at about 2716 cm^{-1} , reflecting the transformation of highly crystalline graphitic material. The Raman spectra of other samples particularly origin based along with ARA fraction reveal similar patterns irrespective of different feed quality.

The ratio of I_D/I_G estimated for the studied specimens are denoted in Table 8. While the G-band is produced by the C—C stretching and exists in all carbon structures, the d-band evolves from the breathing mode of aromatic rings [50]. The d-band indicates presence of disorder carbon in material. The intensity ratio of the D and G band (I_D/I_G) may thus be an indirect assessment of the disorder within the sample. The I_D/I_G value for the ARA fraction of the green sample were in the range 0.6164–0.6890, representing disordered structure. Slightly higher I_D/I_G values were noted for graphitized resin as well green and calcined asphaltene. The I_D/I_G value once again increases which later decreases with increase in temperature, indicating the changes in arrangement of carbon within the material from random to highly ordered carbon like graphitic carbon.

4. Conclusion

The characteristics of LCO, HCO and EHCO crudes and their vacuum residual fractions i.e. feed quality are varying significantly due to effect of different origin. These three crudes vacuum residues and their fractions exhibited an ascending trend in terms of both total metals percentage and ash %, with the lighter fractions having lower values and the heavier fractions having higher values. The HCO aromatic fractions have a larger presence of heteroatoms and aliphatic protons ($-\text{CH}_3$, $-\text{CH}_2$) as observed directly through ^1H NMR and ^{13}C NMR. ARA fractions were explored as a sustainable precursor to produce graphitic carbon like materials. The incomplete conversion for green carbon were revealed by several decomposition stages during TGA studies. Both XRD and Raman indicate that graphitic carbon like material was successfully synthesized from aromatic, resin and asphaltene fraction via the pyrolysis and high temperature treatment of cured derived carbon. The results of XRD revealed that the diffraction lines at $2\theta = 25.46^\circ$, and the interlayer spacing of green carbon were in the range 3.505–3.538 Å, and subsequent reduction with high temperature treatment to 3.38 Å which shows formation of high ordered graphitic carbon. Likewise, the Raman spectrum of green carbon exhibits presence of D band at 1355 cm^{-1} and G band at 1575 cm^{-1} that supports the presence of graphitic carbon. The intensity ratio of the D and G band (I_D/I_G) from Raman spectra confirmed the transformation of present amorphous like carbon to highly ordered graphitic carbon after high temperature treatment. Further, the thermal stability of the calcined and graphitized carbon have been proven by TGA analysis. The XRD, Raman and TGA of the samples determined no difference irrespective of different feed quality for the preparation of graphitic carbon like material from cured based carbon.

CRedit authorship contribution statement

Ravi Dalsania: Writing – original draft, Validation, Supervision, Methodology, Investigation, Formal analysis. **Hasmukh Gajera:** Writing – review & editing, Supervision, Project administration, Investigation, Data curation, Conceptualization. **Mahesh Savant:** Writing – review & editing, Supervision, Project administration, Conceptualization.

Declaration of competing interest

The authors declare the following financial interests/personal

relationships which may be considered as potential competing interests: Ravi Dalsania reports administrative support was provided by Atmiya University. Ravi Dalsania reports a relationship with Reliance Industries Ltd that includes: employment. If there are other authors, they declare that they have no known competing financial interests or personal relationships that could have appeared to influence the work reported in this paper.

Acknowledgments

The authors thank Dr. Harender Bisht (the Geological Survey of Namely Light crude oil (LCO) from Middle East, Middle crude oil (MCO) from Canada and Heavy crude oil (HCO) from South America respectively) for helpful discussions. This work was supported by Reliance industries Ltd, India.

Data availability

Data will be made available on request.

References

- [1] N.A. Alawani, S.K. Panda, A.R. Lajami, T.A. Al-Qunaysi, H. Muller, Characterization of crude oils through alkyl chain-based separation by gel permeation chromatography and mass spectrometry, *Energy Fuels* 34 (2020) 5414.
- [2] D. Stratiev, I. Shishkova, I. Tankov, A. Pavlova, Challenges in characterization of residual oils. A review, *J. Petroleum Science and Engineering* 178 (2019) 227.
- [3] J. Sainbayar, D. Monkhoor, B. Avid, Determination of trace elements in the tamsagbulag and tagaans crude oils and their distillation fractions using by ICP-OES, *Advances in Chemical Engineering and Science* 2 (2012) 113.
- [4] A.R.S. Nazar, L. Bayandory, Investigation of asphaltene stability in the Iranian crude oils, *Iranian J. Chem. Eng.* 5 (2008).
- [5] T.V. Le Doan, N.W. Bostrom, A.K. Burnham, R.L. Kleinberg, A.E. Pomerantz, P. Allix, Green river oil shale pyrolysis: semi-open conditions, *Energy Fuels* 27 (2013) 6447.
- [6] M. Nikookar, M.R. Omidkhan, G.R. Pazuki, A.H. Mohammadi, An insight into molecular weight distributions of asphaltene and asphalt using Gel Permeation Chromatography, *J. Mol. Liq.* 362 (2022) 119736.
- [7] S.L.S. Sarowha, Determination of molecular weights of petroleum products using gel permeation chromatography, *Pet. Sci. Technol.* 23 (2005) 573.
- [8] B. Azinfar, M. Zirrahi, H. Hassanzadeh, J. Abedi, Characterization of heavy crude oils and residues using combined Gel Permeation Chromatography and simulated distillation, *Fuel* 233 (2018) 885.
- [9] M. Makowska, T. Pellinen, Thin layer chromatography performed in stages to identify the presence of aromatic like fraction in chosen bitumen modifiers, *J. Traffic and Transport. Eng.* 8 (2021) 453.
- [10] D.A. Karlson, S.R. Larter, Analysis of petroleum fractions by TLC-FID: applications to petroleum reservoir description, *Org. Geochem.* 17 (1991) 603.
- [11] H.S. Bisht, M. Reddy, M.A. Malvanker, R. Patil, A. Gupta, B. Hazarika, A. Das, Efficient and quick method for saturates, aromatics, resins, and asphaltenes analysis of whole crude oil by thin-layer chromatography-flame ionization detector, *Energy Fuels* 27 (2013) 3006.
- [12] S.A. Khan, S. Sarfraz, D. Price, TLC-FID calibration and accurate weight determination of SARA fractions in heavy crude oil, *Pet. Sci. Technol.* 30 (2012) 2401.
- [13] M.A. Azam, N.E. Safie, H.H. Hamdan, Effect of sulfur content in the crude oil to the corrosion behaviour of internal surface of API 5L X65 petroleum pipeline steel, *Manuf. Technol.* 21 (2021) 561.
- [14] G.H.C. Prado, Y. Rao, A.D. Klerk, Nitrogen removal from oil: a Review, *Energy Fuels* 31 (2017) 14.
- [15] C.E. Chukwunke, J.O. Madu, B.O. Agboola, Determining ash content and trace metal concentration in crude oil samples to teach students sample preparation and instrumental analysis, *J. Chem. Educ.* 98 (2021) 633.
- [16] J.S. Mandlate, A.S. Henn, P.A. Mello, E.M.M. Flores, J.S. Barin, F.A. Duarte, Determination of Cl and S in crude oil by ICP-OES after sample digestion by microwave-induced combustion in disposable vessels, *Anal. Chim. Acta* 1273 (2023) 341536.
- [17] F. Low, L. Zhang, Microwave digestion for the quantification of inorganic elements in coal and coal ash using ICP-OES, *Talanta* 101 (2012) 346.
- [18] A. Saydut, Microwave acid digestion for the determination of metals in subbituminous coal bottom ash by ICP-OES, *Energy Explor. Exploit.* 28 (2010) 105.
- [19] J.M. Santos, A. Vetere, A. Wisniewski Jr, M.N. Eberlin, W. Schrader, Comparing crude oils with different api gravities on a molecular level using mass spectrometric analysis. Part 2: resins and asphaltenes, *Energy Fuels* 11 (2018) 2767.
- [20] J.P. Arenaz-Diaz, D.C. Palacio, C.X. Ramirez, R. Cabanzo, A. Guzman, E. Mejia-Ospino, Chemical characterization of polar species in colombian vacuum residue and its supercritical fluid extraction subfractions using electrospray ionization FT-ICR mass spectrometry, *Chem. Eng. Transact.* 57 (2017) 2283.
- [21] Z. Farmani, W. Schrader, A detailed look at the saturate fractions of different crude oils using direct analysis by ultrahigh resolution mass spectrometry (UHRMS), *Energies* 12 (2019) 3455.
- [22] M. Pudenzi, N. Eberlin, Assessing relative electrospray ionization, atmospheric pressure photoionization, atmospheric pressure chemical ionization, and atmospheric pressure photo- and chemical ionization efficiencies in mass spectrometry petroleomic analysis via pools and pairs of selected polar compound standards, *Energy Fuels* 30 (2016) 7125.
- [23] A. Wick, G. Fink, T.A. Ternes, Comparison of electrospray ionization and atmospheric pressure chemical ionization for multi-residue analysis of biocides, UV-filters and benzothiazoles in aqueous matrices and activated sludge by liquid chromatography–tandem mass spectrometry, *J. Chromatogr.* 1217 (2010) 2088.
- [24] A.K. Huba, K. Huba, P.R. Gardinali, Understanding the atmospheric pressure ionization of petroleum components: the effects of size, structure, and presence of heteroatoms, *Sci. Total Environ.* 568 (2016) 1018.
- [25] I. Zojaji, A. Esfandiarian, J. Taheri-Shakib, Toward molecular characterization of asphaltene from different origins under different conditions by means of FT-IR spectroscopy, *Adv. Colloid Interface Sci.* 289 (2021) 102314.
- [26] N. Esmaeilian, N. Rabiei, M. Mahmoudi, B. Dabir, Asphaltene structure determination: FTIR, NMR, EA, ICP-OES, MS, XRD and computational chemistry considerations, *J. Molecul. Liquids* 385 (2023) 122279.
- [27] M. Asemani, A.R. Rabbani, Detailed FTIR spectroscopy characterization of crude oil extracted asphaltenes: curve resolve of overlapping bands, *J. Pet. Sci. Eng.* 185 (2020) 106618.
- [28] S.B. Yang, J. Moreira, Z. Li, Predicting crude oil properties using fourier-transform infrared spectroscopy (FTIR) and data-driven methods, *Digital Chem. Eng.* 3 (2022) 100031.
- [29] G. Gao, J. Cao, T. Xu, H. Zhang, Y. Zhang, K. Hu, Nuclear magnetic resonance spectroscopy of crude oil as proxies for oil source and thermal maturity based on ¹H and ¹³C spectra, *Fuel* 271 (2020) 117622.
- [30] T.F. Canan, S. Ok, W. Al-Bazzaz, S. Ponnuswamy, M. Fernandes, M. Al-Shamali, A. Qubian, A. Sagidullin, Rapid characterization of crude oil by NMR relaxation using new user-friendly software, *Fuel* 320 (2022) 123793.
- [31] I. Rakhmatullin, S. Efimov, V. Tyurin, M. Gafurov, A. Al-Muntaser, M. Varfolomeev, V. Klochkov, Qualitative and quantitative analysis of heavy crude oil samples and their SARA fractions with ¹³C nuclear magnetic resonance, *Processes* 8 (2020) 995.
- [32] D. Stratiev, I. Shishkova, V. Toteva, G. Georgiev, R. Dinkov, I. Kolev, I. Petrov, G. Argirov, V. Bureva, S. Ribagin, K. Atanassov, S. Nenov, S. Sotirov, Experience in processing alternative crude oils to replace design oil in the refinery, *Resources* 13 (2024) 86.
- [33] A.B. Garmarudi, M. Khanmohammadi, H.G. Fard, M. Guardia, Origin based classification of crude oils by infrared spectrometry and chemometrics, *Fuel* 236 (2019) 1093.
- [34] O. Galtier, O. Abbas, Y. Dreau, C. Rebufa, J. Kister, J. Artaud, N. Dupuy, Comparison of PLS1-DA, PLS2-DA and SIMCA for classification by origin of crude petroleum oils by MIR and virgin olive oils by NIR for different spectral regions, *Vib. Spectrosc.* 55 (2011) 132.
- [35] M. Salehzadeh, M.M. Husein, C. Ghotbi, B. Dabir, V. Taghikhani, In-depth characterization of light, medium and heavy oil asphaltenes as well as asphaltenes subfractions, *Fuel* 324 (2022) 124525.
- [36] X. Zhai, W. Lin, J. Liu, X. Chen, J. Yong, W. Yang, Fe₃C/Fe, N-codoped porous carbon from petroleum vacuum residual for highly efficient oxygen reduction, *J. Electroanal. Chem.* 866 (2020) 114170.
- [37] J.L. Tirado, R. Santamaria, G.F. Ortiz, R. Menendez, P. Lavela, J.M. Jimenez-Mateos, F.J.G. Garcia, A. Concheso, R. Alcantara, Tin-carbon composites as anodic material in Li-ion batteries obtained by copolyrolysis of petroleum vacuum residue and SnO₂, *Carbon N Y* 45 (2007) 1396.
- [38] H. Chao, J. Liu, Preparation of the 3D porous carbon based on vacuum residue and its application in lithium ion capacitors, *J. Phys.:Conf. Ser.* 2044 (2021) 012117.
- [39] K.H. Lim, S. Kim, H. Kweon, S. Moon, C.H. Lee, H. Kim, Preparation of graphene hollow spheres from vacuum residue of ultra-heavy oil as an effective oxygen electrode for Li-O₂ batteries, *J. Mater. Chem. A* 6 (2018) 4040.
- [40] M. Paliukaite, A. Vaitkus, A. Zofka, Evaluation of bitumen fractional composition depending on the crude oil type and production technology, in: *The 9th international conference "Environmental Engineering"*, 2014.
- [41] T.R. Penha, J.R. Almeida, R.M. Sousa, E.V.R. Castro, M.T.W.D. Carneiro, G. P. Brandao, Multielement analysis of crude oil produced water by ICP OES after acid digestion assisted by microwave, *J. Anal. At. Spectrom.* 30 (2015) 1154.
- [42] A.C.S. Berna, V.C. Moran, E.T.R. Guzman, M.J. Yacaman, Asphaltene aggregation from vacuum residue and its content of inorganic particles, *Pet. Sci. Technol.* 24 (2013) 1055.
- [43] G.A. Mansoori, D. Vazquez, M.S. Niassar, Polydispersity of heavy organics in crude oils and their role in oil well fouling, *J. Petroleum Science and Engineering* 58 (2007) 375.
- [44] D. Oldham, X. Qu, H. Wang, E.H. Fini, Investigating change of polydispersity and rheology of crude oil and bitumen due to asphaltene oxidation, *Energy Fuels* 34 (2020) 10299.
- [45] C.O.E. Eromosele, C.N. Onwucha, S.O. Ajayi, G. Melinte, A.L. Hansen, S. Indris, H. Ehrenberg, Ionothermal preparation of activated carbon from waste PET bottles as anode materials for lithium ion batteries, *RSC Adv.* 12 (2022) 34670.
- [46] P.D. Filippis, L.D. Palma, E. Petrucci, M. Scarsella, N. Verdone, Production and characterization of adsorbent materials from sewage sludge by pyrolysis, *Chem. Eng. Transact.* 32 (2013) 1974.

- [47] A.D. Jara, G. Woldetinsae, A. Betemariam, J.Y. Kim, Mineralogical and petrographic analysis on the flake graphite ore from Saba Boru area in Ethiopia, *Int. J. Mining Sci. Technol.* 30 (2020) 715.
- [48] S.N. Alam, N. Sharma, L. Kumar, Preparation of Graphene Oxide (GO) by modified hummers method and its thermal reduction to obtain reduced graphene oxide (rGO), *Graphene* 6 (2017) 1.
- [49] Z. Zhang, Q. Wang, The new method of XRD measurement of the degree of disorder for anode coke material, *cryst.* 7 (2017) 5.
- [50] V. Scardaci, G. Compagnini, Raman spectroscopy investigation of graphene oxide reduction by laser scribing, *J. Carbon Res.* 7 (2021) 48.